A STUDY OF STEADY STATE AND NON-STEADY STATE DEFORMATION KINETICS

by

Bernard Faucher

A thesis submitted to the School of Graduate Studies
of the University of Ottawa
in partial fulfillment of the requirements
for the degree of
Doctor of Philosophy
in Civil Engineering

Ottawa, Canada

November, 1978

A STUDY OF STEADY STATE AND NON-STEADY STATE DEFORMATION KINETICS

PREFACE

The time dependent plastic deformation of solids is a thermally activated process: plastic flow results from the movement of flow units over energy barriers. Accordingly, the determination of the plastic strain rate is based on deformation kinetics and on the transition state theory of rate processes. This study develops further the steady state kinetics and introduces the non-steady state kinetics of processes that occur over consecutive energy barriers. The results are valid for any deformation mechanism associated with a consecutive system.

Stress relaxation experiments have been carried out on lithium fluoride in the temperature range of 274 - 319 K. The plastic strain rate of LiF in the range of 10^{-3} - 10^{-7} min^{-1} is well described by the kinetics associated with a system of two consecutive energy barriers. Although the experimental activation volume increases when either the stress decreases or the temperature increases, the true activation volumes are stress and temperature independent. This is a general property of consecutive systems.

Dislocations, or flow units, are waiting in front of each energy barrier of a consecutive system. Because the dislocation distribution depends on the stress, a change of stress produces a redistribution that is considered instantaneous in the quasi-steady state approximation.

It is shown that this is valid only when the rate of activation is high or when the redistribution is not extensive. The non-steady state kinetics that prevails in other circumstances is described by a system of differential equations.

The dislocation redistribution that occurs during constant strain rate tests produces yield drop. Two characteristics of this type of yield drop are that its magnitude has a maximum in function of the strain rate and of the temperature, and that the stress oscillates around its steady state value when the yield drop is large. Dislocation redistribution occurs also at the beginning of repeated relaxation tests. It is shown that, in this case, the plastic strain rate increases as the stress decreases, contrary to the usual behavior. This recently recognized behavior is observed in LiF. The explanation of these two phenomena illustrates the importance of deformation kinetics in plastic deformation studies.

ACKNOWLEDGEMENTS

The author wishes to express his deep sense of gratitude to his advisor, Dr. A. S. Krausz, not only for the guidance, encouragement and critical suggestions throughout this project, but also for the teaching of the art and the joy of carrying out a research project.

Sincere thanks are due to all the staff members of the Department of Mechanical Engineering, especially to Mr. D. Seaman and to Mr. G. Toth for their help in the solution of administrative and technical problems.

The generosity of Dr. A. S. Krausz in providing financial assistance from his NRC grant is particularly acknowledged.

The typing of the difficult text by Mrs. L. Sprouse, and the drawing of the figures by Mr. R. Pelot are warmly appreciated.

TABLE OF CONTENT

LIST OF FIGURES

LIST OF TABLES

NOMENCLATURE

a	cross section area
b	Burgers vector
h	Planck's constant
k	Boltzmann's constant
ℓ	distance moved after activation or gage length
m	coefficient
$\bar{s}$	standard error of estimate
t	time
v	dislocation velocity
y	ratio of dislocations in front of second energy barrier ($y=\rho_2/\rho_t$)
A	constant
E	Young's modulus or energy
E'	combined elastic modulus
F	flow over an energy barrier
G	Gibbs free energy
H	work hardening coefficient
K	stiffness
Q	partition function
S	nominal pulling rate
T	absolute temperature
V	activation volume
W	work
α	geometrical factor
δ	contribution to the deformation after activation
ε	strain
η	δ_1/δ_t

κ	transmission coefficient
ρ	dislocation density
σ	normal stress
τ	shear stress
Δ	change of
Σ	summation of
∂	partial derivative
k	rate constant

Superscripts

.	rate
$\ddagger$	activated state
-	average
*	transition
ss	steady state

Subscripts

a	applied
b	backward
e	elastic empirical
exp	experimental
f	forward
i	internal
o	initial
p	plastic
r	reactant
t	total
y	yield
1,2,i,j	index
M	machine

Note

The rate constants, activation energies, and activation volumes are labelled as, for example, ${}_{i}k^{j}$ or ${}^{j}k_{i}$, where i represents the reactant state and j the product state. The numerals i and j are arranged as ${}_{i}k^{j}$ in the case of forward activation and as ${}^{j}k_{i}$ in the case of backward activation.

A STUDY OF STEADY STATE AND NON-STEADY STATE DEFORMATION KINETICS

CHAPTER 1

INTRODUCTION

> This being the universal structure of things, in every inquiry about anything we are always to presuppose a single Form, for we shall certainly discover its presence. If we have found it, we are next to look for two Forms to follow on the one, or, if we cannot find two, for three or some other number. Each of the units thus found should be treated in the same fashion, until we discover not simply that our initial one is also many, or indefinitely numerous, but actually how many it is.
>
> (Plato, Philebus)

Matter in solid state is characterized by a definite shape, or by the ability to sustain shear stress. At high stress level, however, solids undergo a permanent change of shape, that is flow, at a rate that depends on the temperature. This is a general property of solids - metals, polymers, and even usually brittle materials. The formability of metals has been utilized since the Bronze and Iron Ages of civilization. Today this property is used by the manufacturing industry to produce a variety of objects, some of which are as simple as a coin, and others as complex as a spacecraft. The plasticity of polymers is utilized in every day life. The fibers of clothing are "permanently" elongated under the high temperature and stress used in ironing. The keratin of the hair is set into a "permanent" form with the necessary humidity and heat. Although ice is usually considered

as a brittle material, ice needles may be bent into loops (1)[1]. Even rocks can be folded under the tremendous pressures that result from the very slow movement of the plates forming the earth's outer shell. Geomechanics is in fact an integral part of plasticity theory (2).

Although plasticity is a favorable property whenever it facilitates the forming of materials, it becomes undesirable whenever it leads to the failure of engineering components. A puzzling problem in plasticity occurred when the first European railway cars had made extensive travelling. Their axles started to fracture even though the applied stress was well below the yield stress - the stress required to cause large amount of plastic flow. Investigations that followed the work of Ewing and Humfrey (3) have shown that plastic deformation occurs even at these low stress levels and that this is associated with fatigue failure. The sudden fracture of T-2 tankers during the Second World War raised another challenging problem related to plasticity (4). It led to the development of fracture mechanics and the understanding of the role of plasticity in crack propagation. Failure results also from the creep of components of, for example, steam-generating units, gas turbines, or nuclear reactors. Plastic flow in stressed assemblies may cause another form of failure that is due to stress relaxation.

To cope with the various problems associated with plastic flow, engineers need a functional relationship between the parameters that control the plastic deformation process. As early as 1909, Ludwig (5) found a logarithmic relation between the flow stress and the rate of

---

1. Numerical in parentheses refer to corresponding items in the List of References.

deformation. Somewhat later, Becker (6) took into account the effect of temperature through an Arrhenius type equation. Holloman and Zener (7) proposed that a functional relationship, of the same kind as the equation of state of a perfect gas, may hold for the plastic deformation of metals. Following the work of Hart (8), there have been many attempts (see for example Ref. 9, 10) to take into consideration the structure of the material. However, because the dislocation configuration, and therefore the structure, of a deformed material is not in thermodynamic equilibrium there could be no physical validity to a mechanical equation of state (11). It is well known that the structure of a deformed material depends on its previous strain-temperature history.

The establishment of the relationship, even though it may be valid only under specific conditions, between the various parameters that govern plastic deformation is extremely valuable for engineering purposes. A sound relationship must be based on a rigorous theory, and conform to experimental observations. As will be shown later, the fundamental physical processes of plastic deformation and chemical reaction are identical. Chemical kinetics, based on statistical mechanics, should therefore be utilized to study plasticity.

The experimental part of this thesis describes the behavior of lithium fluoride during stress relaxation experiments. This material has been selected because its dislocation structure has been thoroughly studied, large single crystals of high purity may be easily obtained,

and it presents a well-pronounced yield drop. The deformation kinetics analysis of the experimental results has led in this study to the further development of the steady state and non-steady state kinetics associated with consecutive energy barrier systems.

1.1 THEORY OF DEFORMATION KINETICS

The fundamental physical process of both chemical reactions and plastic deformations is the breaking of atomic bonds and establishment of new bonds. A chemical reaction produces a change in the chemical composition of substances, and a "deformation reaction" produces a change of shape. Similarly to plastic deformation, an isomerization reaction changes only the atomic configuration of the reacting substance. A deforming body may thus be conceived as a giant molecule, the isomerization of which is the plastic flow. Deformation kinetics must therefore be identical to chemical reaction kinetics.

1.1.1 DEFORMATION OF CRYSTALLINE MATERIALS

The bond breaking process in crystalline materials at low temperature occurs with high probability at line defects - the dislocations. The concept of dislocation was introduced in 1934 by Orowan (12), Polanyi (13), and Taylor (14) to explain the discrepancy between the calculated (see for example Ref. 15) and observed yield stress of metal single crystals. The effect of an applied stress on the potential energy along a dislocation slip plane is shown in Fig. 1 (14). It was already recognized that thermal fluctuations can

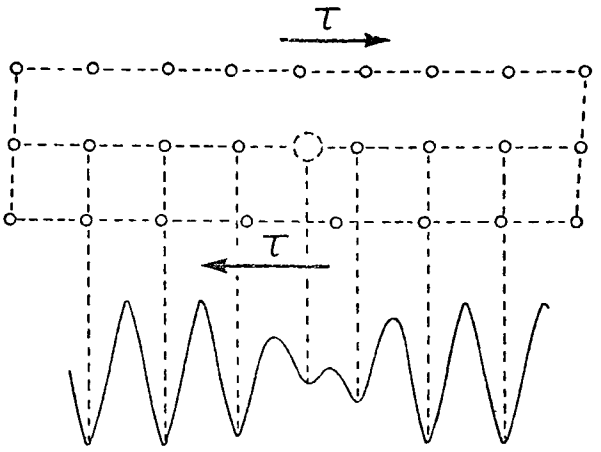

FIGURE 1. The effect of a shear stress on the potential energy along a dislocation slip plane (14).

facilitate the displacement of the dislocations in the direction favored by the shear stress. Extensive studies of the properties of dislocations have since been carried out (16-21), and numerous observations have been made (22).

A dislocation moving in a crystal produces in the swept area a relative displacement equal to the magnitude of its Burgers vector, b. The plastic strain rate, $\dot{\varepsilon}_p$, resulting from the displacement of dislocations at the average velocity $\bar{v}$ is given by Orowan's equation (23) as:

$$\dot{\varepsilon}_p = \alpha \, b \, \rho \, \bar{v} \qquad (1.1)$$

where α is a geometrical factor, and ρ is the total length of dislocations

per unit volume. The limiting velocity of a dislocation is the speed of transverse-sound-waves (Ref. 21 p. 156). In the usual stress and temperature ranges, the motion of dislocations occurs at a much lower rate because it is impeded by obstacles. A dislocation passes over an obstacle when it can acquire enough energy, either from the applied stress or from the random fluctuations of energy in the crystal, that is from thermal activation.

Following Seeger (24), two types of obstacles to dislocation motion are usually considered: those that raise long-range stress fields, and those that raise short range stress fields. It is generally considered (25-29) that the large amount of energy required to overcome the former type of obstacles can be acquired only through the applied stress. Thermal activation can assist dislocations in overcoming only the short range obstacles. The applied stress, τ_a, is accordingly the sum of two components: the internal (or athermal) stress, τ_i, that is needed to overcome long range obstacles, and the effective (or thermal) stress, τ, that is needed to overcome short range obstacles. The athermal stress depends weakly on the temperature through the elastic modulus, and the thermal stress depends strongly on the strain rate and the temperature.

According to Conrad (27), some common thermally activated dislocation mechanisms are illustrated in Fig. 2. Obstacles to the motion of dislocations in the slip plane are the Peierls-Nabarro stress (periodic stress field of the lattice), the "forest dislocations"

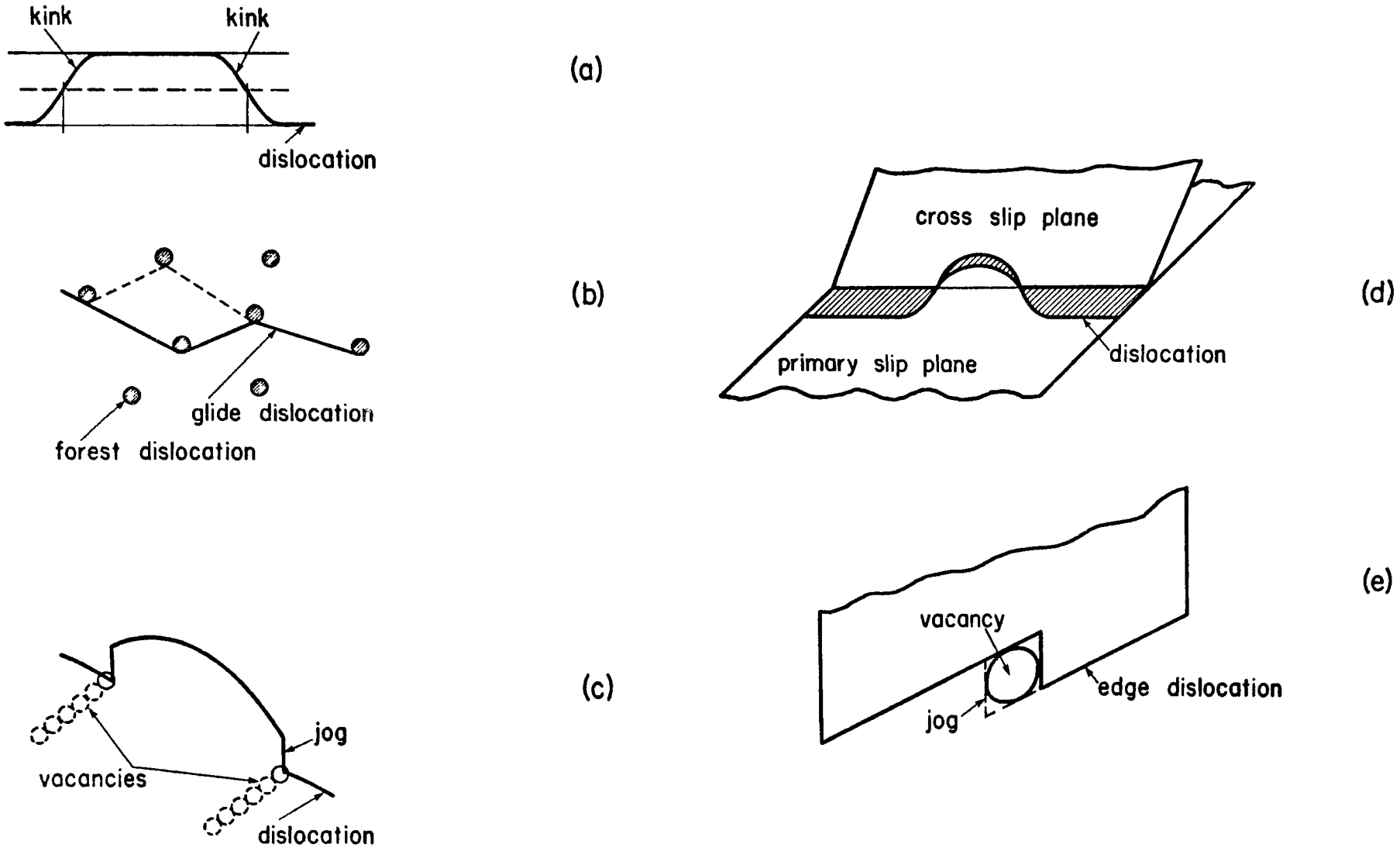

FIGURE 2: Thermally activated dislocation mechanisms (27).

(dislocations threading the glide plane), the motion of jogs in screw dislocations. Mechanisms that produce motion of dislocations out of the slip plane are the cross-slip of extended screw dislocations, and the climb of edge dislocations.

The plastic strain rate produced by the motion of dislocations over an average distance $\bar{\ell}$ is expressed as (23)

$$\dot{\varepsilon}_p = \alpha\ b\ \rho\ \bar{v} = \alpha\ b\ \rho\ \bar{\ell}\ k = \delta\ \rho\ k$$

where k is the net rate of activation over the velocity-limiting energy barrier, and δ is the average contribution to the strain. The rate of activation k depends on the kinetics of the process, and is usually a combination of elementary rate constants. Each rate constant is obtained from the properties of each energy barrier, according to the transition state theory.

1.1.2 THE TRANSITION STATE THEORY

The first attempt to take into account the strong temperature dependence of the rate, k, of a chemical reaction was made by Arrhenius (30) who expressed it as

$$k = A_e \exp\ (-\ \Delta E_e / kT)$$

where A_e is a frequency factor, ΔE_e is an empirical activation energy, k is the Boltzmann's constant, and T is the absolute temperature. This was a purely empirical relationship, and theoretical justification had to wait for the development of statistical thermodynamics. Marcellin (31) was the first to suggest that the reacting molecules should go through a critical surface in phase space. The concept that reactants

must be in an activated state before becoming products was further developed by Rodebush (32-35), Rice and Gershinowitz (36,37). The theory was brought to its present form by Eyring (38,39), Evans and Polanyi (40-42) and its relevance to plasticity was already considered (43,51). The transition state theory (44) and its application to deformation kinetics (45) are now firmly established.

For dislocation movement, the reacting molecule is the group of N atoms around the dislocation. The potential energy of this molecule is represented in a configuration space of 3N-5 dimensions, and may theoretically be calculated from quantum mechanics. The configuration associated with the passage of the dislocation over an obstacle is shown schematically in two dimensions in Fig. 3. A molecule in the low energy level - indicated as R - corresponding to the reactant state can go to the low energy level - indicated as P - corresponding to the product state, only if it becomes activated to the transition state - indicated as ‡. The activated state is a saddle point, that is, presents negative curvature in the direction corresponding to the reaction path - the reaction coordinate, indicated with a dashed line - and positive curvature in all other orthogonal directions. The potential energy along the reaction coordinate is shown schematically in Fig. 4. The passage of the activated complexes over the top of the energy barrier may be treated as a translation or as a loose vibration (46). The frequency of decomposition of the activated complexes is found, in both cases, to be kT/h. The rate of the reaction in the forward direction, that is from reactant to product, is obtained as (44-46):

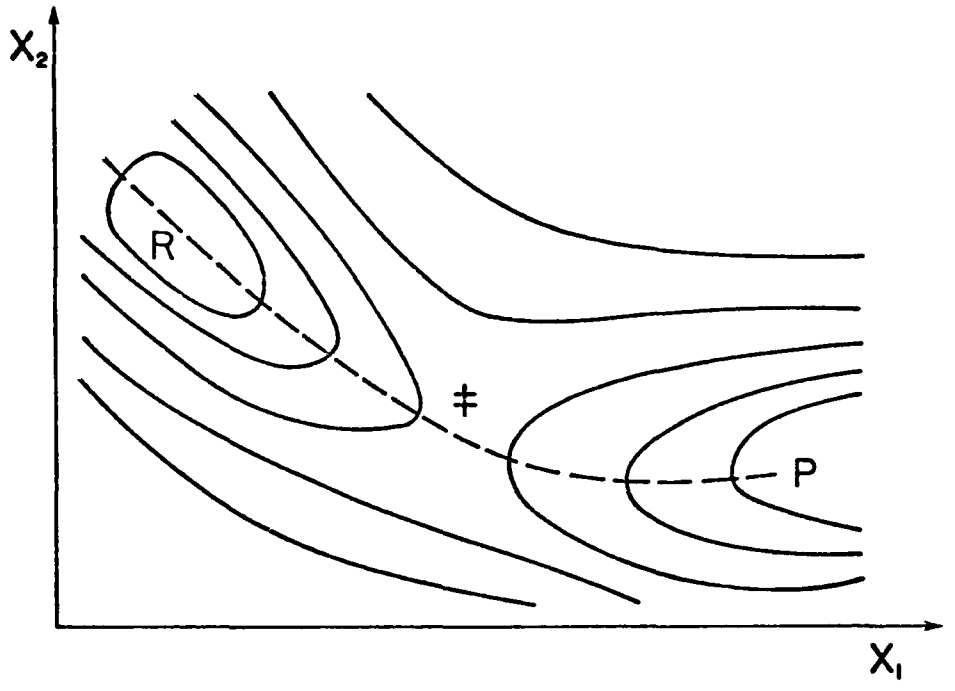

FIGURE 3: Equipotential lines in phase space, and the reaction path.

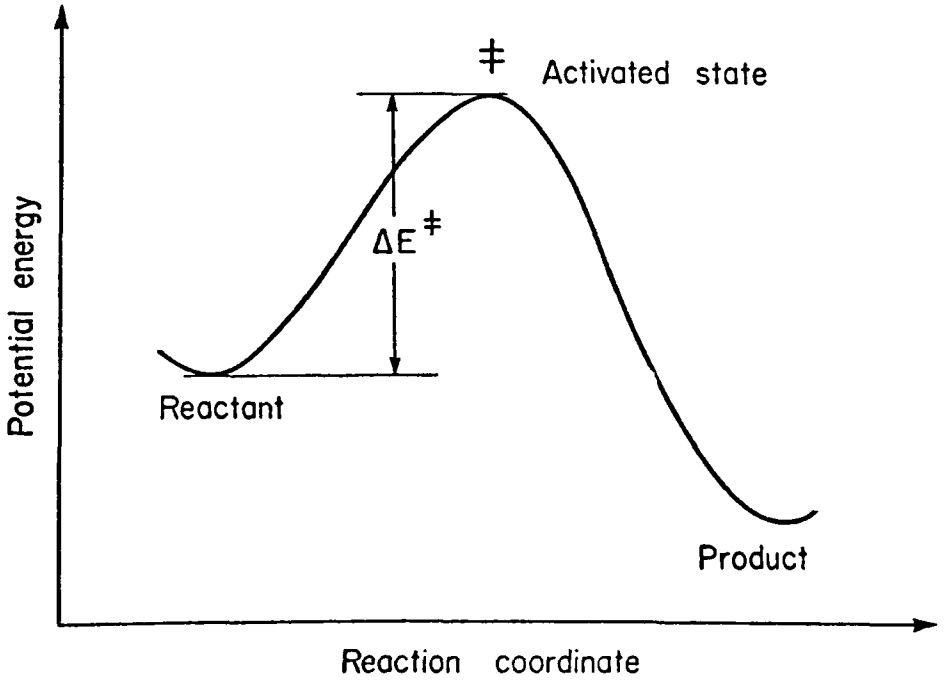

FIGURE 4: Variation of the potential energy along the reaction coordinate.

$$\text{Rate}_f = \rho_r k_f^{\ddagger} = \rho_r \kappa \frac{kT}{h} \frac{Q^{\ddagger}}{Q_r} \exp\left(-\frac{\Delta E^{\ddagger}}{kT}\right)$$

where $\Delta E^{\ddagger}$ is the energy of activation at 0K, that is the difference between the zero-point energy of the activated complexes and that of the reactants, $Q^{\ddagger}$ represents the partition functions of the 3N-7 degrees of vibrational freedom in the activated state (the degree of freedom corresponding to the reaction coordinate has been utilized), Q_r represents the partition functions of the reactant state, ρ_r is the number of reacting molecules (atom groups forming dislocations), k and h are respectively the Boltzmann and Planck constants, T is the absolute temperature, and κ is a transmission coefficient that takes into account the possibility that a complex may be reflected back or tunnel through the energy barrier. From the statistical thermodynamics definition of the Gibbs free energy ΔG, the rate constant $k_f^{\ddagger}$ may be written as

$$k_f^{\ddagger} = \kappa \frac{kT}{h} \frac{Q^{\ddagger}}{Q_r} \exp\left(-\frac{\Delta E^{\ddagger}}{kT}\right) = \kappa \frac{kT}{h} \exp\left(-\frac{\Delta G_f^{\ddagger}}{kT}\right) .$$

Because the passage of a dislocation over an energy barrier produces strain, the effective stress, τ, acting on the dislocation does the work $W_f(\tau)$. The potential energy surface is then modified, and the rate constant k_f is expressed as

$$k_f = \kappa \frac{kT}{h} \exp\left[-\frac{\Delta G_f^{\ddagger} - W_f(\tau)}{kT}\right] = k_f^{\ddagger} \exp\left[\frac{W_f(\tau)}{kT}\right] .$$

1.1.3 DEFORMATION KINETICS

The first step of a deformation kinetics analysis is to consider the effect of "backward activation", that is the reaction from product

to reactant. In fact, the transition state theory is rigorously exact only for equilibrium states, that is when forward and backward rates are equal. The two basic combinations of elementary processes - in parallel and in series - should then be investigated. The corresponding behavior has been described by Gifkins (47) and Li (48). Krausz and Eyring (45,49) have developed the associated kinetics, and Hanley and Krausz (50) a method for the analysis of deformation kinetics.

In the following description of deformation kinetics theory, only kinetics associated with fundamental processes will be discussed: backward activation over a single energy barrier, parallel and consecutive systems. When necessary, more elaborate systems may be easily constructed.

SINGLE BARRIER KINETICS

The net rate of any reaction, that is the difference between forward and backward rates, is expressed as

$$\text{Rate} = \text{Rate}_f - \text{Rate}_b = \rho_f k_f - \rho_b k_b,$$

where the subscripts f and b indicate that the process is associated with the forward and backward activation, respectively. In plastic flow there is no difference between product and reactant states, because, after overcoming an energy barrier, the dislocations, which are the reacting molecules are usually stopped in front of a similar energy barrier. This situation, as outlined by Gifkins (47) is very different from chemical kinetics. The difference between forward and backward directions results only from the work, W, done by the effective stress,

τ, during activation. A dislocation moving in the forward direction "sees" the energy barrier reduced by $W(\tau)$, and moving in the backward direction sees the same energy barrier increased by $W(\tau)$, as illustrated in Fig. 5. The plastic strain rate is then expressed as

$$\dot{\varepsilon}_p = \delta\rho k = \delta\rho\ (k_f - k_b) = \delta\rho k^{\ddagger}\left\{ \exp\left[\frac{W(\tau)}{kT}\right] - \exp\left[-\frac{W(\tau)}{kT}\right] \right\}$$

$$\dot{\varepsilon}_p = 2\delta\rho k^{\ddagger} \sinh\left[W(\tau)/kT\right] \qquad (1.2)$$

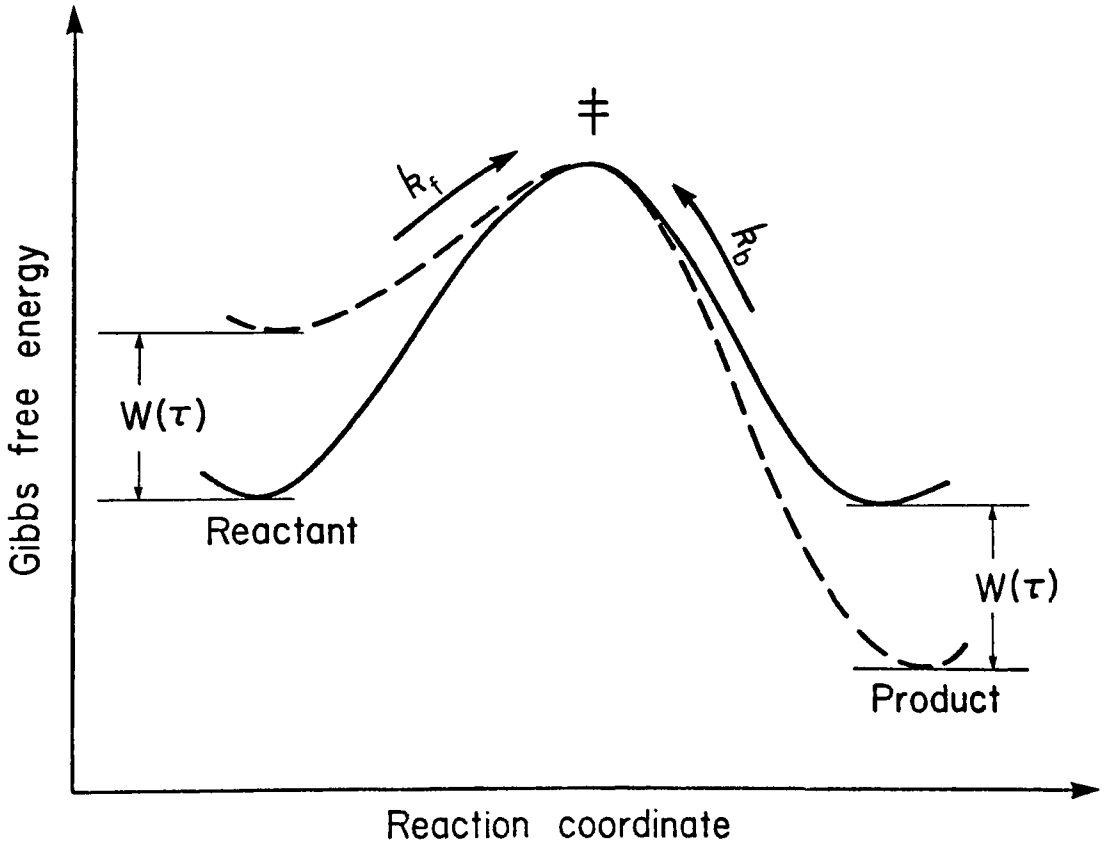

FIGURE 5: Schematic representation of the effect of the shear stress on the energy barrier associated with the plastic flow.

This expression was used by Orowan (51), Eyring (43), Kauzmann (52) with a linear stress dependence of the work, that is

$$W(\tau) = V.\tau$$

where the "activation volume" V is defined as

$$V = - \left(\frac{\partial \Delta G}{\partial \tau}\right)_T .$$

At low stress level or high temperature, when $W(\tau)$ is much less than kT, Eq. (1.2) becomes

$$\dot{\varepsilon}_p = 2\delta\rho k^{\ddagger} \sinh (V\tau/kT) \simeq 2\delta\rho k^{\ddagger} \frac{V\tau}{kT} .$$

This relation expresses the often observed proportionality between the plastic strain rate and the stress. At high stress level, or low temperature, when $W(\tau)$ is much larger than kT, the plastic strain rate is obtained as

$$\dot{\varepsilon}_p = 2\delta\rho k^{\ddagger} \sinh (V\tau/kT) \simeq \delta\rho k^{\ddagger} \exp (V\tau/kT) .$$

This relation expresses the fact that activation in the backward direction is then negligible. According to Schoeck (53), backward activation is effective only when the dislocation does not move too far away from the barrier, and in the case of point defect controlled plastic flow.

Alefeld (54) showed that even with constant activation volume, Eq.(1.2)could describe adequately some experimental results. Krausz (55) considered the more general case of a non-symmetrical energy barrier. The plastic strain rate is then expressed as

$$\dot{\varepsilon}_p = \delta_f \rho k_f - \delta_b \rho k_b$$

where

$$k_f = \kappa \frac{kT}{h} \exp\left(-\frac{\Delta G_f^{\ddagger} - V_f \tau}{kT}\right) = k_f^{\ddagger} \exp\left(V_f \tau / kT\right)$$

$$k_b = \kappa \frac{kT}{h} \exp\left(-\frac{\Delta G_b^{\ddagger} + V_b \tau}{kT}\right) = k_b^{\ddagger} \exp\left(-V_b \tau / kT\right)$$

Non-symmetrical energy barrier takes into account the facts that the structure, hence the energy, of the group of atoms around the dislocation may change after activation, and that the activation distance, hence the activation volume, may be different for forward and backward activation. Krausz was thus able to explain the observed stress dependence of dislocation velocity in LiF, Ge, Si ... (55), as well as the effect of temperature on the behavior of Ge, Si, CaF_2 ... (56). Backward activation over non-symmetrical energy barrier could also explain the stress dependence of the experimental activation volume measured in bcc metals (57).

PARALLEL SYSTEMS

In general, plastic deformation occurs over several slip planes, while simultaneous processes may occur in one slip plane. The macroscopically observed strain rate is the sum of all individual events (45, 47-50, 59, 60):

$$\dot{\varepsilon}_p = \sum_i \alpha_i b_i \rho_i v_i = \sum_i \delta_i \rho_i k_i \qquad (1.3)$$

where the k_i's are of the form

$$k_i = k_{if} - k_{ib} .$$

The largest term in Eq. (1.3) controls the rate of deformation, and, in general, is sufficient to describe the plastic strain rate at a given temperature. Kauzmann (52) found that two terms were needed to explain the creep behavior of tin single crystals (61). The experimental

results of Heard, obtained on Yule marble (62), were analyzed by Eyring and co-workers (63). They found that the stress dependence of the deformation rate could be explained only by considering two mechanisms, dislocation glide and grain boundary glide associated with vacancy diffusion. Li (48) refers to a large number of materials in which deformation is thought to be controlled by parallel processes.

CONSECUTIVE SYSTEMS

A system of consecutive energy barriers may be represented by a series such as ABCABCA ... Dislocations pass successively over each barrier A, B, and C. In a specific stress range, one of the barriers may be higher than the others and would, therefore, control the rate. The Peierls-Nabarro mechanism, diffusive climb, and glide of jogged dislocations are processes associated with consecutive energy barrier systems.

The Peierls-Nabarro mechanism, which results from the periodical stress field of the lattice, operates by the nucleation of a double kink that propagates along the dislocation line (64). Celli et al. (65) have considered that the spreading may be retarded by dragging points. Figure 6a illustrates the system of two consecutive energy barriers corresponding to the nucleation and point defect pinning of the double kink. Hanley, Krausz and Krishna (66) have shown that dragging due to n identical point defects has formally the same effect as a single energy barrier. Hirth (60) has delimited the stress range where either kink nucleation or kink diffusion is rate controlling. The contribution

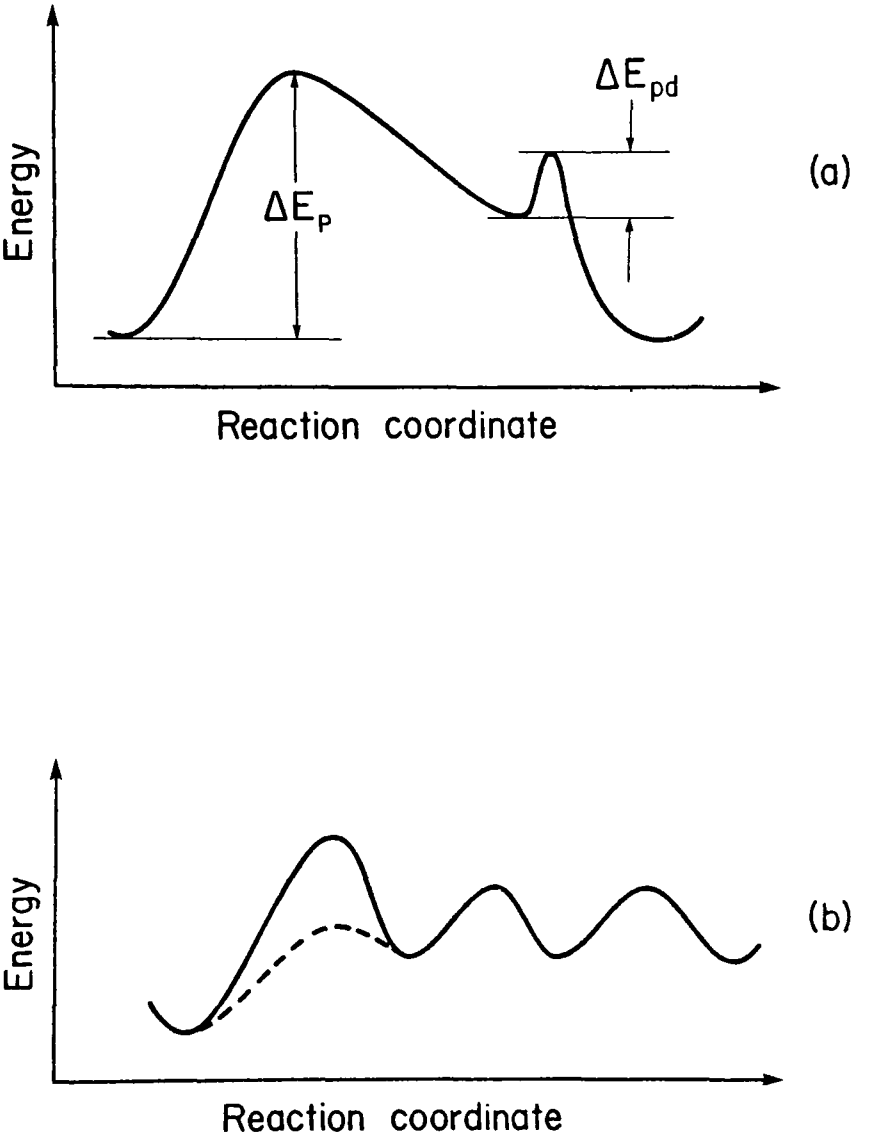

FIGURE 6: Two examples of consecutive energy barriers. (a) Peierls mechanism (65). The first barrier is associated with the Peierls stress and the second with the dragging by point defects. (b) Two alternatives for the glide of jogged dislocations (Ref. 21 p. 538). The first barrier is associated with the motion of the jog and the subsequent with the diffusion of the vacancy in the lattice.

of dislocation climb to plastic deformation becomes significant at high temperature (67,68). Dislocation climb proceeds by the formation of a jog that grows by vacancy (or interstitial) emission. The emission of the point defect and its following diffusion over a short distance (17,21) constitute a consecutive system. Similarly, the glide of jogged dislocations occurs by the emission of vacancies that diffuse into the lattice (69,70). Consequently, the glide of jogged dislocations (Fig. 6b) is controlled by consecutive energy barriers kinetics.

The plastic strain rate associated with consecutive energy barriers is often written as (47,48,71,72)

$$\dot{\varepsilon}_p = \varepsilon_o / \sum_i t_i \tag{1.4}$$

where t_i is the waiting time in front of the i-th energy barrier. The kinetics analysis (45,49) takes into account backward activation. For the two-consecutive-energy-barrier system shown in Fig. 7, the net flow F_1 and F_2 over each individual barrier is (73)

$$F_1 = \rho_1 \, {}_1k^1 - \rho_2 \, {}^1k_2 = F_2 = \rho_2 \, {}_2k^2 - \rho_1 \, {}^2k_1$$

where ${}_ik^j$ represents the rate of activation in the forward direction from barrier i to the top of barrier j, and ${}^jk_i$ represents the rate of activation in the backward direction. Because the total number of dislocations is

$$\rho_t = \rho_1 + \rho_2$$

it follows that

$$\rho_1 = \rho_t - \rho_2 = \rho_t \frac{{}_2k^2 + {}^1k_2}{{}_1k^1 + {}_2k^2 + {}^1k_2 + {}^2k_1} \tag{1.5}$$

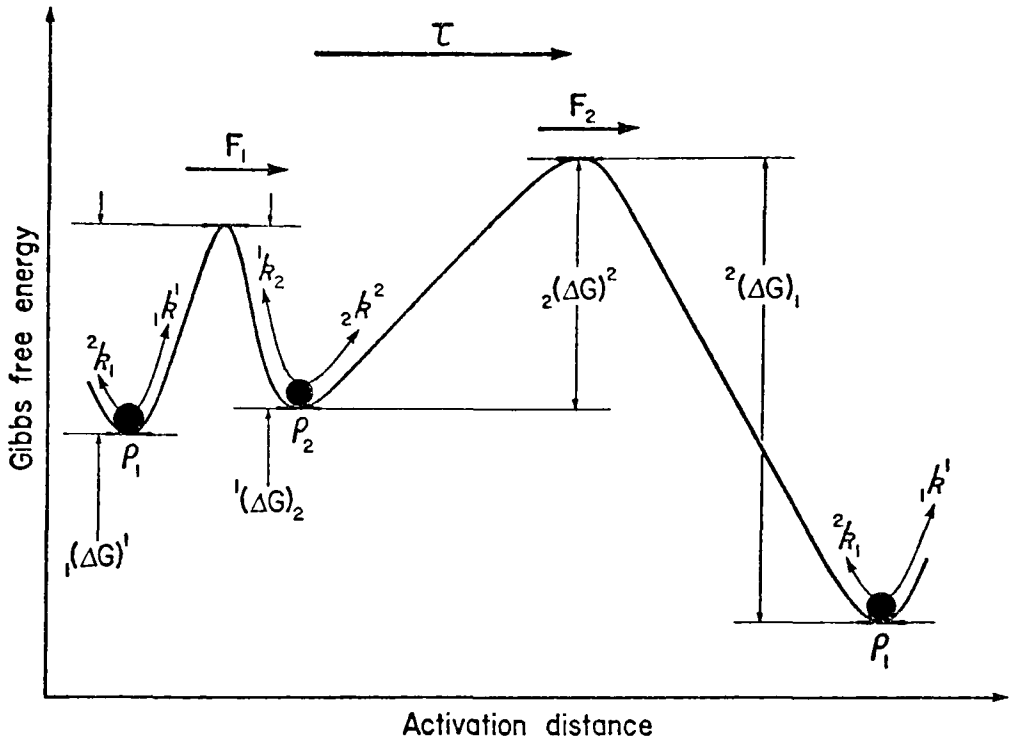

FIGURE 7: Schematic representation of a system of two consecutive energy barriers under the influence of a shear stress.

The plastic strain rate is then

$$\dot{\varepsilon}_p = \delta F = \delta \rho_t \frac{{}_1k^1\ {}_2k^2 - {}^1k_2\ {}^2k_1}{{}_1k^1 + {}_2k^2 + {}^1k_2 + {}^2k_1}$$

or

$$\dot{\varepsilon}_p = \delta \rho_t \frac{1 - \dfrac{{}^1k_2\ {}^2k_1}{{}_1k^1\ {}_2k^2}}{\dfrac{1}{{}_1k^1} + \dfrac{1}{{}_2k^2} + \dfrac{1}{{}_1k^2} + \dfrac{1}{{}_2k^1}} \qquad (1.6)$$

where ${}_1k^2 = {}_1k^1\ {}_2k^2/{}^1k_2$ and ${}_2k^1 = {}_2k^2\ {}_1k^1/{}^2k_1$.

In this equation the numerator is

$$1 - \exp\left\{ \frac{{}_1\Delta G^{\ddagger 1} + {}_2\Delta G^{\ddagger 2} - {}^1\Delta G_2^{\ddagger} - {}^2\Delta G_1^{\ddagger} - \left[{}_1W^1(\tau) + {}_2W^2(\tau) + {}^1W_2(\tau) + {}^2W_1(\tau)\right]}{kT} \right\}$$

Since the strain rate is zero when the stress is zero, it follows immediately that, for the investigated system,

$$ {}_1\Delta G^{\ddagger 1} + {}_2\Delta G^{\ddagger 2} = {}^1\Delta G_2^{\ddagger} + {}^2\Delta G_1^{\ddagger} \qquad (1.7) $$

The two first terms in the denominator of Eq. (1.6) are of the form

$$ \frac{1}{{}_i k^i} = \frac{h}{kT} \exp\left[\frac{{}^i\Delta G^{\ddagger i} - {}_i W^i(\tau)}{kT}\right]. $$

They are waiting times for activation over each of the energy barriers in the forward direction. The third term is expressed explicitly as

$$ \frac{1}{{}_1 k^2} = \frac{{}^1 k_2}{{}_1 k^1 \, {}_2 k^2} = \frac{h}{kT} \exp\left[\frac{{}^1\Delta G^{\ddagger 1} + {}_2\Delta G^{\ddagger 2} - {}^1\Delta G_2^{\ddagger} - {}_1 W^1(\tau) - {}_2 W^1(\tau) - {}_2 W^2(\tau)}{kT}\right] $$

or using Eq. (1.7)

$$ \frac{1}{{}_1 k^2} = \frac{h}{kT} \exp\left[\frac{{}^2\Delta G_1^{\ddagger} - {}_1 W^1(\tau) - {}_2 W^1(\tau) - {}_2 W^2(\tau)}{kT}\right] $$

This term is identical to a waiting time for activation over an energy barrier corresponding to the forward free energy difference between position 1 and the top of the second barrier. Similarly, the fourth term in the denominator of Eq. (1.6) is identical to a waiting time for activation over an energy barrier corresponding to the forward free energy difference between position 2 and the top of the first barrier.

Equation (1.6) describes the properties of a system of two consecutive energy barriers. It can be generalized to systems of more than two energy barriers (58) and it can be included in the equation describing parallel processes. Although more general and more satisfactory than Eq. (1.4), equation (1.6) has been derived under the

condition of steady state flow. Because steady state is only an approximation, its validity will be determined from a non-steady state analysis.

1.2 EXPERIMENTAL METHODS

Several experimental techniques were developed for the determination of the deformation kinetics of materials. Mechanical models help the visualization of the behavior of materials under these various experimental conditions. The elastic deformation is represented by a spring, and the time dependent plastic deformation by a dashpot. The behavior of materials may then be represented by the combination of springs and dashpots shown in Fig. 8 (Ref. 45 p. 129). The deformation of the dashpot is usually non-Newtonian and is described by a constitutive relation between the stress, σ, deformation, ε_p, rate $\dot{\varepsilon}_p$, and temperature, T, as

$$F(\sigma, \varepsilon_p, \dot{\varepsilon}_p, T) = 0 \tag{1.8}$$

The exact form of Eq. (1.8) depends on the kinetics associated with the mechanisms that control plastic flow. Equation (1.8) defines a deformation surface (74), shown in Fig. 9. The surface is determined by various tests during which one of the variables is usually kept constant. The tests are represented by intersections of the surface with planes perpendicular to the axis: constant strain rate test (or tensile test), constant stress (or creep test), and constant strain (or stress relaxation test).

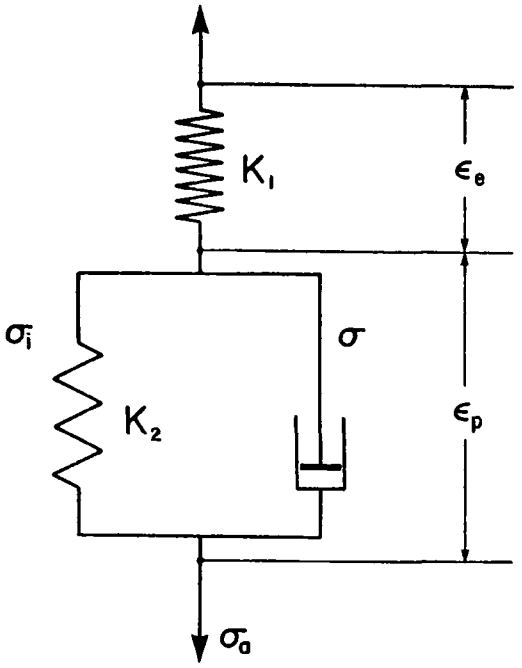

FIGURE 8: The mechanical model used in the study of plastic deformation. ϵ_e and ϵ_p are, respectively, the elastic and plastic strain . σ, σ_i, and σ_a are the effective, internal, and applied stress.

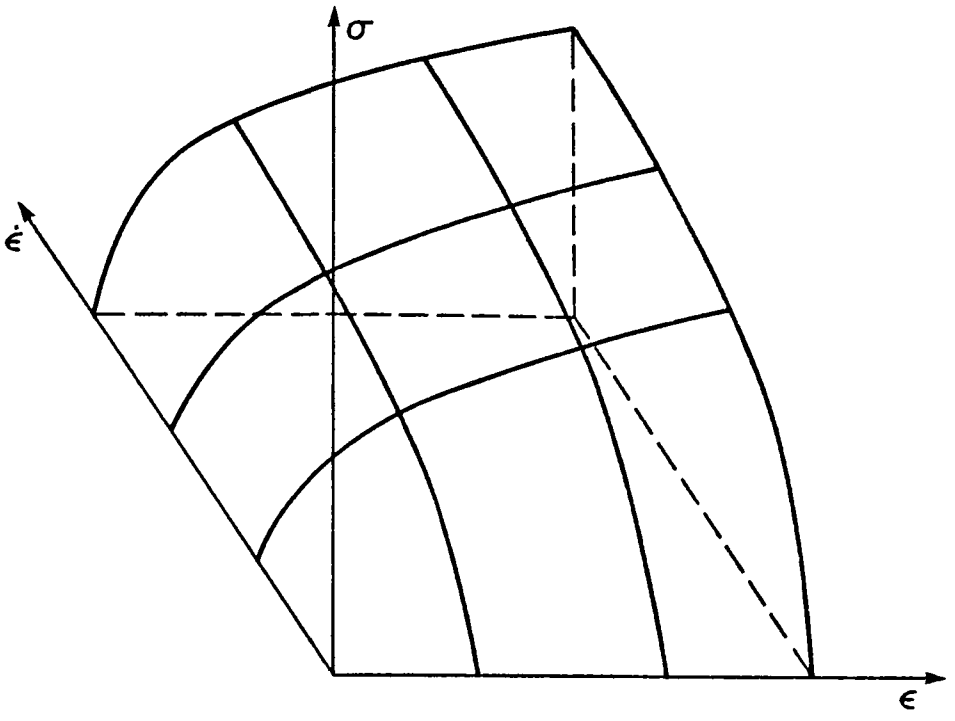

FIGURE 9: Deformation surface for the model of Fig. 8 (Ref. 74 p. 418).

CONSTANT STRAIN RATE TEST

Figure 10a shows the input corresponding to a constant strain rate test, and the response of the model of Fig. 8. The elongation rate of the dashpot is zero at the beginning of the test, and reaches the imposed rate at the end of the test. The elastic modulus of the specimen, E (initial slope in Fig. 10a), is represented by the spring K_1, and spring K_2 represents the work-hardening coefficient, H (final slope). Depending on the properties of the dashpot, materials may exhibit an upper and lower yield stress as indicated with the dashed line in Fig. 10a.

The tensile test is probably the oldest method used for the investigation of the plastic properties of materials (74). It is now usually carried out in hard testing machines at constant crosshead velocity. These machines provide a good approximation of the constant strain rate condition at small elongations. Tensile tests may be carried out over a very large temperature range and at various strain rates. A variant, the strain rate change test, facilitates the determination of the experimental activation volume, V_{exp}, defined as

$$V_{exp} = kT \left(\frac{\partial \ell n \dot{\varepsilon}}{\partial \tau}\right) .$$

The yield drop phenomena that are observed during constant strain rate tests have been explained by Cottrell (16) and Johnston (75).

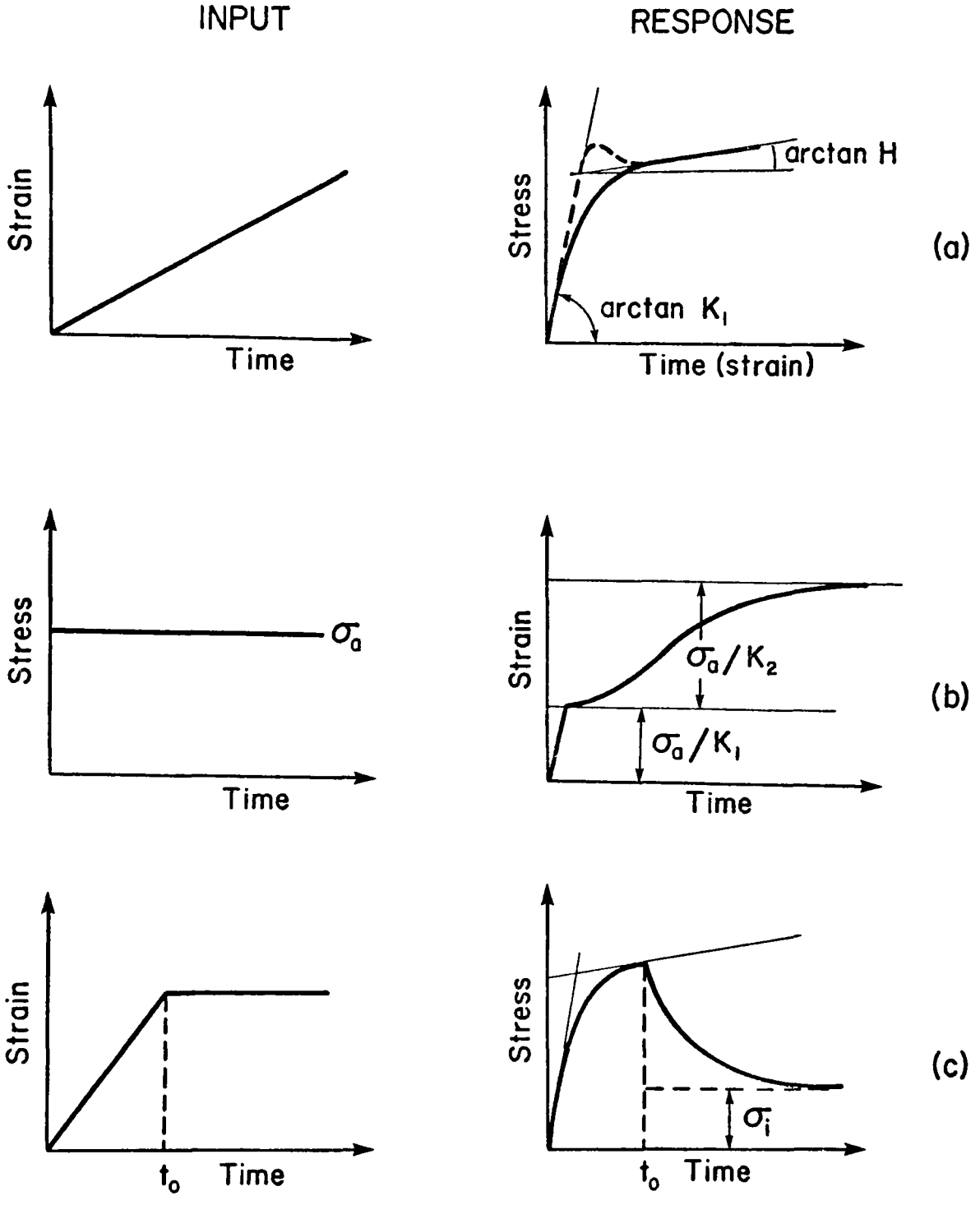

FIGURE 10: Schematic representation of the constant strain rate (a), creep (b), and stress relaxation (c) experiments (Input) and of the response of the model of Fig. 8.

CREEP TEST

The constant stress input and the response typical of low temperature creep are shown in Fig. 10b. The initial strain results from the deformation of the spring K_1. As the dashpot displaces, the load is transferred to spring K_2 until no more load acts on the dashpot. Phillips (76) and Andrade (77) were among the first to investigate the creep behavior of various materials. Creep test is usually approximated by a constant load test, even if the applied stress changes as a result of the deformation of the specimen. Even when the applied stress is constant, the effective stress does change during a creep experiment. Discrete stress change tests in creep (78,79) allow the determination of the experimental activation volume, similarly to strain rate change tests. Experimental activation energies may be calculated from temperature change tests in creep (80-82).

STRESS RELAXATION TEST

The behavior under constant strain condition is shown in Fig. 10c. The specimen is first deformed under constant strain rate, then, after time t_o, the elongation is kept constant. Just before t_o, the dashpot deforms at the imposed rate under the effect of a stress σ_o. Just after t_o, the stress σ_o, is still acting on the dashpot that keeps on elongating. The constant elongation condition requires a contraction of the spring K_1 equal to the elongation of the dashpot. The applied stress, therefore, decreases until no more load acts on the dashpot.

One of the first investigations was made as early as 1904 by

Trouton and Rankine (83). Extensive studies have since been made by Feltham (84,85) and others. Stress relaxation tests are usually carried out in a hard testing machine. The decrease of the load following the arrest of the crosshead produces a small deformation of the machine. The analysis of the test, following Guiu and Pratt (86), takes into consideration the interrelation between the machine and the specimen. This is represented in Fig. 11, where the machine deforms only elastically with a stiffness K, and the specimen deforms both elastically and plastically according to the model of Fig. 8. The combined elastic modulus E' takes into account the elastic deformation of the machine, ε_m, and of the specimen, ε_e. It is defined as

$$\frac{1}{E'} = \frac{a_o}{K\ell_o} + \frac{1}{E}$$

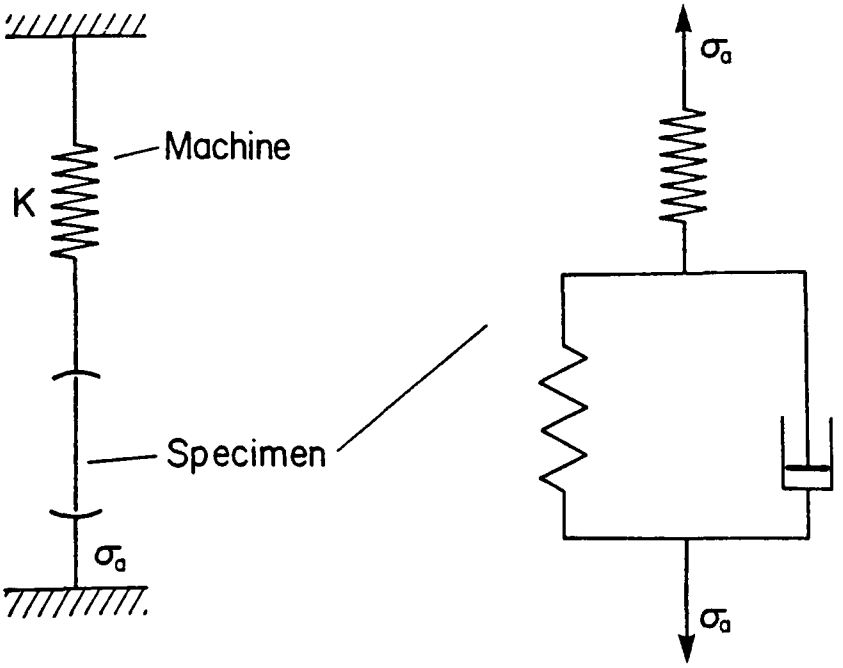

FIGURE 11: Schematic representation of the interaction between the machine and the specimen.

where a_o and ℓ_o are, respectively, the initial cross-sectional area and length of the specimen, K is the stiffness of the testing machine, and E is the elastic modulus of the specimen. The plastic strain rate, $\dot{\varepsilon}_p$, is the difference between the constant pulling rate of the machine, S, and the elastic rates:

$$\dot{\varepsilon}_p = S - (\dot{\varepsilon}_e + \dot{\varepsilon}_m) = S - \dot{\sigma}_a/E'$$

hence

$$\dot{\sigma}_a = E' (S - \dot{\varepsilon}_p). \tag{1.9}$$

Because the applied stress is the sum of the effective and the internal stresses,

$$\dot{\sigma}_a = \dot{\sigma} + \dot{\sigma}_i = \dot{\sigma} + H \dot{\varepsilon}_p,$$

the effective stress rate is obtained from Eq. (1.9) as

$$\dot{\sigma} = E' (S - \dot{\varepsilon}_p) - H \dot{\varepsilon}_p = E' \left[S - (1 + \frac{H}{E'}) \dot{\varepsilon}_p \right].$$

In stress relaxation $S = 0$, then

$$\dot{\sigma} = - E' (1 + \frac{H}{E'}) \dot{\varepsilon}_p = - (E' + H) \dot{\varepsilon}_p$$

When the deformation of the machine is not purely elastic, the total strain of the specimen, ε, should be measured. The plastic strain rate is then expressed as

$$\dot{\varepsilon}_p = \dot{\varepsilon} - \dot{\varepsilon}_e = \dot{\varepsilon} - \dot{\sigma}_a/E \tag{1.10}$$

This relation holds in all situations and shows that the plastic strain rate can be determined from a knowledge of the total strain rate and the stress rate.

Combining Eqs. (1.9) when $S = 0$ and (1.10), the total strain rate during stress relaxation is expressed as

$$\dot{\varepsilon} = - \dot{\sigma}_a (\frac{1}{E'} - \frac{1}{E}).$$

This equation shows that the relation between the stress and the total strain measured during stress relaxation should be linear if the deformation of the machine is linearly elastic. It could also be used for the measurement of the combined elastic modulus.

Because plastic deformation is kept to a minimum during stress relaxation experiments, structural changes are minimized. The plastic strain rate is measured over a wide range as the stress decreases. The stress relaxation test appears, therefore, to be well suited for the determination of the deformation surface.

INTERNAL STRESS

Only the effective stress does work when a dislocation surmounts an obstacle by thermal activation. Because the effective stress is the difference between applied stress - easily measured - and internal stress, the latter must be known in order to determine activation parameters. The first method developed by Seeger (24) is based on the fact that the internal stress depends on the temperature only through the shear modulus. The temperature dependence of the ratio of the flow stress to the shear modulus yields the values of internal stress and effective stress at each temperature (Fig. 12). This method, however, presents certain shortcomings: a large number of tests are required over a wide range of temperature, the internal structure may change with the temperature (72).

The incremental unloading method avoids these shortcomings and is

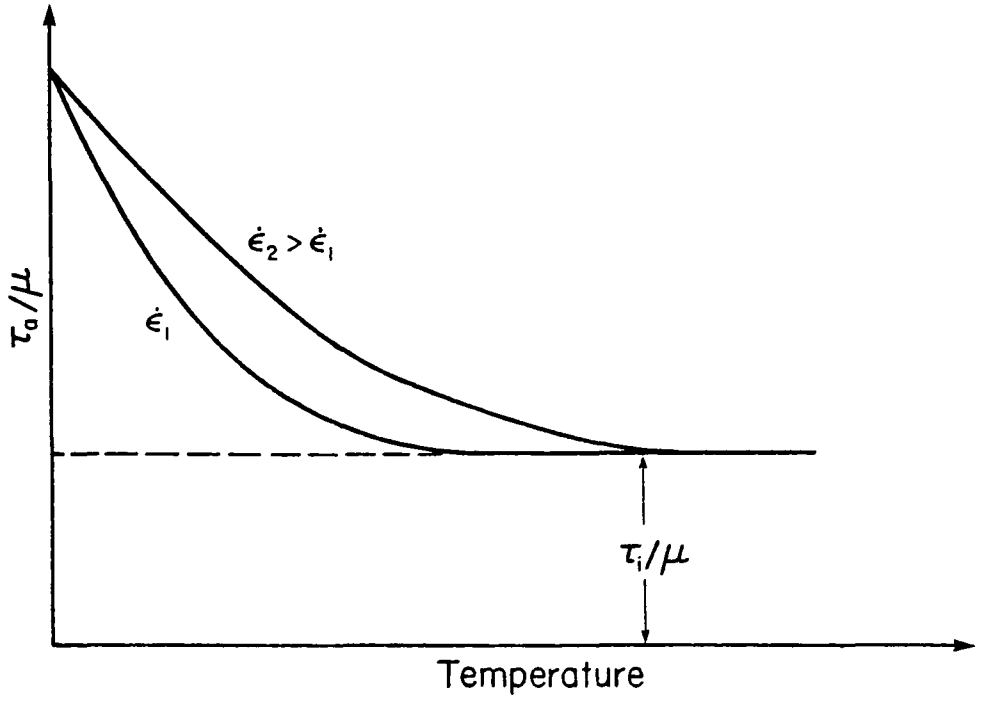

FIGURE 12: Schematic temperature dependence on τ_a/μ. τ_a is the flow stress corresponding to the strain rate $\dot{\epsilon}$, and μ is the shear modulus at the same temperature.

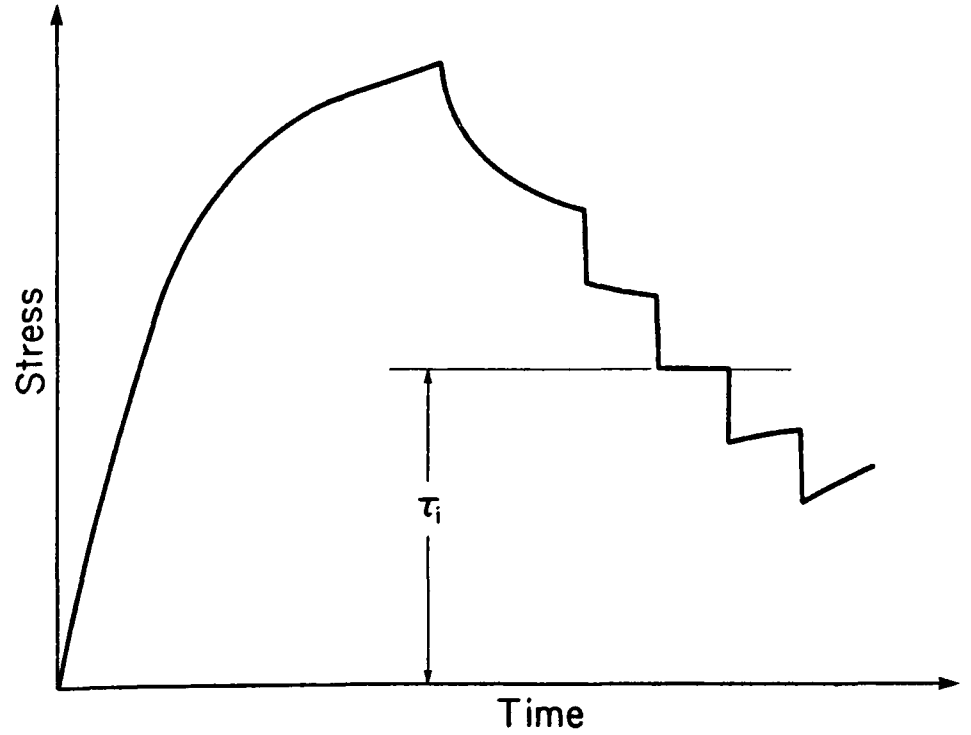

FIGURE 13: Schematic representation of the incremental unloading method to measure the internal stress.

widely used (87-93). The principle of this method is shown in Fig. 13. At zero effective stress, the plastic strain rate must be zero. At stress below the internal stress level negative relaxation occurs. The internal stress is then simply the applied stress at zero strain rate. Besides the fact that machine relaxation may render the measurement very difficult (91), the determination of zero rate is a practical impossibility. The method brackets only a stress range within which the strain rate is vanishingly small (92). The width of this stress range depends on the sensitivity of the equipment and the properties of the material: a specific material will have a more or less broad stress range within which its plastic strain rate will be less than the sensitivity of the equipment. The precaution required to use the method is further illustrated by the recent observation of a positive relaxation that followed a negative relaxation (93). The advantage of this method is that the evaluation is made on the same specimen that was used in a preceding test.

CHAPTER 2

EXPERIMENTAL PROCEDURE AND RESULTS

2.1 EXPERIMENTAL SPECIFICATIONS

2.1.1 MATERIAL

Two batches of lithium fluoride single crystals of vacuum ultraviolet quality were obtained from the Harshaw Chemical Company. The crystals were cleaved along {100} planes to a square cross-section of about 10 mm^2, and a length of 5 cm. The specimens were cemented to the grips of the tensile machine, as shown in Fig. 14, with methyl-2-cyanoacrylate type cement (loctite 12). The contact length was 12 mm on two sides at each end. The load was, therefore, transmitted through a contact area of twice 12 x 3.2 mm^2. The specimens had a pale yellowish coloration, and a relatively high elastic limit. They yielded at a normal stress of about 18 MPa, fractured before 2% strain could be achieved, and did not work-harden.

2.1.2 EQUIPMENT

TESTING MACHINES

Most of the tests were performed on an Instron TTCM machine, with a 50 lb. capacity load cell. The combined elastic modulus, E', with this load cell, was 5000 MPa, which corresponds to a stiffness of 2 MN/m. Some tests were made with a stiffer, 100 kg capacity, load cell with which E' was 10,000 MPa. A few tests were carried out in a

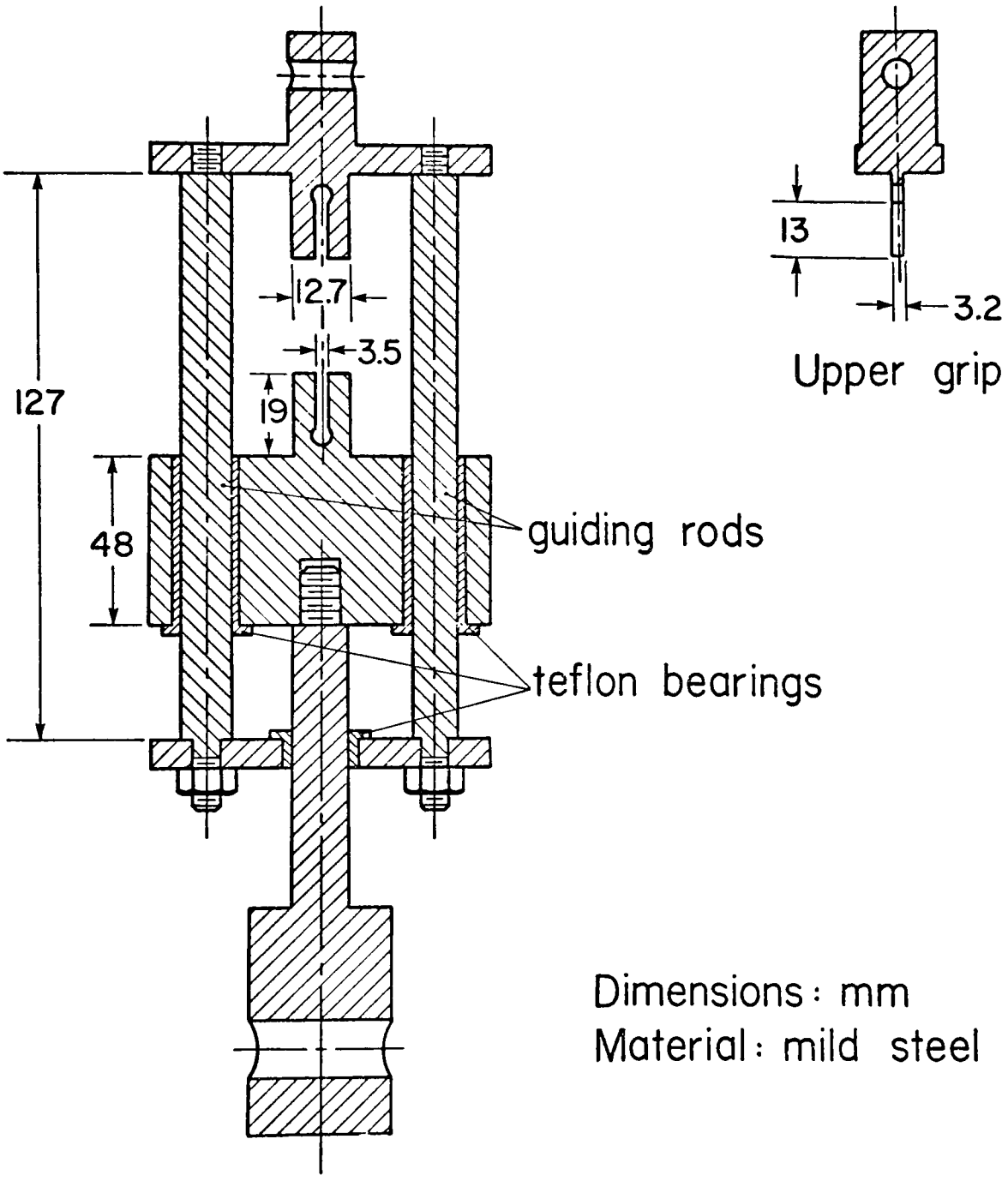

FIGURE 14: Grips used to load LiF single crystals in tension.

Hounsfield tensometer to decrease E' to 2000 MPa. The nominal cross-head velocity of the machines was 2×10^{-3} min^{-1}. The specified full load and time scale accuracy of the Instron recorder is 0.25%. The load cell of the Hounsfield was modified to allow a direct recording of the load: a Hewlett-Packard 7DCDT-050 transducer was used to measure the deflection of the spring beam (94). The control of the synchronous stepping motor, that replaced the manual loading device (95), was modified to obtain a nominal strain rate of 2×10^{-3} min^{-1}. The accuracy of the load measurement on the modified Hounsfield was estimated to be only 5%. Hysteresis resulting from friction in various parts of the Hounsfield load cell was significant at the beginning of the relaxation test.

STRAIN MEASUREMENT

The total strain of the specimens was measured with an Instron G51-11MA strain gauge extensometer, that was mounted on teflon pads attached to the specimen (Fig. 15). This arrangement reduced the damage to the specimen, and prevented the slippage of the extensometer. The strain of the extensometer was measured with an Intertechnology P-350 strain indicator set to a gauge factor of 1.03 and maximum sensitivity. The calibration, that was made with an Instron A18-3C extensometer calibrator, did not change by more than 1% in the temperature range of 258-303K. The output of the strain indicator (10.05±0.05 V/mm) depended weakly on the operating range of the apparatus, and was linear over a ± 250 mV range. The voltage was recorded with a Hewlett-Packard 7100B strip chart recorder. The noise

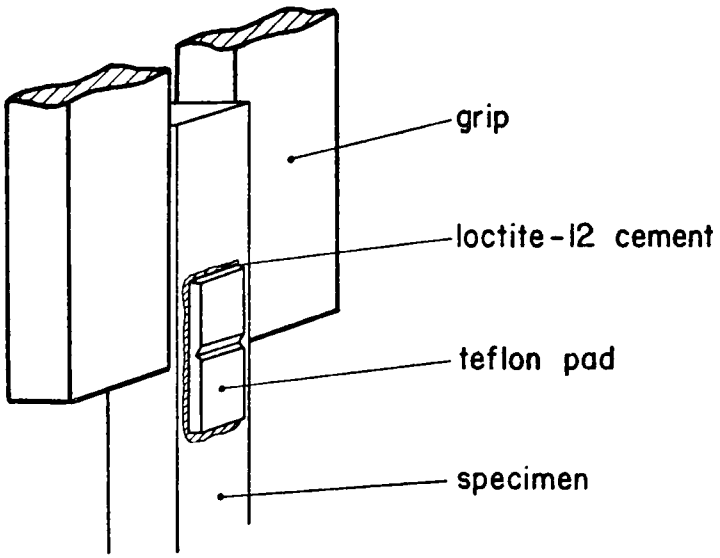

FIGURE 15: Detail of the specimen arrangement.

of the strain indicator was about 1 mV, which limited the sensitivity of the strain measurements to 4×10^{-6}. With the selected gauge factor the strain indicated by the strain indicator was about ten times less than the actual strain of the specimen. Because the specified accuracy of the strain indicator is 0.1%, the accuracy of the total strain was estimated to be 1%.

TEMPERATURE CONTROL

The stress relaxation measured during constant elongation tests results from the elastic contractions of the machine and the specimen that compensate the plastic elongation of the specimen. Because a

small strain change produces a large stress change (the ratio is the combined elastic modulus), it is important to minimize the length changes caused by temperature fluctuations. Furthermore, to be able to measure low strain rates, the temperature has to be stable over a long period of time. This was accomplished by surrounding the test frame of the machine with a double styrofoam insulation. During tests above room temperature, the temperature between the two enclosures was controlled with a Thermoelectric 400 temperature controller, model 32422. During tests below room temperature, the machine and the double insulation were placed in a cold room. During each test the temperature was monitored by a thermocouple placed near the specimen. The fluctuations were typically within a 0.2°C range, and their effect was not noticeable.

EQUIPMENT PERFORMANCE

Stress relaxation tests were carried out at 29°C and -17°C with steel dummy specimens to determine the performance of the equipment. The specimens were submitted to a load corresponding to the yield stress of LiF (about 200N), and their relaxation was measured during 100 hours. The observed load relaxation corresponded to an apparent negative strain rate that was orders of magnitude less than the relaxation rate of LiF. This apparent rate was typically of the order of 10^{-6} min^{-1} at the beginning of the test, and decreased afterwards. After a few minutes the maximum apparent strain rate was less than 4×10^{-8} min^{-1}. The lower limit of strain measurement was set at 2×10^{-7} min^{-1}. Comparison of this value with the initial value of 2×10^{-3} min^{-1} - the nominal

crosshead speed - indicates that the strain rate could be measured with at least 10% accuracy over four orders of magnitude range.

2.1.3 EXPERIMENTAL PROCEDURE AND DATA PROCESSING

The specimens were submitted to two different types of test: "conventional" and "repeated" stress relaxation. In conventional relaxation, the specimen was strained until a predetermined strain was reached. The crosshead was then stopped and the subsequent load relaxation and elongation were recorded. In repeated relaxation the specimen was reloaded elastically to a predetermined load, and the relaxation test repeated. Figure 16 illustrates the difference between the two test types. The duration of the tests was, in general, one day.

The plastic strain rates were calculated according to Eq. (1.10):

$$\dot{\varepsilon}_p = \dot{\varepsilon} - \dot{\sigma}_a/E.$$

The stress and strain rates were determined from smooth spline functions fitted to the experimental load and elongation recordings (Appendix A). The elastic modulus of LiF was obtained from the data of Briscoe and Squire (95). Because it changes only from 103 GPa to 88 GPa as the temperature changes from 0 to 300 K, an average value of 98 GPa was used at each testing temperature.

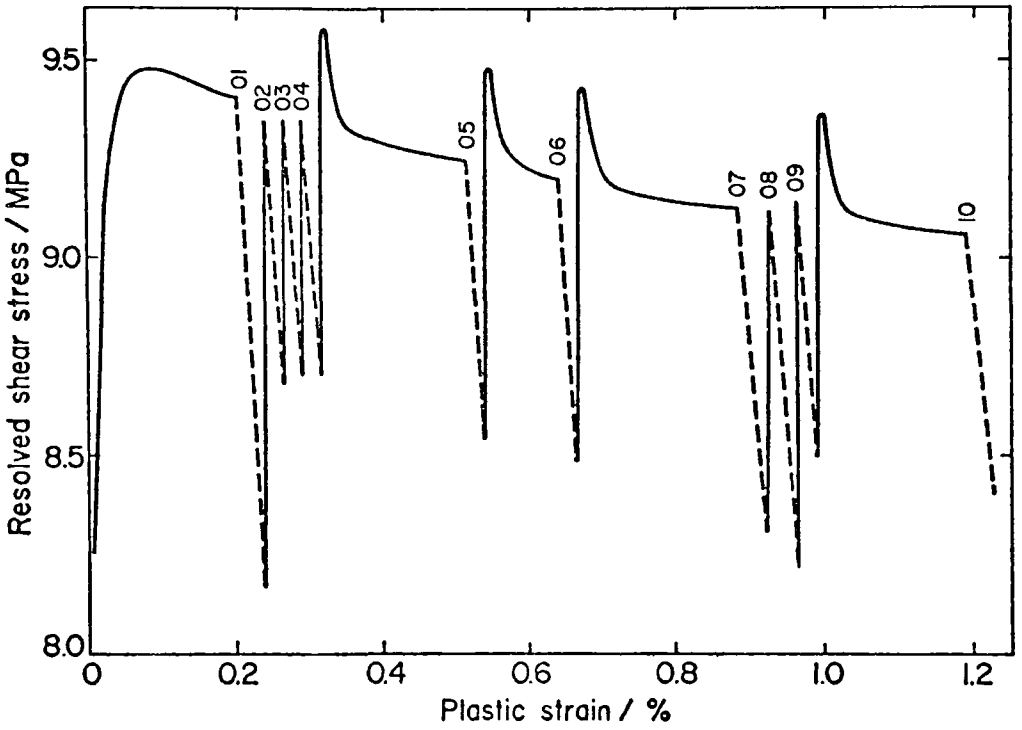

FIGURE 16: Typical test sequence showing conventional relaxations (tests 01, 05, 06, 07, 10) and repeated relaxations (tests 02, 03, 04, 08, 09).

2.2 EXPERIMENTAL RESULTS

Stress relaxation results are often represented in the log $(-\dot{\sigma})$-vs-τ coordinate system, in which the slope of the curve is proportional to the experimental activation volume. Because useful information can be also obtained from the shape of these rate diagrams, some typical results will be presented in the log $\dot{\varepsilon}_p$-vs-$(\tau_a-\tau_o)$ coordinate system. The use of $\dot{\varepsilon}_p$ eliminates the non-elastic behavior of the machine. The difference $\tau_a-\tau_o$ is utilized to obtain a reference, the initial applied stress τ_o, that will allow a comparison of the results regardless of the value of the internal stress.

EFFECT OF DEFORMATION

The first group of tests was carried out to determine the effect of deformation on the relaxation behavior of LiF. As many tests as possible were carried out on each specimen before it fractured; a typical sequence is shown in Fig. 16. These tests were made on specimens 2, 4, 6, and 7 of the first batch of crystals, at 302 K in the Instron machine with a combined elastic modulus of 5000 MPa. The initial conditions are shown in Table I, and the results in Appendix B.

Figure 18 shows the characteristic features of the rate diagrams obtained in conventional relaxation: a long straight line at low strain rates (2-3 orders of magnitude), and a convex curvature at higher rates. The observed scatter is well within the limits of experimental error, and the results indicate that deformation of less than 2% has no measurable effect on the relaxation of LiF.

TABLE I

The initial conditions of group I tests. Each quantity is illustrated in Fig. 17.

TEST NO	TEMPERATURE (K)	INITIAL STRAIN (PCT)	TOTAL STRAIN (PCT)	INITIAL SHEAR STRESS (MPA)
2.01	302	0.20	0.20	8.360
2.02	302	0.23	0.47	8.290
2.03	302	0.20	0.70	8.272
2.04	302	0.00	0.74	8.197
2.05	302	0.00	0.76	8.199
2.06	302	0.21	1.00	8.232
4.01	302	0.20	0.20	9.432
4.02	302	0.00	0.23	9.369
4.03	302	0.00	0.26	9.379
4.04	302	0.00	0.29	9.379
4.05	302	0.20	0.51	9.297
4.06	302	0.10	0.64	9.262
4.07	302	0.20	0.88	9.213
4.08	302	0.00	0.92	9.201
4.09	302	0.00	0.95	9.215
4.10	302	0.20	1.19	9.170
6.01	302	0.12	0.12	8.735
6.02	302	0.00	0.15	8.716
6.03	302	0.00	0.18	8.718
6.04	302	0.00	0.18	8.716
7.01	302	0.08	0.08	8.955
7.02	302	0.00	0.11	8.958
7.03	302	0.00	0.11	8.923

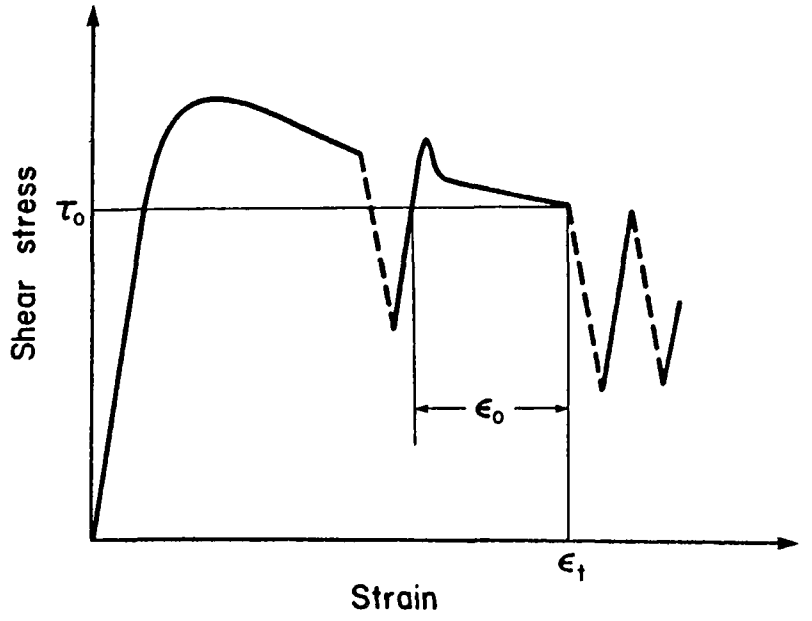

FIGURE 17: Schematic illustration of the initial conditions. τ_0 is the initial stress, ϵ_0 is the initial strain (the initial strain of repeated relaxation tests if 0), ϵ_t is the total strain.

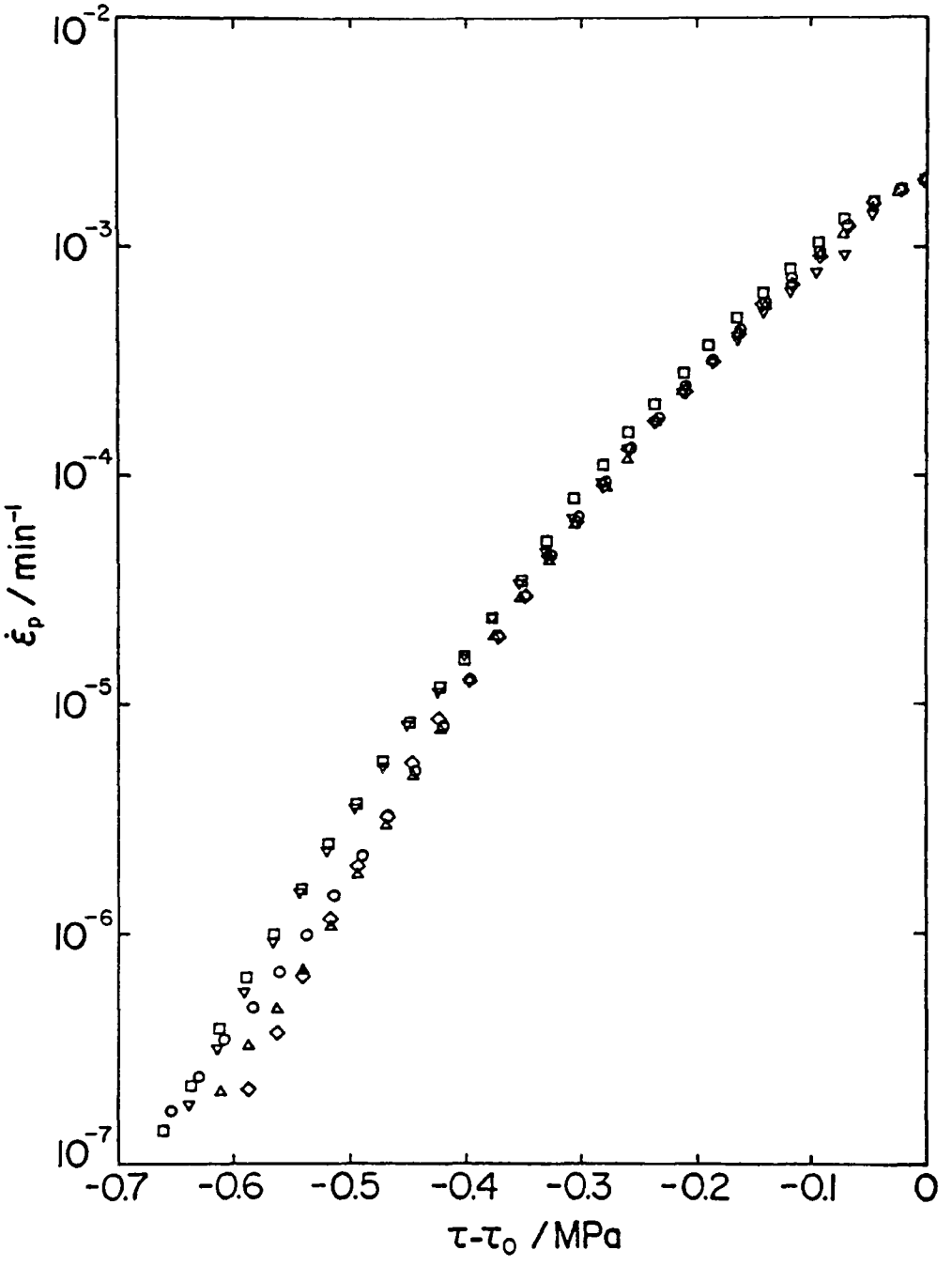

FIGURE 18: Typical behavior observed in conventional stress relaxation. Tests 4.01 (○), 4.05 (◇), 4.06 (△), 4.07 (□), and 4.10 (▽), at room temperature.

EFFECT OF TEMPERATURE

A second group of tests was carried out to measure the effect of temperature on the relaxation of lithium fluoride. Tests were made on specimens 20 to 26 of the second batch of crystals. Each specimen was submitted to a test sequence similar to that shown in Fig. 16. The tests were carried out in the Instron machine (E' = 5000 MPa), in the temperature range of 258-319 K. Specimen 26 was tested at various temperatures. The initials conditions are shown in Table II, and the results in Appendix B.

TABLE II

The initial conditions of group II tests.

TEST NO	TEMPERATURE (K)	INITIAL STRAIN (PCT)	TOTAL STRAIN (PCT)	INITIAL SHEAR STRESS (MPA)
20.01	300	0.07	0.07	8.729
20.02	300	0.00	0.14	8.474
20.03	300	0.00	0.19	8.488
21.01	300	0.06	0.06	8.592
21.02	300	0.00	0.10	7.646
21.03	300	0.00	0.12	7.931
21.04	300	0.00	0.14	8.208
21.05	300	0.00	0.20	8.329
21.06	300	0.18	0.43	8.237
21.07	300	0.00	0.48	8.225
21.08	300	0.00	0.54	8.238
21.09	300	0.20	0.78	8.239
21.10	300	0.21	1.05	8.327
21.11	300	0.18	1.28	8.322
21.12	300	0.21	1.53	8.327
22.01	281	0.06	0.06	8.564
23.01	281	0.08	0.08	8.450
23.02	281	0.00	0.17	8.389
23.03	281	0.10	0.34	8.472
23.04	281	0.20	0.63	8.543
24.01	258	0.00	0.04	10.181
24.02	258	0.21	0.35	9.347
24.03	258	0.00	0.45	9.182
24.04	258	0.17	0.70	9.045
24.05	258	0.16	0.92	9.025
24.06	258	0.11	1.12	9.118
25.01	258	0.07	0.07	11.133
25.02	258	0.20	0.38	10.137
25.03	258	0.00	0.46	10.154
26.01	319	0.14	0.14	9.082
26.02	319	0.00	0.22	9.161
26.03	319	0.19	0.50	8.524
26.04	319	0.00	0.56	8.529
26.05	319	0.19	0.82	8.353
26.06	305	0.12	1.00	7.600
26.07	294	0.17	1.23	7.913
26.08	282	0.20	1.49	8.141
26.09	274	0.20	1.75	8.376

Figure 19 shows the effect of temperature on the relaxation behavior of specimen 26. All curves, except those at 319 K in the low strain rate range, are identical. The experimental activation volume, therefore, increases with temperature because the slope is proportional to V/kT.

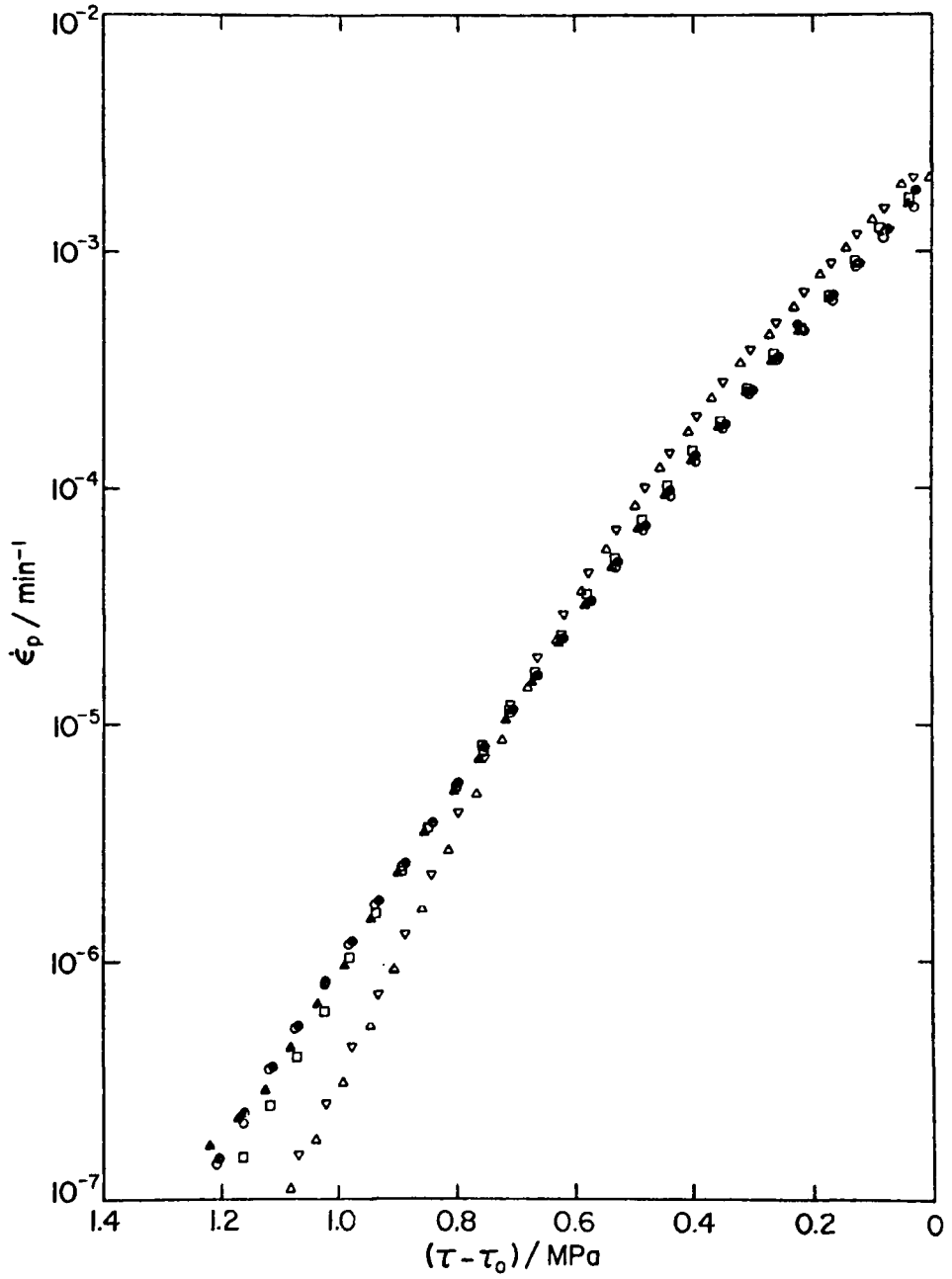

FIGURE 19: Effect of temperature on relaxation behavior. Tests 26.03 (△), 26.05 (▽) at 319 K, 26.06 (□) at 305 K, 26.07 (o) at 294 K, 26.08 (●) at 282 K, and 26.09 (▲) at 274 K.

EFFECT OF MACHINE STIFFNESS

A third group of tests were carried out to determine the effect of machine stiffness on the relaxation behavior of LiF. The tests were made on specimen 33 of the second batch of crystals at about 305 K. The specimen was tested alternatively in the Instron (E' = 10,000 MPa) and in the Hounsfield tensile machine (E' = 2000 MPa). The initial conditions are shown in Table III.

TABLE III

The initial conditions of group III tests.

TEST NO	TEMPERATURE (K)	INITIAL STRAIN (PCT)	TOTAL STRAIN (PCT)	INITIAL SHEAR STRESS (MPA)
33.01*	305	0.13	0.13	7.897
33.02*	305	0.00	0.24	7.897
33.03	305	0.14	0.46	7.446
33.05	305	0.18	0.67	7.387
33.06	305	0.00	0.70	7.409
33.07*	303	0.17	0.90	8.240
33.08*	303	0.00	1.00	7.946
33.09*	303	0.17	1.30	8.314
33.10	306	0.19	1.60	7.933
33.11	306	0.17	1.80	7.949

* Tests carried out in the Hounsfield tensometer.

It appears from Fig. 20 that the softer is the machine, the larger is the experimental activation volume (slope). This effect, however, is weak and difficult to establish. That would require a more accurate method of load measurement than was possible with the Hounsfield tensometer.

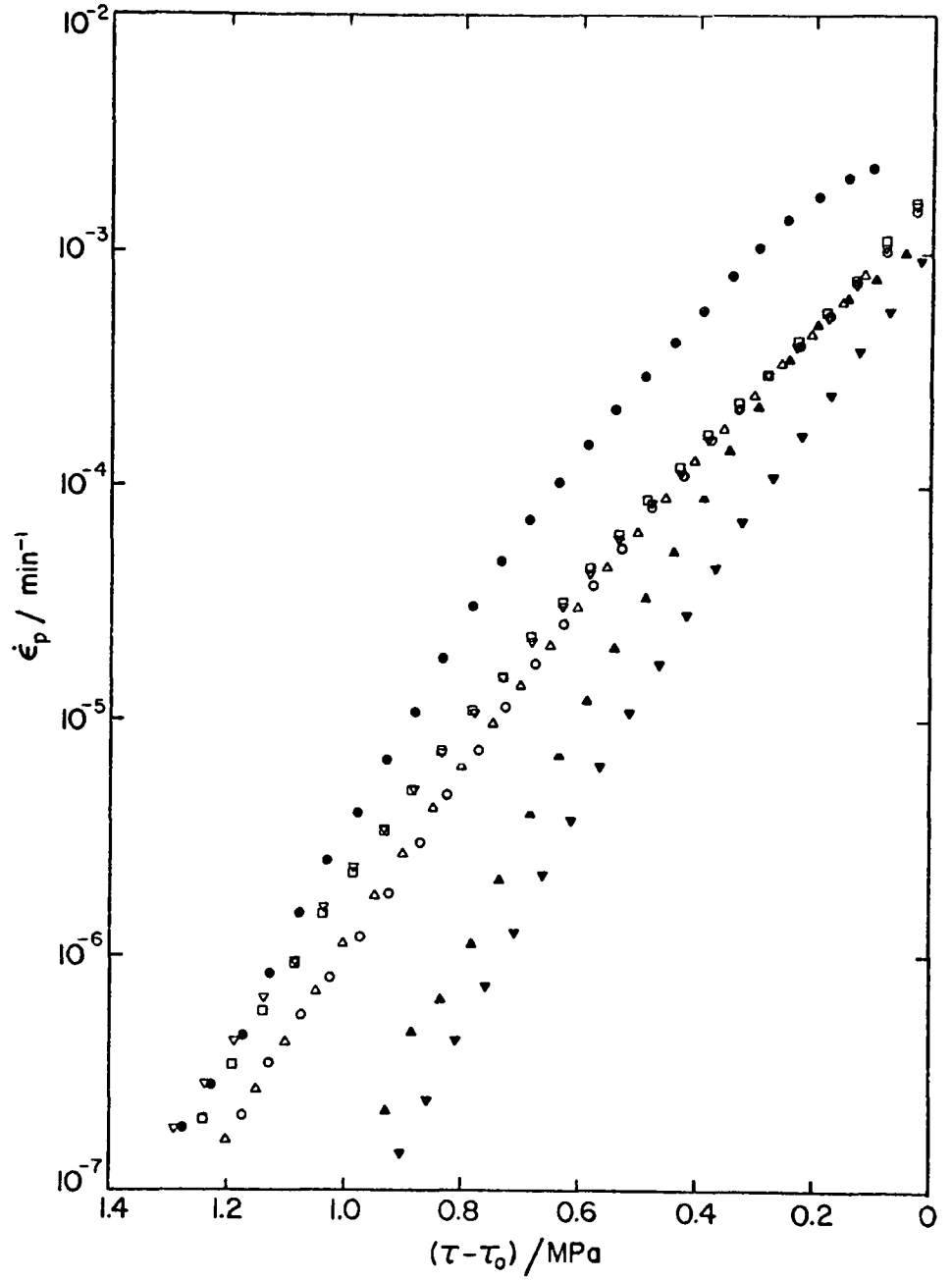

FIGURE 20: Effect of machine stiffness on relaxation behavior. The combined elastic modulus of tests 33.01 (●), 33.07 (▲), and 33.09 (▼), was 2000 MPa. That of tests 33.03 (o), 33.05 (△), 33.10 (▽), and 33.11 (□) was 10,000 MPa.

REPEATED RELAXATION

Most specimens were submitted to repeated relaxation, as indicated in Tables I to III by 0 initial strain. The behavior of the first batch of crystals is shown in Fig. 21. At the beginning of the repeated

relaxation, the strain rate increases as the stress decreases, an unusual behavior. At low strain rates, however, the curves become similar to those obtained in conventional relaxation. In general, this increasing plastic strain rate was not observed in specimens of the second batch of crystals. The exceptions have been noticed at the two extreme testing temperatures: tests 24.01 and 25.03 at 258 K, and tests 26.02 and 26.04 at 319 K.

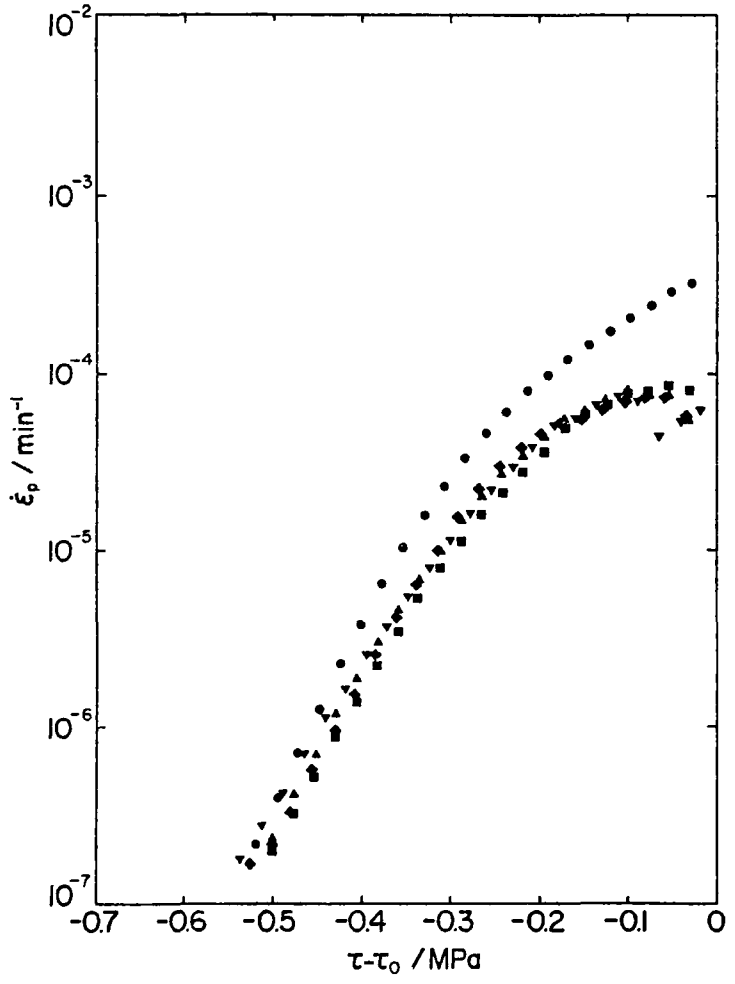

FIGURE 21: Typical behavior observed in repeated relaxation. Tests 4.02 (●), 4.03 (◆), 4.04 (▲), 4.08 (■), and 4.09 (▼), at 302 K.

CHAPTER 3

DISCUSSION

SYSTEMS OF TWO CONSECUTIVE ENERGY BARRIERS

The first step in the identification of the process that governs the plastic flow of a specific material must be the determination of the deformation kinetics. Only then is it possible to relate the energy barriers to particular mechanisms. This study is, accordingly, concerned with the development of deformation kinetics in general, and with the application of these results to the plastic flow of solids. The analysis of the deformation process in LiF gave the impetus to theoretical developments that are of interest for other materials. Some of the conclusions are thus fully general.

The analysis will be guided by two characteristic features of the rate diagrams: the long straight line in the low stress region, and the convex curvature. A straight line in a rate diagram denotes a constant activation volume; it indicates that the Gibbs free energy is a linear function of the stress, and can be expressed, in this range, as

$$\Delta G(\tau) = \Delta G^{\ddagger} - W(\tau) = \Delta G^{\ddagger} - V\tau \qquad (3.1)$$

where $\Delta G^{\ddagger}$ is the value - or the extrapolated value - of $\Delta G(\tau)$ at zero stress. The straight line also implies that the preexponential factor in the rate equation is constant. Deformation kinetics analysis (45,50)

have shown that in case of constant activation volume a convex curvature results either from backward activation at low stress level, or from the motion of dislocations over a system of consecutive energy barriers. Figure 22 demonstrates that the characteristic features of the rate diagrams obtained during conventional relaxation (Figs. 18 and 19) are those of a consecutive system. It is thus appropriate to study the properties of systems of two consecutive energy barriers.

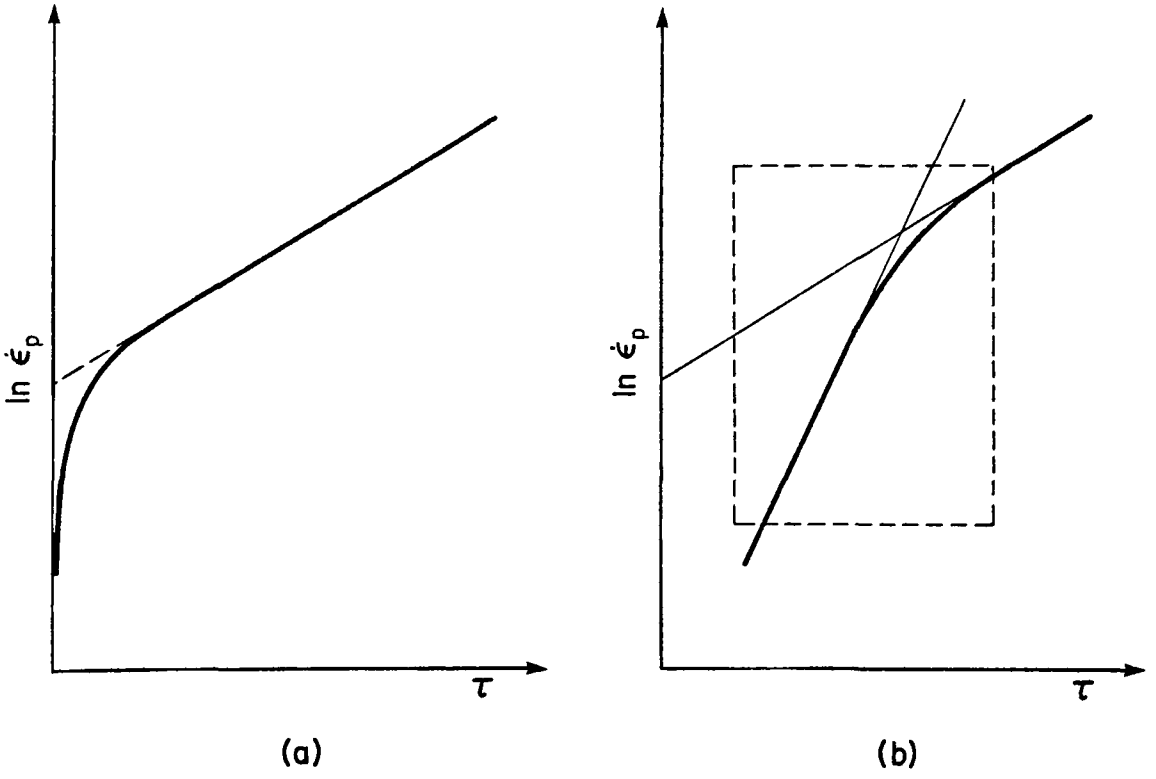

FIGURE 22: Schematic rate diagrams for backward activation over a single energy barrier (a), and activation over a consecutive system (b), in case of constant activation volumes. The results of conventional relaxation are well described by the part of the curve in the dashed rectangle in (b).

3.1 STEADY STATE ANALYSIS OF CONSECUTIVE PROCESSES

3.1.1 PROPERTIES OF THE SYSTEM (73)

A system composed of two consecutive energy barriers is schematically represented in Fig. 7 p. 19, and the associated plastic strain rate is given by Eq. (1.6). In case of linearly stress-dependent Gibbs free energies the plastic strain rate is written as

$$\dot{\varepsilon}_p = \delta\rho_t \frac{kT}{h} \frac{1 - \exp\left[-\left({}_1V^1 + {}_2V^2 + {}^1V_2 + {}^2V_1\right)\tau/kT\right]}{\exp\left(\frac{{}^1\Delta G^1}{kT}\right) + \exp\left(\frac{{}^2\Delta G^2}{kT}\right) + \exp\left(\frac{{}^1\Delta G^2}{kT}\right) + \exp\left(\frac{{}^2\Delta G^1}{kT}\right)} \tag{3.2}$$

where

$${}_i\Delta G^i = {}_i\Delta G^{i\ddagger} - {}_iV^i\,\tau, \quad i = 1,2$$

$${}_1\Delta G^2 = {}_1\Delta G^1 + {}_2\Delta G^2 - {}^1\Delta G_2 = {}^2\Delta G_1{}^{\ddagger} - \left({}_1V^1 + {}_2V^2 + {}^1V_2\right)\tau$$

$${}_2\Delta G^1 = {}^1\Delta G_2{}^{\ddagger} - \left({}_1V^1 + {}_2V^2 + {}^2V_1\right)\tau.$$

The properties of a consecutive system of two energy barriers will be determined from Eq. (3.2) for constant $\delta\rho_t$ (constant structure). An experimental activation energy, ΔG_{exp}, may be defined from the relation

$$\dot{\varepsilon}_p = \delta\rho_t \frac{kT}{h} \exp\left[-\frac{\Delta G_{exp}(\tau)}{kT}\right],$$

that is

$$\Delta G_{exp}(\tau) = -\,kT\,\ell n\left(\frac{\dot{\varepsilon}_p\, h}{\delta\rho_t\, kT}\right)$$

The stress dependence of ΔG_{exp} represents in an essentially temperature independent form the stress dependence of the plastic strain rate. From Eq. (3.2) the experimental activation energy may be written as

$$- \Delta G_{exp} = kT \ln \left\{ \frac{1 - \exp \left[- ({}_1V^1 + {}_2V^2 + {}^1V_2 + {}^2V_1)\, \tau/kT \right]}{\exp \left(\frac{{}_1\Delta G^1}{kT} \right) + \exp \left(\frac{{}_2\Delta G^2}{kT} \right) + \exp \left(\frac{{}_1\Delta G^2}{kT} \right) + \exp \left(\frac{{}_2\Delta G^1}{kT} \right)} \right\} \quad (3.3)$$

This relation is represented in Fig. 23. Because the exponential in the numerator of Eq. (3.3) is much less than 1, it may be neglected except in the low stress range, where the strain rate becomes very small.

In the region where the first term in the denominator, $\exp ({}_1\Delta G^1/kT)$, is much larger than the others, Eq. (3.2) reduces to

$$\dot{\varepsilon}_p = \delta \rho_t \frac{kT}{h} \exp \left(\frac{{}_1\Delta G^1}{kT} \right)$$

from which

$$- \Delta G_{exp} = - {}_1\Delta G^1 = - {}_1\Delta G^{1\ddagger} + {}_1V^1 \tau \ .$$

In the region where the second term, $\exp ({}_2\Delta G^2/kT)$ is much larger

$$- \Delta G_{exp} = - {}_2\Delta G^2 = - {}_2\Delta G^{2\ddagger} + {}_2V^2 \tau \ .$$

These two straight lines intercept at

$$\tau_1^* = \frac{{}_2\Delta G^{2\ddagger} - {}_1\Delta G^{1\ddagger}}{{}_2V^2 - {}_1V^1} \quad \text{and} \quad \Delta G_1^* = \frac{{}_1V^1 \, {}_2\Delta G^{\ddagger 2} - {}_2V^2 \, {}_1\Delta G^{\ddagger 1}}{{}_2V^2 - {}_1V^1}$$

The intercept will be noticed when τ_1^* and ΔG_1^* are positive. In the region where the third term is much larger than the others,

$$- \Delta G_{exp} = - {}_1\Delta G^2 = - {}^2\Delta G_1^{\ddagger} + ({}_1V^1 + {}_2V^2 + {}^1V_2)\, \tau \ .$$

This straight line intercepts the second one at

$$\tau_2^* = \frac{{}^2\Delta G_1^{\ddagger} - {}_2\Delta G^{2\ddagger}}{{}_1V^1 + {}^1V_2}$$

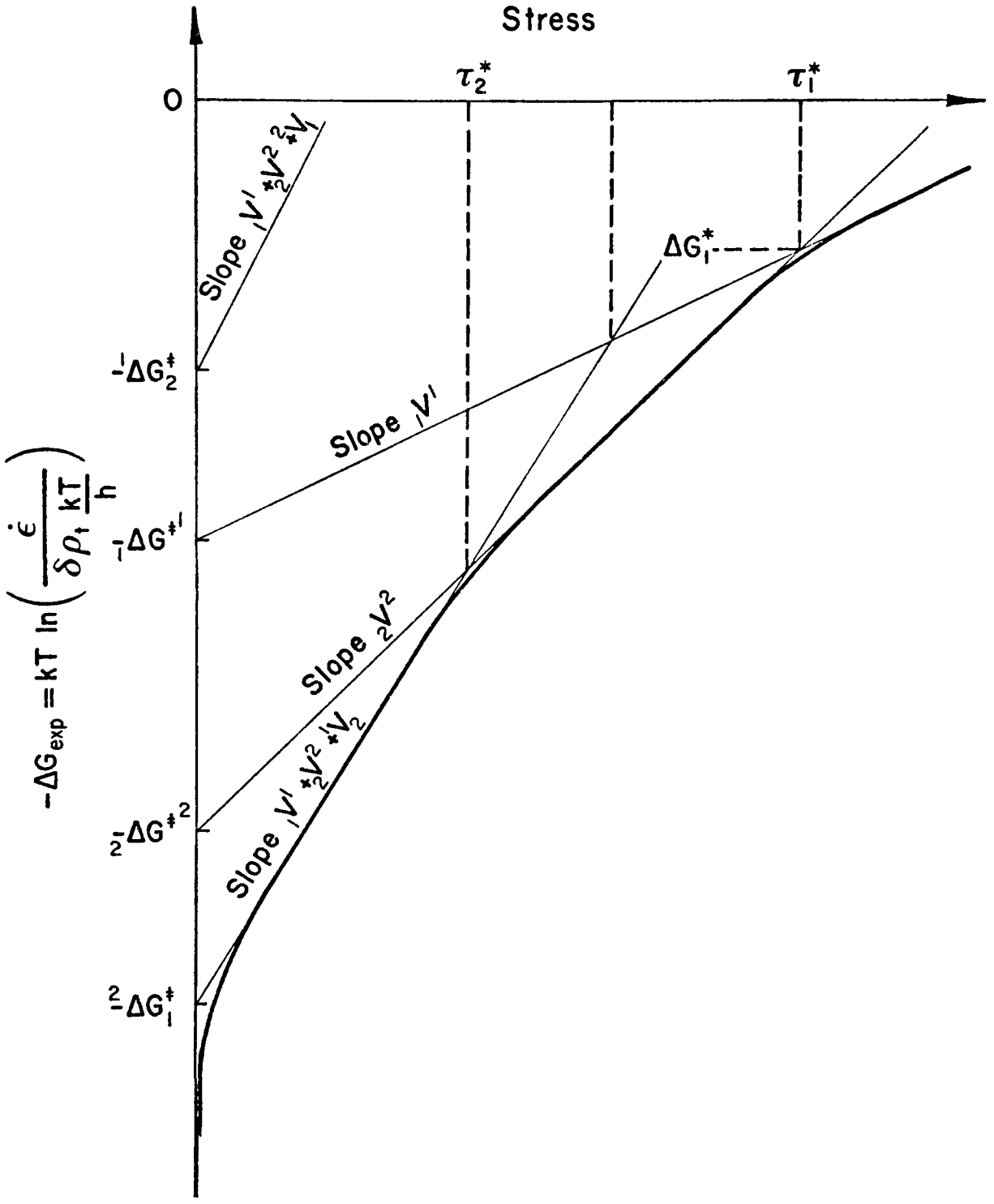

FIGURE 23: Stress dependence of the experimental activation energy for a system of two consecutive energy barriers.

This third term will be effective only when τ_2^* is positive, that is when ${}^2\Delta G_1^{\ddagger}$ is greater than ${}_2\Delta G^{2\ddagger}$. From Eq. (1.7) it follows that ${}^1\Delta G_2^{\ddagger}$ will be smaller than ${}_1\Delta G^{1\ddagger}$ and as a result the fourth straight line corresponding to the fourth term in the denominator of Eq. (3.3) will intercept the previous lines at a negative stress. Therefore, the fourth term cannot have any separate effect on the resultant strain rate.

It also follows from the analysis that when three terms are separately controlling the rate in each of the specific stress ranges, τ_2^* is smaller than τ_1^*. Thus

$$ {}^1V_2 > \frac{({}_2V^2 - {}_1V^1)\ {}^2\Delta G_1^{\ddagger} - ({}_2V^2\ {}_2\Delta G^{2\ddagger} - {}_1V^1\ {}_1\Delta G^{1\ddagger})}{{}_2\Delta G^{2\ddagger} - {}_1\Delta G^{1\ddagger}} . $$

When τ_2^* is larger than τ_1^*, which may be the case when ${}^2\Delta G_1^{\ddagger}$ is large and ${}^1V_2$ small, only the first and third term in the denominator of Eq. 3.2 will have an effect on the strain rate.

The three different possibilities are illustrated in Fig. 24, as well as the corresponding stress dependence of the dislocation density obtained from Eq. (1.5). In case (1) only the first transition at τ_1^* is noticeable. This happens for

$$ {}_i\Delta G^i < {}^j\Delta G_i < {}_j\Delta G^j $$

In case (2) both transitions at τ_1^* and τ_2^* are noticeable. A differentiation is made between (2) and (2') which depends on the nature of the transition at τ_2^*. This difference does not appear in the rate diagrams and comes only from the dislocation density distribution. For a transition from

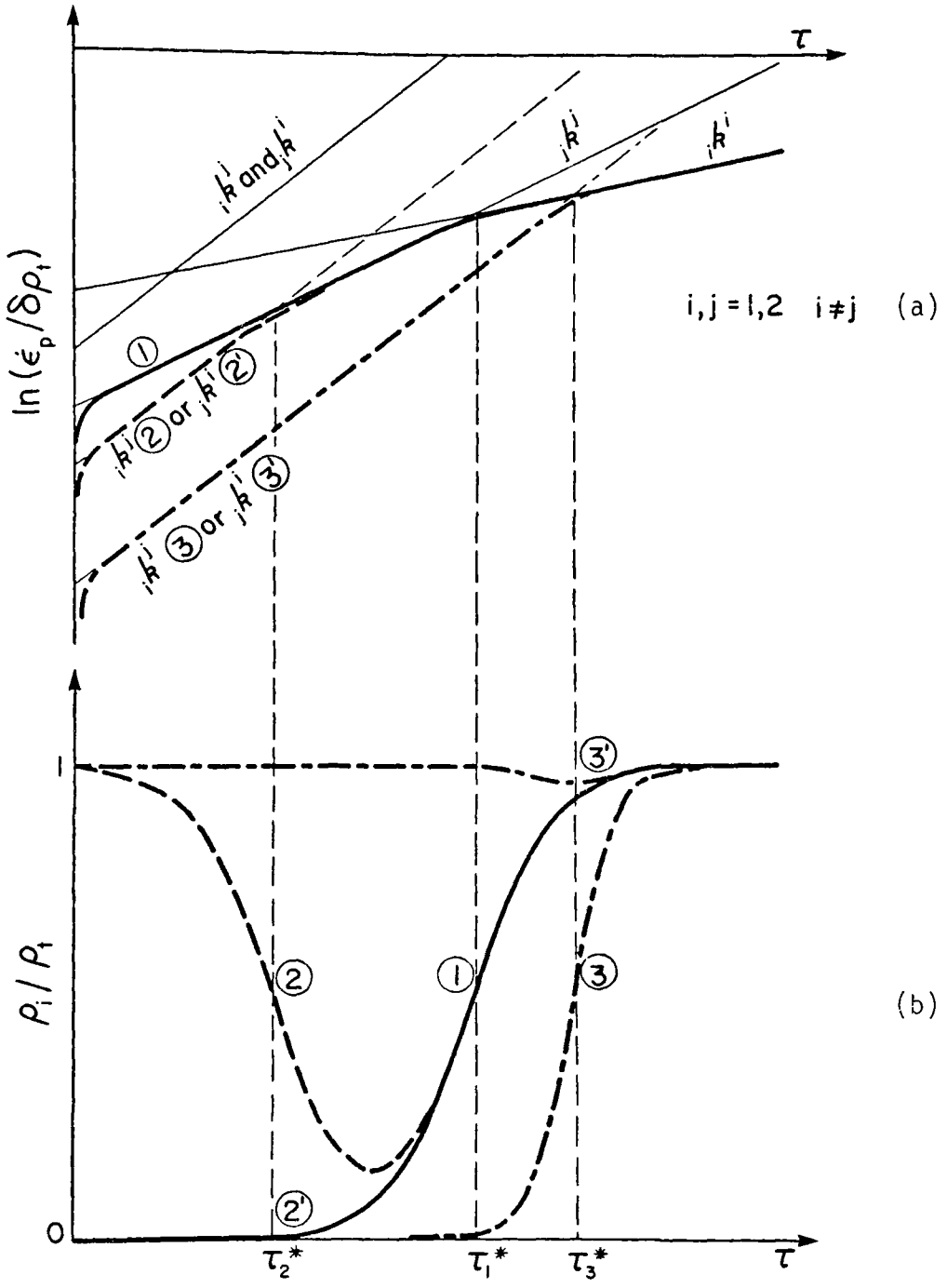

FIGURE 24: (a) The three different rate diagrams for a system of two consecutive energy barriers. The full line corresponds to $\tau_1^* > 0$ and $\tau_2^* < 0$, the dashed line to $\tau_1^* > 0$ and $0 < \tau_2^* < \tau_1^*$, and the broken line with a dot to $\tau_2^* > \tau_1^*$.

(b) The associated dislocation densities.

${}_jk^j$ to ${}_ik^j$, the dislocation distribution changes rapidly at τ_2^* (case ②); for a transition from ${}_jk^j$ to ${}_jk^i$ there is no change in the dislocation distribution (case ②'). Case ③ corresponds to τ_2^* larger than τ_1^*; only the transition at τ_3^* is observed on the rate diagram but again the dislocation distribution introduces a difference similar to the previous one. It is of interest to note that, from an analytical point of view, cases ①, ③, and ③' are identical. The steady state analysis leads to only two types of rate diagrams associated with systems of two consecutive energy barriers: according to the properties of the system considered, the rate diagram will consist of two straight lines and one transition, or three straight lines and two transitions.

It is also of interest to note that while the analysis was presented for systems characterized by linearly stress-dependent activation free energies (Eq. 3.1), the theory can be extended to systems in which

$$\Delta G_i(\tau) = \Delta G_i^{\ddagger} \pm m_i f(\tau) .$$

In this case, the analysis should be developed in function of $f(\tau)$ instead of τ. In particular, when $f(\tau) = \ell n (\tau/\tau_o)$, it can be shown that the stress exponent n, defined from the relation

$$\dot{\varepsilon}_p = \dot{\varepsilon}_o \left(\frac{\sigma}{\sigma_o}\right)^n \exp\left(-\frac{Q}{kT}\right)$$

is related to the various m_i. The analysis is developed in function of $\ell n\ \tau$, and the conclusions are similar to those obtained.

3.1.2 APPLICATION TO EXPERIMENTAL RESULTS

The rate diagram associated with a system of two consecutive energy barriers consists of straight lines connected by transition regions. In general, the plastic strain rate is controlled by two terms in the transition region, and can be expressed as

$$\dot{\varepsilon}_p \simeq \frac{\delta\rho_t}{\frac{1}{k_I} + \frac{1}{k_{II}}} = \frac{\delta\rho_t \frac{kT}{h}}{\exp\left(\frac{\Delta G_I^{\ddagger} - V_I \tau}{kT}\right) + \exp\left(\frac{\Delta G_{II}^{\ddagger} - V_{II} \tau}{kT}\right)} \tag{3.4}$$

This equation has the same form as Eq. (1.4) that is often used to describe consecutive systems. It should be noted, however, that $1/k_I$ and $1/k_{II}$ do not necessarily represent the waiting time in front of each energy barrier; one of them may be a composite term, in case of transitions of type ② or ③.

The transition stress, τ^*, may be defined from the relation

$$k_I = \frac{kT}{h} \exp\left[-\frac{\Delta G_I(\tau^*)}{kT}\right] = k_{II} = \frac{kT}{h} \exp\left[-\frac{\Delta G_{II}(\tau^*)}{kT}\right]$$

that is

$$\Delta G_I^{\ddagger} - V_I \tau^* = \Delta G_{II}^{\ddagger} - V_{II} \tau^* = \Delta G^*$$

hence

$$\tau^* = \frac{\Delta G_I^{\ddagger} - \Delta G_{II}^{\ddagger}}{V_I - V_{II}} \quad \text{and} \quad \Delta G^* = \frac{V_I \Delta G_{II}^{\ddagger} - V_{II} \Delta G_I^{\ddagger}}{V_I - V_{II}} .$$

The plastic strain rate at the transition stress is given by Eq. (3.4) as

$$\dot{\varepsilon}_p(\tau^*) = \frac{1}{2} \delta\rho_t \frac{kT}{h} \exp\left(-\frac{\Delta G^*}{kT}\right) .$$

If $\dot{\varepsilon}^*$ is defined as twice $\dot{\varepsilon}_p(\tau^*)$, that is,

$$\dot{\varepsilon}^* = \delta\rho_t \frac{kT}{h} \exp\left(-\frac{\Delta G^*}{kT}\right) \tag{3.5}$$

then, Eq. (3.4) may be written as

$$\dot{\varepsilon}_p = \frac{\dot{\varepsilon}^*}{\exp\left(V_I \frac{\tau^* - \tau}{kT}\right) + \exp\left(V_{II} \frac{\tau^* - \tau}{kT}\right)} \tag{3.6}$$

This relation is represented in Fig. 25, and shows that the plastic strain rate is fully determined in the transition region by four quantities V_I, V_{II}, τ^*, $\dot{\varepsilon}^*$. Although identical to Eq. (3.4), this later description presents two main advantages:

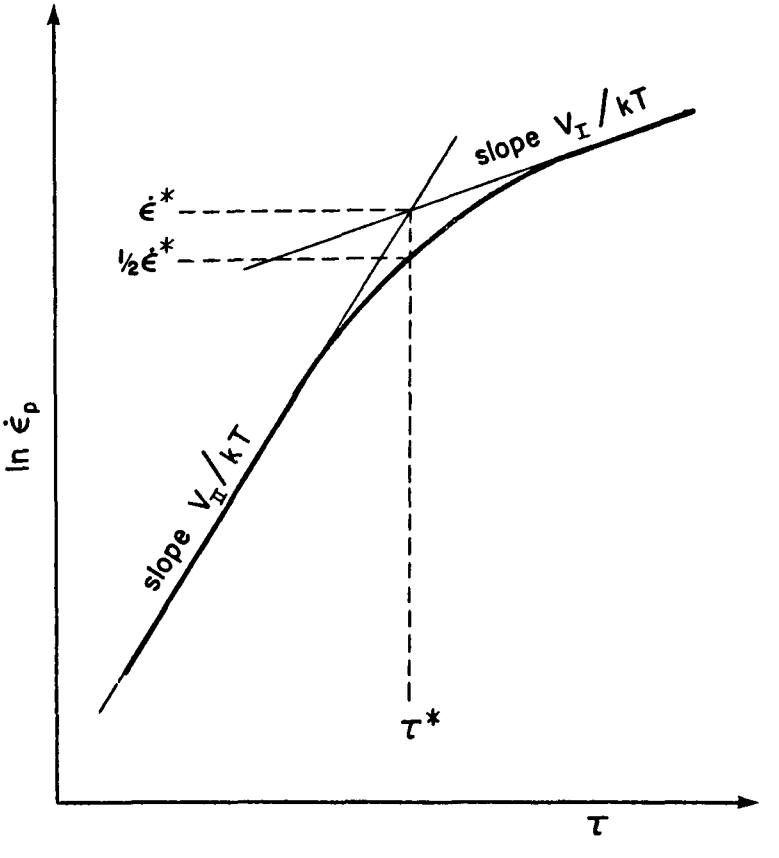

FIGURE 25: Schematic rate diagram at the transition stress.

1) - The analysis is valid for non-linear stress dependence of the activation energies. Both functions $\Delta G_I(\tau)$ and $\Delta G_{II}(\tau)$ may be developed in series with respect to the transition stress:

$$\Delta G(\tau) = \Delta G(\tau^*) + V\,(\tau-\tau^*) + \ldots$$

$$\Delta G(\tau) \simeq \Delta G^* + V\,(\tau-\tau^*)$$

thus Eq. (3.6) is always valid in the vicinity of τ^*.

2) - Of the four quantities defining the plastic strain rate, three are temperature independent: V_I, V_{II}, τ^*. The temperature dependence of $\dot{\varepsilon}^*$ allows the determination of ΔG^*. From Eq. (3.5), the free energy at the transition stress is

$$\Delta G^* = - k \frac{\partial\, \ell n\, (\dot{\varepsilon}^*/T)}{\partial\, 1/T} \tag{3.7}$$

Then, $\Delta G_I^{\ddagger}$ and $\Delta G_{II}^{\ddagger}$ are obtained from

$$\Delta G_{I,II}^{\ddagger} = \Delta G^* + V_{I,II}\,\tau^*. \tag{3.8}$$

The constancy of $V_{I,II}$ may serve to verify the validity of the analysis, and the constancy of τ^* may be useful in providing a reference for the effective stress.

CONVENTIONAL RELAXATION

All conventional relaxation experiments (Appendix B) have been analyzed according to Eq. (3.6). The results, together with the initial conditions, are shown in Tables IV, V, VI for tests of groups 1, 2, 3 respectively. A steepest descent method has been utilized to minimize the subjectivity in the graphical method (66,96,97) used to determine the activation parameters. The activation volumes are given in units

TEST NO	TEMPERATURE (K)	INITIAL STRAIN (PCT)	TOTAL STRAIN (PCT)	INITIAL SHEAR STRESS (MPA)	ACTIVATION VOLUMES (B**3)		TRANSITION SHEAR STRESS (MPA)	TRANSITION STRAIN RATE (/MIN)	DEVIATION (PCT)
2.01	302	0.20	0.20	8.360	1202	3552	8.304	2.83E-03	4.90
2.02	302	0.23	0.47	8.290	2714	4653	7.892	8.75E-06	4.22
2.03	302	0.20	0.70	8.272	1776	3647	8.087	4.43E-04	3.85
2.04	302	0.21	1.00	8.262	2930	5601	7.744	1.32E-06	6.87
4.01	302	0.20	0.20	9.442	850	3106	9.291	1.21E-03	7.84
4.05	302	0.20	0.51	9.397	1778	4157	8.968	9.39E-05	5.35
4.06	302	0.10	0.64	9.262	1471	3649	9.011	2.90E-04	5.69
4.07	302	0.20	0.88	9.213	1411	3475	8.958	3.34E-04	7.67
4.10	302	0.20	1.19	9.170	1874	3803	8.765	3.33E-05	5.96
6.01	302	0.12	0.12	8.730	1303	3654	8.519	6.14E-04	2.48
7.01	302	0.08	0.08	8.955	1439	4318	8.664	2.17E-04	7.33

TEST NO	TEMPERATURE (K)	INITIAL STRAIN (PCT)	TOTAL STRAIN (PCT)	INITIAL SHEAR STRESS (MPA)	ACTIVATION VOLUMES (B**3)		TRANSITION SHEAR STRESS (MPA)	TRANSITION STRAIN RATE (/MIN)	DEVIATION (PCT)
20.01	300	0.07	0.07	8.729	1081	1662	8.314	2.00E-04	4.19
21.01	300	0.06	0.06	8.582	878	1809	8.184	3.86E-04	4.46
21.06	300	0.18	0.43	8.237	1323	2070	7.775	8.70E-05	3.83
21.09	300	0.20	0.78	8.239	1167	1925	8.004	5.85E-04	3.93
21.10	300	0.21	1.05	8.327	1330	1989	7.856	8.07E-05	3.90
21.11	300	0.18	1.28	8.322	1358	1921	8.008	2.90E-04	4.70
21.12	300	0.21	1.53	8.327	1283	1784	8.439	1.32E-02	5.66
22.01	281	0.06	0.06	8.584	774	1178	7.812	6.96E-05	3.99
23.01	281	0.08	0.08	8.450	759	1281	7.412	1.27E-05	3.20
23.03	281	0.10	0.34	8.472	588	1188	8.006	5.03E-04	3.16
23.04	281	0.20	0.63	8.543	862	1659	6.900	4.81E-07	7.96
24.02	258	0.21	0.35	9.347	579	1153	8.332	4.59E-05	2.72
24.04	258	0.17	0.70	9.045	599	1126	8.352	1.31E-04	1.74
24.05	258	0.16	0.92	9.025	639	1153	8.262	8.44E-05	2.21
24.06	258	0.11	1.12	9.118	586	1083	8.542	4.66E-04	1.29
25.01	258	0.07	0.07	11.133	464	1117	10.036	3.09E-05	10.11
25.02	258	0.20	0.38	10.137	609	1394	9.591	2.75E-04	4.31
26.01	319	0.14	0.14	9.082	801	2100	8.538	2.80E-04	6.30
26.03	319	0.19	0.50	8.524	1041	2433	8.000	1.37E-04	3.85
26.05	319	0.19	0.82	8.353	1089	2467	7.783	9.57E-05	3.44
26.06	305	0.12	1.00	7.600	1135	1948	6.908	2.94E-05	3.08
26.07	294	0.17	1.23	7.913	1194	1867	6.985	3.83E-06	2.28
26.08	282	0.20	1.49	8.141	1133	1700	7.294	7.65E-06	2.40
26.09	274	0.20	1.75	8.376	1029	1528	7.805	7.13E-05	5.65
26.09	274	0.20	1.75	8.376	737	1419	8.203	1.36E-03	4.98

TEST NO	TEMPERATURE (K)	INITIAL STRAIN (PCT)	TOTAL STRAIN (PCT)	INITIAL SHEAR STRESS (MPA)	ACTIVATION VOLUMES (B**3)		TRANSITION SHEAR STRESS (MPA)	TRANSITION STRAIN RATE (/MIN)	DEVIATION (PCT)
33.01	305	0.13	0.13	7.897	806	1909	7.300	2.97E-04	5.51
33.03	305	0.14	0.46	7.446	986	1744	6.907	2.03E-05	4.30
33.05	305	0.18	0.67	7.307	1022	1817	6.715	3.73E-05	1.76
33.07	303	0.17	0.90	8.240	466	2070	8.014	7.73E-04	6.34
33.09	304	0.17	1.30	8.314	1247	2108	7.964	1.07E-04	2.41
33.10	306	0.19	1.60	7.933	1100	1817	6.940	4.40E-06	3.24
33.11	306	0.17	1.80	7.949	1136	2151	6.902	2.71E-06	3.00

TABLE IV, V, VI
The analysis of conventional relaxation tests, according to Eq. (3.6).

of cubic Burgers vector (b^3). In lithium fluoride b is $\frac{a}{2}$ [110] and because the side of the fcc unit cell is a = 4.03Å, the value b = 2.85Å was used. The last column presents the standard error of estimate, $\bar{s}$. This is the quantity that was minimized by the steepest descent method, and was defined as

$$\bar{s} = 100 \left\{ \frac{\sum_{i=1}^{n} \left[(\dot{\varepsilon}_{cal} - \dot{\varepsilon}_i)/\dot{\varepsilon}_i \right]^2}{N - 2} \right\}^{\frac{1}{2}}$$

where $\dot{\varepsilon}_i$ are the N experimental strain rate values, and $\dot{\varepsilon}_{cal}$ are the corresponding calculated values. The factor N-2 has been used because the method served to determine V_I and V_{II}. Utilizing the notation

$$A_{1,2} = \dot{\varepsilon}^{*-1} \exp (V_{I,II}\, \tau^*/kT) \qquad (3.9)$$

$$m_{1,2} = V_{I,II}/kT \ ,$$

Eq. (3.6) may be written as

$$\frac{1}{\dot{\varepsilon}_p} = A_1 e^{-m_1\tau} + A_2 e^{-m_2\tau} \ ,$$

Multiplying each side by exp ($m_1\tau$) results in

$$\frac{e^{m_1\tau}}{\dot{\varepsilon}_p} = A_1 + A_2 e^{(m_1-m_2)\tau} \qquad (3.10)$$

For any selected values of V_I and V_{II}, Eq. (3.10) may be read as

$$Y = A_1 + A_2 X \ ,$$

and A_1 and A_2 can be determined from least square fit. Because this least square analysis did not always lead to the smallest value of $\bar{s}$, a second steepest descent method was used for the determination of A_1 and A_2. After the best values - in the least square sense - of V_I and V_{II} were determined, $\dot{\varepsilon}^*$ and τ^* could be calculated from Eqs. (3.9). The activation volumes V_I and V_{II} are shown as the function of temperature in Fig. 26 for all tests. The experimental scatter is partly caused

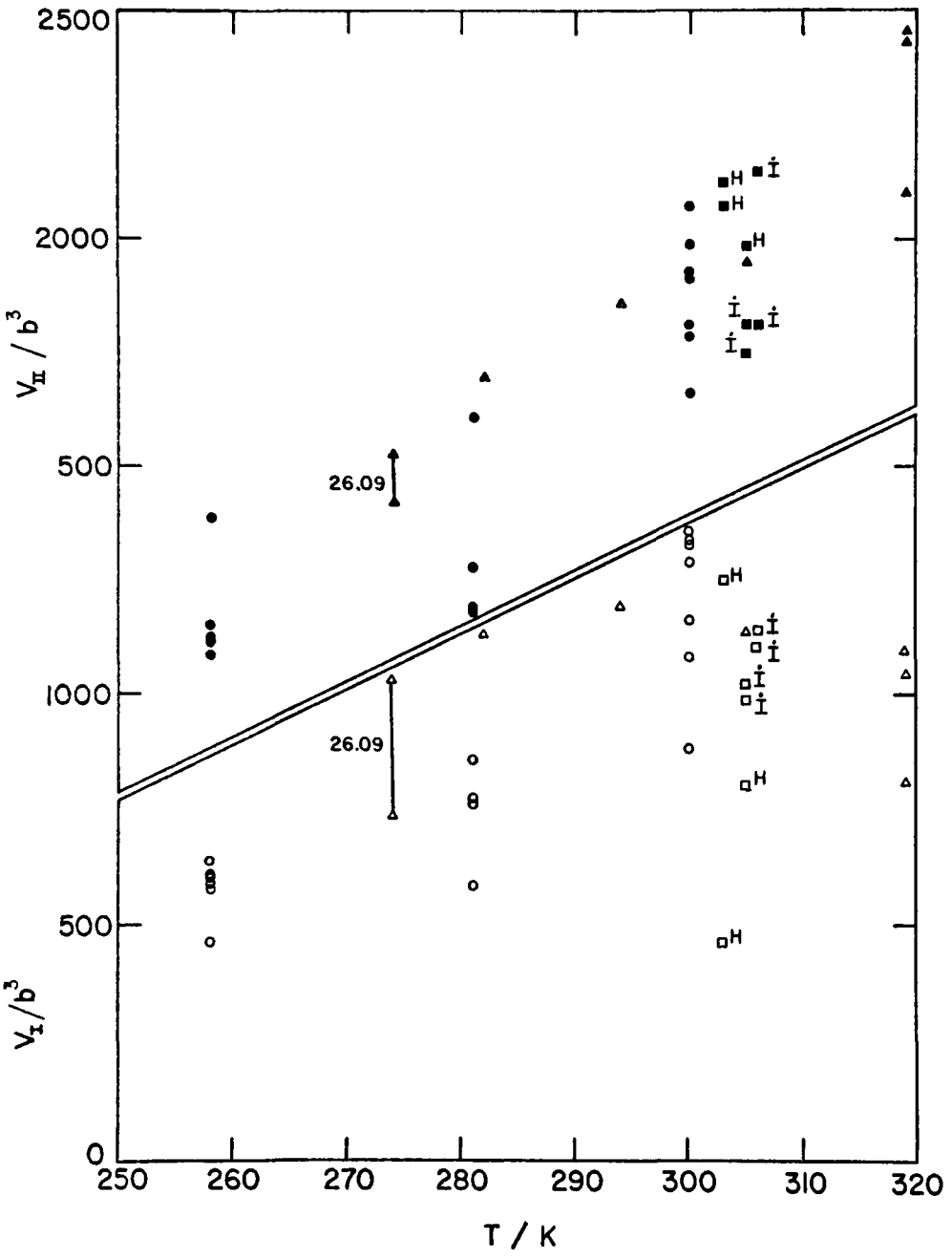

FIGURE 26: Temperature dependence of both activation volumes calculated from the analysis of usual relaxations. Specimens 20 to 25 (O), 26 (Δ), and 33 (□). For specimen 33, the tests were carried out with the Hounsfield (H) and Instron (I) machines. The open symbols are for the high stress range ($\tau > \tau^*$) and the full symbols (high values) are for the low stress range ($\tau < \tau^*$).

by the use of different specimens that have different structure and partly by the inaccuracy that results from fitting a sum of exponential terms to experimental data. Test 26.09 (Fig. 26 and Table IV) illustrates an extreme case to the point: the analysis yielded two minima. Nevertheless, the analysis can provide information on the effect of machine stiffness and temperature.

MACHINE STIFFNESS

Tests on specimen 33 were carried out in either the Instron ($E' = 10{,}000$ MPa) or the Hounsfield testing machine ($E' = 2000$ MPa). The results shown in Figs. 19,25 and Table VI indicate that there is a large scatter in the calculated activation volumes. Furthermore, the precision of load measurement at the beginning of relaxation experiments with the Hounsfield extensometer was poor. Therefore, it can be only concluded that there is no apparent effect of the machine stiffness on the relaxation behavior of LiF.

This conclusion is in agreement with the observation that the specimens did not work-harden (Fig. 16). When the analysis is done in function of the applied stress the calculated activation volume, V_a, is defined as

$$V_a = \frac{\partial \Delta G}{\partial \tau_a}$$

Because the true activation volume, V, is defined as

$$V = \frac{\partial \Delta G}{\partial \tau} \quad ,$$

these two quantities are not equal. During stress relaxation the internal stress changes as (Fig. 27)

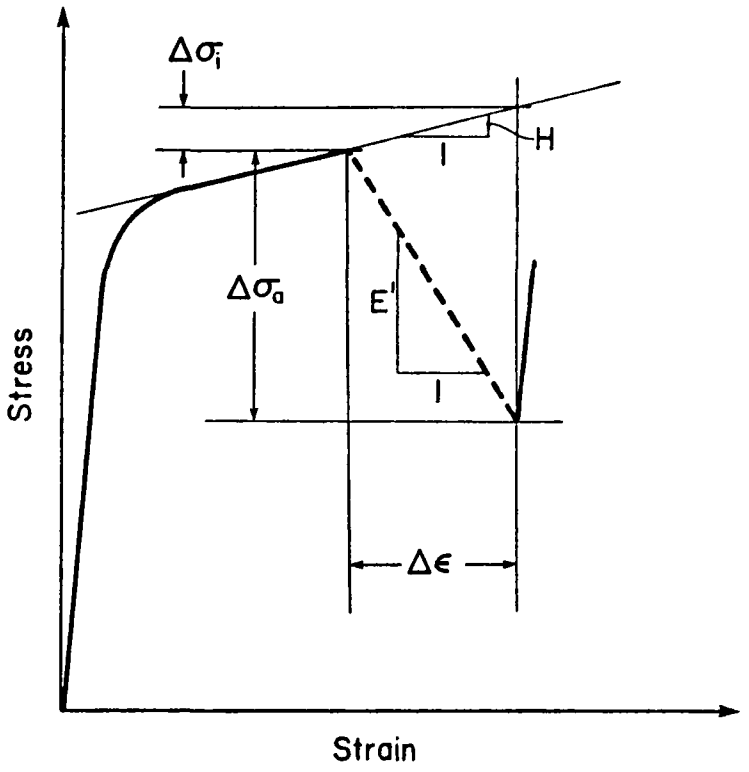

FIGURE 27: Change in internal stress, $\Delta\sigma_i$, during a stress relaxation experiment (98).

$$\Delta\sigma_i = H\ \Delta\varepsilon_p$$

and $$\dot{\sigma}_i = H\ \dot{\varepsilon}_p = -\frac{H}{E'}\ \dot{\sigma}_a .$$

The relation between the measured and true activation volumes is then obtained as

$$V_a = \frac{\partial\ \Delta G}{\partial\ \tau_a} = \frac{\partial\ \Delta G}{\partial \tau}\ \frac{\partial \tau}{\partial \tau_a} = V\ \frac{\partial \tau}{\partial \tau_a} = V\ \frac{\partial \sigma}{\partial \sigma_a}$$

The applied stress is the sum of the internal and effective stress:

$$\sigma_a = \sigma + \sigma_i .$$

Thus

$$\frac{\partial \sigma}{\partial \sigma_a} = \frac{\dot{\sigma}}{\dot{\sigma}_a} = \frac{\dot{\sigma}_a - \dot{\sigma}_i}{\dot{\sigma}_a} = 1 - \frac{\dot{\sigma}_i}{\dot{\sigma}_a}$$

and the relation between measured and true activation volumes becomes

$$V_a = V \left(1 + \frac{H}{E'}\right) .$$

This relation, first derived by Sargent (99), shows that the activation volumes V_a, determined from change of the applied stress must be corrected to take into account the stiffness of the testing machine. However, because E' is large, and H was very small, in the present study $V_a \simeq V$.

Rhode and Nordstrom (100) used this correction for activation volumes determined from stress relaxation. Nevertheless, they found that the activation volume of several metals depends on the stiffness of the testing machine. They claimed that this was a result of dislocation density change. Because the strain rate is

$$\dot{\varepsilon}_p = \delta \rho k,$$

the experimental activation volume, V_{exp}, measured in stress relaxation when ρ changes, is

$$V_{exp} = kT \frac{\partial \ell n \dot{\varepsilon}_p}{\partial \tau} = kT \left(\frac{\partial \ell n \rho}{\partial \tau} + \frac{\partial \ell n k}{\partial \tau}\right)$$

Because the stress rate is proportional to the strain rate during relaxation, V_{exp} can be expressed as

$$V_{exp} = - \frac{kT}{E'} \frac{\partial \ell n \rho}{\partial \varepsilon} \frac{\partial \sigma}{\partial \tau} + V,$$

when only one rate constant controls the deformation. Considering the linear relation $\rho = \rho_o + 10^9 \varepsilon$, established by Gilman and Johnston in LiF (101), the correction factor would be

$$2 \frac{kT}{E'} \frac{\partial \ell n \rho}{\partial \varepsilon} \leq 2 \frac{kT}{E' \varepsilon} \quad .$$

At 305°K, with $E' = 2000$ MPa and $\varepsilon = 0.1\%$ (test 33.01), the correction factor is only 18 b^3. This small correction factor is negligible and proves that it was legitimate to neglect dislocation multiplication in the analysis of the stress relaxation behavior of LiF.

TEMPERATURE EFFECTS

The measured activation volumes seem to increase with temperature. The increase of V_{II}, the activation volume at low stress level, is more pronounced (Fig. 26). It has been shown before (73) that this effect is a general feature of consecutive energy barrier systems, even if the true activation volumes are constant. From Fig. 23 p. 50, it is seen that the measured activation volume, that is the slope of the curve, is a decreasing function of the stress. Furthermore, the stress needed to achieve a fixed strain rate is a decreasing function of the temperature. The activation volume measured at a fixed strain rate is, therefore, an increasing function of the temperature. Because the true activation volumes that are associated with each of the free energies are constant, the temperature dependence of the measured activation volume is only an apparent effect that results from the properties of consecutive energy barrier systems. This observation was considered in the analysis of the results obtained with the single specimen (26) tested at various temperatures. The steepest descent method was changed so that all tests could be analyzed simultaneously with the same activation volumes, and that the sum of the standard errors of estimate be minimum. Test 26.01 was excluded because its large deviation

would have biased the analysis. The results (Table VII) indicate that the behavior of LiF can be well described with two terms in the rate equation for consecutive energy barriers, and temperature independent activation volumes. The use of a third term in the rate equation would yield a better fit. Because the average deviation (last column in Table VII) was already less than 10%, that is of the same order as the error in the measurement of the rates, this was not deemed necessary in the temperature range considered. The activation energy at the transition stress is obtained from the temperature dependence of the transition strain rate. According to Eq. (3.5) p. 54, the least square analysis of the results (Fig. 28) gave the values

$$\Delta G^{*} = 11363\ k = 1.6\ 10^{-19}\ J = 1.0\ eV$$

$$\delta\rho_t = 1.86\ 10^{-4}$$

with a correlation factor of 0.97. The activation energies at zero stress, $\Delta G^{\ddagger}$, may be determined from the equation (Eq. 3.8):

$$\Delta G^{\ddagger}_{I,II} \quad \Delta G^{*} + V_{I,II}\ \tau^{*} = \Delta G^{*} + V_{I,II}\ (\tau^{*}_{a} - \tau_i)$$

The applied transition stress, τ^{*}_{a}, is obtained from Table VII, but the internal stress, τ_i, must be determined for each test since it may be a function of the strain. Some attempts were made to measure the level

TABLE VII

The analysis with temperature independent activation volumes.

TEST NO	TEMPERATURE (K)	INITIAL STRAIN (PCT)	TOTAL STRAIN (PCT)	INITIAL SHEAR STRESS (MPA)	ACTIVATION VOLUMES (BAS)	TRANSITION SHEAR STRESS (MPA)	TRANSITION STRAIN RATE (/MIN)	DEVIATION (PCT)
26.03	319	0.19	2.45	8.524	1273 2572	7.878	4.03E 05	8.88
26.05	319	0.19	4.02	8.353	1273 2572	7.637	3.55E 05	7.21
26.06	305	0.12	4.90	7.600	1273 2572	6.620	2.34E 06	7.53
26.07	294	0.17	6.03	7.913	1273 2572	6.771	5.42E 07	6.34
26.08	282	0.20	7.31	8.141	1273 2572	6.922	2.46E 07	6.11
26.09	274	0.20	8.58	8.376	1273 2572	7.055	9.58E 08	11.13

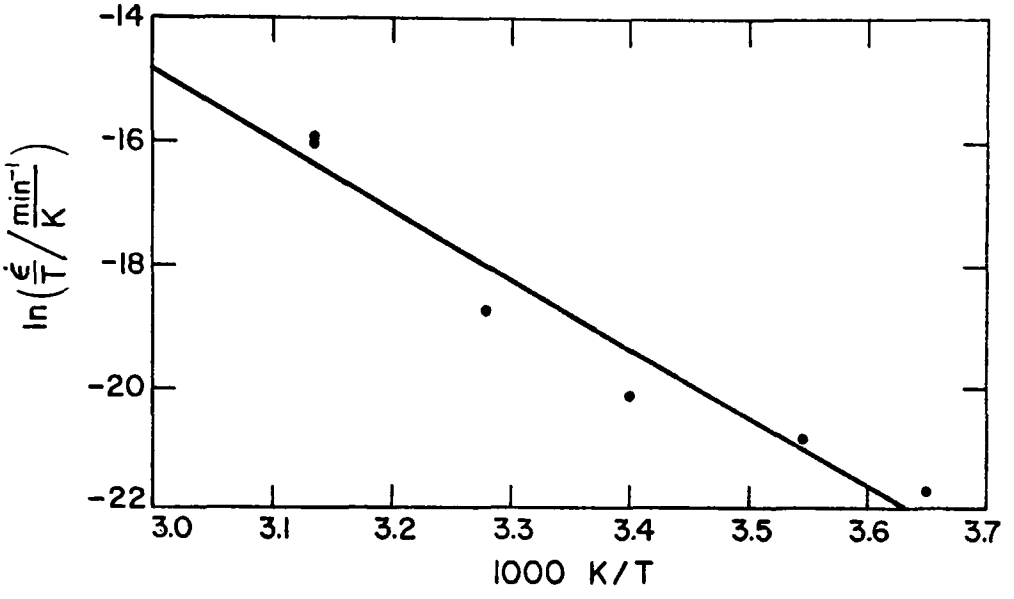

FIGURE 28: Determination of the activation energy at the transition stress for specimen 26.

of internal stress. It was found that the stress range where the plastic strain rate is negligible (that is between $\pm 10^{-7}$ min^{-1}, the limit of sensitivity of the equipment) was too large to yield meaningful results. The effective transition stress was estimated to be

$$\tau^* = (3 \pm 2) \text{ MPa},$$

whence $\Delta G_I^{\ddagger} = (2.5 \pm 0.6) \times 10^{-19}$ J $= 1.5 \pm 0.4$ eV

$\Delta G_{II}^{\ddagger} = (3.4 \pm 1.2) \times 10^{-19}$ J $= 2.1 \pm 0.7$ eV.

The plastic deformation of LiF is then described by the relation

$$\dot{\varepsilon}_p = \frac{2 \times 10^{-4} \; kT/h}{\exp\left(\frac{2.5\times10^{-19} - 2.95\times10^{-26} \times \tau}{kT}\right) + \exp\left(\frac{3.4\times10^{-19} - 5.95\times10^{-26} \times \tau}{kT}\right)} \qquad (3.11)$$

where τ is the effective shear stress in Pascals. This relation is in excellent agreement with the experimental values as shown in Fig. 29.

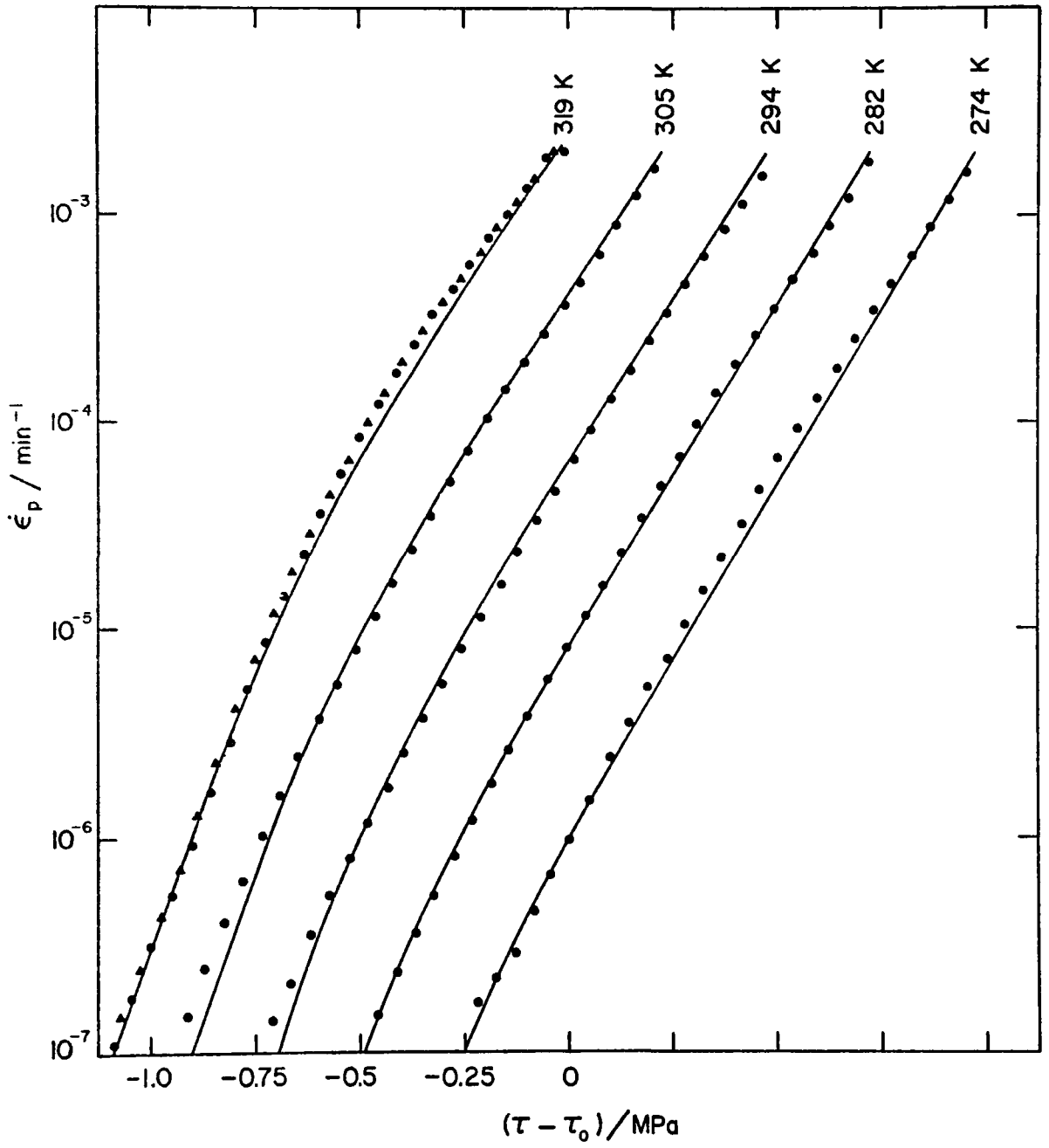

FIGURE 29: Effect of temperature on the relaxation behavior of specimen 26. The symbols represent the experimental values (Appendix B and Fig. 19), and the curves are calculated with Eq. 3.11.

Because of the variation in specimens (see for example specimens 24 and 25, Table V, p. 57), the temperature dependence of the flow stress is difficult to establish. It is, however, possible to use the results of specimen 26 that was tested at various temperatures. Table VII shows that the applied flow stress has a minimum at 305K. Such minimum has been observed by Reppich (108), although at a higher temperature. The applied stress is the sum of the internal stress, which is temperature independent, and of the effective stress which increases as the temperature decreases. Because $\delta\rho_t$ was considered constant, the minimum in the applied flow stress can result only from a decrease in the internal stress as the elongation increases (the low temperature tests were carried out at large strains). Utilizing the fact that the transition stress is temperature independent, it is possible to determine the temperature dependence of the effective flow stress, τ_y, without evaluating the internal stress, τ_i. The applied flow stress, τ_{ya}, measured at the beginning of the relaxation test is

$$\tau_{ya} = \tau_y + \tau_i$$

and the transition stress, τ_a^*, obtained from the analysis of the test, is

$$\tau_a^* = \tau^* + \tau_i$$

The internal stress, τ_i, does not change appreciably during the test; thus the difference of the stresses gives

$$\tau_y - \tau^* = \tau_{ya} - \tau_a^* .$$

Because $d\tau^*/dT = 0$, the temperature dependence of the effective flow stress is

$$\frac{d\,\tau_y}{dT} = \frac{d\,(\tau_y - \tau^*)}{dT} = \frac{d}{dT}\,(\tau_{ya} - \tau_a^*) .$$

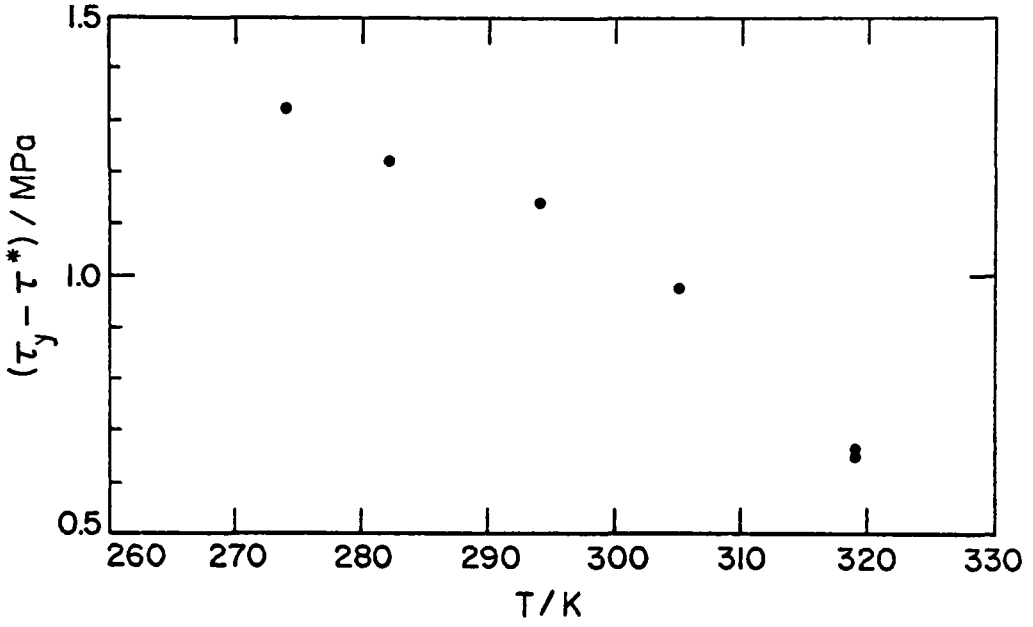

FIGURE 30: Temperature dependence of the effective flow stress (the effective transition stress, τ^*, is temperature independent).

The results, obtained from the data listed in Table VII, are shown in Fig. 30.

DEFORMATION OF LITHIUM FLUORIDE

Since the work of Gilman and Johnston (101) it is well established that single crystals of LiF deform by slip on {110} planes in the <1T0> direction. For axially loaded specimen, slip may start on any of the four {110} planes shown in Fig. 31, and deformation develops by the broadening of glide bands parallel to these planes (101-103).

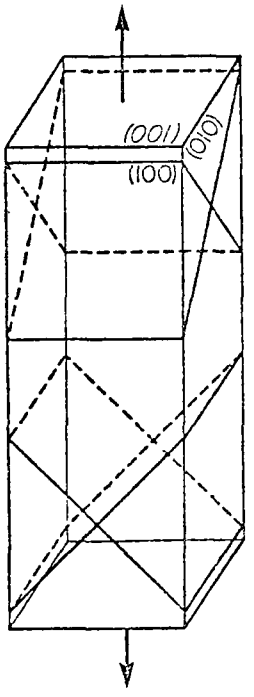

FIGURE 31: The four possible slip planes for rocksalt structure single crystals stressed along [001] direction.

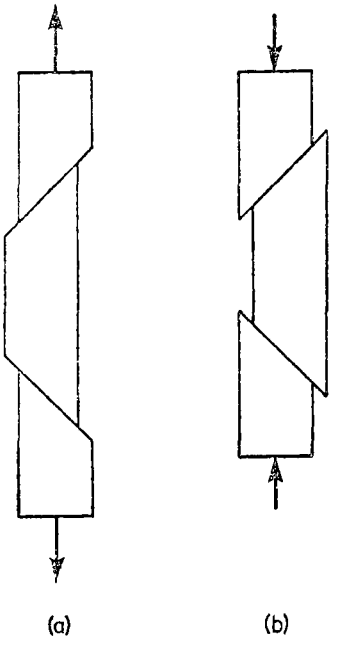

FIGURE 32: The effect of the grips in axial loading under tension (a), and compression (b).

In most tensile machines the deformation of the specimen must accommodate the displacement of the grips, so that the ends remain aligned, as illustrated in Fig. 32. This effect creates a parasitic stress, that is proportional to the square of the ratio w/ℓ between the width, w, and the length, ℓ, of the specimen (102). Even the most recent studies on the flow properties of pure lithium fluoride (103-104), doped with Mg^{++} (105-108), or irradiated (109) were made in compression with a ratio of ℓ/w between 2.5 and 3. The present experiments were carried out in tension with a ratio ℓ/w of 8. Although it has been shown (103) that the critical resolved shear stress and the work-hardening coefficient do not change appreciably with the ratio ℓ/w when it is larger than 2.4, the use of a larger ratio certainly minimizes the end effect and yields more dependable results. Contrary to the tests carried out in compression (103-108), there is no work-hardening in tension (Fig. 16, and Tables IV-VI). This absence of work-hardening - up to 2% strain - may be due to end effects, or geometric effects, or to differences in crystals. In fact the crystals utilized had a yield stress of about one order of magnitude larger than the usual pure crystals (103-109). Because it is necessary to irradiate LiF pure single crystals to be able to cleave them, the high yield stress could correspond to an incompletely annealed specimen (110). This is substantiated by the pale yellowish coloration of the crystals.

The increase in the flow stress of LiF due to the presence of Mg^{2+} impurities has been attributed by Fleischer (111) to the interaction of dislocations with tetragonal distortions produced by Mg^{2+}—vacancy

dipoles. This theory was refined by Gibbs (112) and Barnett and Nix (113), and has been applied successfully to the temperature dependence of the flow stress of LiF (104, 105, 107-109). Deviations from the theory have been found to be significant at about 200K (105). More recently, Fotedar and Stoebe (104) arrived to the conclusion that in pure LiF Fleischer's mechanism was probably rate controlling in the temperature range of 196-250K. They concluded that at higher temperatures several rate controlling mechanisms are present, although without identifying them. Reppich (108) found that Fleischer's mechanism was operating at temperatures below 200°C and that at higher temperatures other mechanisms were rate controlling. These observations are in excellent agreement with the present analysis which, even though it is not complete, has shown that two consecutive energy barriers are rate controlling in the temperature range of 260-320K. A more detailed analysis would require to carry out a larger number of tests, temperature change tests and to take into account the temperature dependence of the elastic modulus. The activation energies that were determined in this analysis are, however, comparable to the values already published for pure crystals (Table VIII). Activation volumes as low as $300b^3$ (105, 107) and higher than $2500b^3$ (104, 105) have been determined in the temperature range of 77-400K. These values may be compared to the calculated values of 1300 and $2600b^3$, but it has been observed that they may change drastically from crystal to crystal as can be seen, for example, by comparing Tables IV and V.

TABLE VIII

Activation energies for plastic flow of lithium fluoride

Investigators	ΔG/eV
Fotedar and Stoebe (104)	1.1 to 1.5
Gaiduchenya et al. (105)	2.0
Guiu and Langdon (107)	1.2
Cagnon (109)	1.33. Increasing up to 2.25 by irradiation
Present study	1.5 and 2.1

Mechanisms may be associated with the consecutive energy barriers that control the plastic deformation of LiF. At small strain level, LiF deforms by slip band broadening (101-103, 114), that occurs by double cross-slip. Dislocation dipoles produced by double cross-slip harden the slip plane and prevent dislocation movement within the band. Only the dislocations at the side of the band can move (114, 115). The mobile dislocation density, therefore, remains unchanged as long as the number of glide bands is constant. The first energy barrier of the consecutive system may be associated with the broadening of the glide bands by the double cross-slip mechanism (or other), and the second energy barrier may be associated with obstacles to dislocation motion. The general softening that results from straining may be caused by an increase in the number of slip bands. A more detailed and definitive study would be outside of the scope of this report.

3.2 NON-STEADY STATE ANALYSIS

The results obtained in repeated relaxation can not be explained with the preceding analysis. The increasing, or sometimes constant, strain rate noticed at the beginning of the repeated test is clearly associated with the yield drop observed in reloading (Fig. 16). Such yield drops, that occur after a relaxation period, have been noticed before in LiF (106). It has been proposed that they are the consequence of strain ageing, more specifically, that the dislocations are weakly pinned by tetragonal strain fields around impurity - vacancy dipoles. This explanation is similar to the Cottrell theory (116) - the breakaway of dislocations from their impurity clouds - that accounts for yield drops in steel. The other cause of yield drop, dislocation multiplication, has been proposed by Johnston (117), to explain the behavior of LiF during constant strain rate tests. Both explanations of yield drop would also be capable of describing the behavior in repeated relaxation. It will be shown, however, that there is no need to resort to any of these mechanisms; yield drops as well as a maximum in repeated relaxation are the direct consequence of the properties of consecutive energy barrier systems.

The steady state proportion of dislocations waiting in front of one of the two consecutive energy barriers is shown schematically as a function of stress in Fig. 33. When, during an experiment, the stress changes from τ_1 to τ_2, the dislocations, that were waiting in front of the second energy barrier at τ_1, will be redistributed so that they will

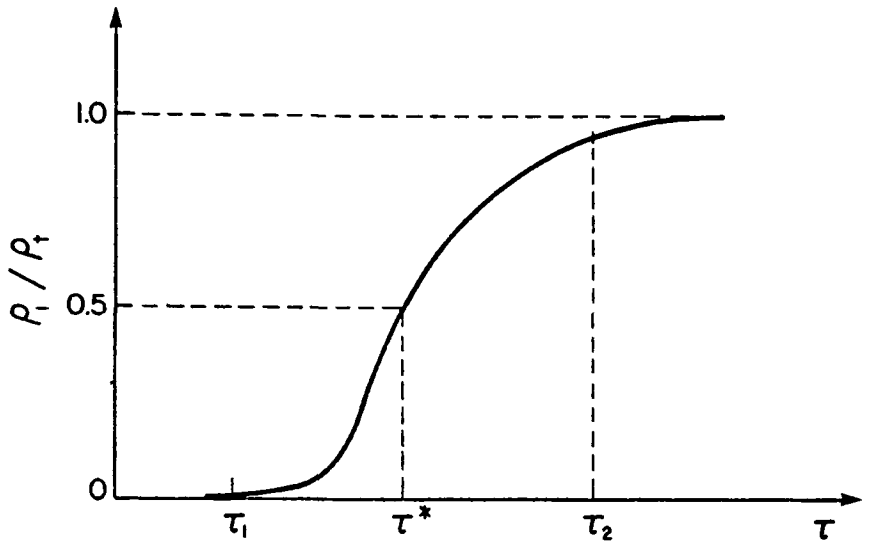

FIGURE 33: Schematic stress dependence of the ratio of dislocations waiting in front of barrier 1, in steady state.

be waiting in front of the first energy barrier at τ_2. The redistribution occurs by non-steady state flow. The associated effects will depend on the amount of redistribution, that is on the values of τ_1 and τ_2 with respect to the transition stress and the type of transition (For types (2') and (3') in Fig. 24b, p. 52 there is no redistribution), and on the time required for the redistribution. This time, which depends on the rate constants, was always assumed to be negligible in consecutive energy barrier system studies (45, 49, 58, 66, 73). The validity of this assumption will be re-investigated following the derivation of the non-steady state kinetics. The results will then be applied successfully to the description of yield drop and repeated relaxation.

3.2.1 NON-STEADY STATE KINETICS (118)

Similarly to paragraph 1.1.3, the net flow of dislocations over each of the two consecutive energy barriers (Fig. 7, p. 19) is described as

$$F_1 = \rho_1 \, {}_1k^1 - \rho_2 \, {}^1k_2 \tag{3.12.a}$$

$$F_2 = \rho_2 \, {}_2k^2 - \rho_1 \, {}^2k_1 \tag{3.12.b}$$

where the k's are functions of stress and temperature. When dislocation multiplication may be neglected, the rate of dislocation density change is simply the difference between the flow in and the flow out:

$$\dot{\rho}_1 = F_2 - F_1 = - \dot{\rho}_2 \tag{3.13}$$

The plastic strain rate resulting from these flows is given by the relation:

$$\dot{\varepsilon}_p = \delta_1 \, F_1 + \delta_2 \, F_2 \tag{3.14}$$

where δ_i is the strain produced by activation over the i-th barrier. The non-steady state behavior is fully described by Eqs. (3.13) and (3.14), and the flows are obtained from Eqs. (3.12). The solution of the system of differential equations (3.13) and (3.14) requires an additional relation between the stress rate and the strain rate. This relation depends on the testing condition.

The importance of the non-steady state effects, and therefore the limit of validity of the steady state analysis, will be demonstrated for constant effective stress. For this condition, that may be achieved during a constant rate test, the individual activation rates in Eqs. (3.12) are constant. The dislocation density change is obtained from Eqs. (3.12) and (3.13) as

$$\dot{\rho}_2 = F_1 - F_2 = \rho_1 \, {}_1k^1 - \rho_2 \, {}^1k_2 - \rho_2 \, {}_2k^2 + \rho_1 \, {}^2k_1 \, .$$

The total number of dislocations, ρ_t, is

$$\rho_t = \rho_1 + \rho_2$$

thus

$$\dot{\rho}_2 = \rho_t \, ({}_1k^1 + {}^2k_1) - \rho_2 \, \Sigma k \tag{3.15}$$

where $\Sigma k = {}_1k^1 + {}_2k^2 + {}^1k_2 + {}^2k_1$.

For constant stress condition, the solution of Eq. (3.15) is expressed as a function of time, t, as

$$\rho_2 = \rho_2^{ss} + (\rho_2^o - \rho_2^{ss}) \, e^{-(\Sigma k) \, t} \tag{3.16}$$

where ρ_2^o is the initial dislocation density and ρ_2^{ss} is defined as

$$\rho_2^{ss} = \rho_t \, ({}_1k^1 + {}^2k_1)/\Sigma k.$$

The steady state dislocation density, ρ_2^{ss}, can be obtained by taking $\dot{\rho}_2 = 0$ in Eq. (3.15), that is when $F_1 = F_2$. The non-steady state solution at constant stress (Eq. 3.16), illustrated in Fig. 34, shows that ρ_2 approaches its steady state value, ρ_2^{ss}, exponentially with a relaxation time equal to $1/\Sigma k$. The sum of exponential terms, Σk, can be estimated by considering the rate constant with the largest value, that is, the k that corresponds to the lowest energy barrier. At 300K, for example, 90% of the redistribution occurs in 0.09 ms when the smallest energy barrier is 0.5 eV, in 0.2 s when it is 0.7 eV, but in 8 min when it is 0.9 eV.

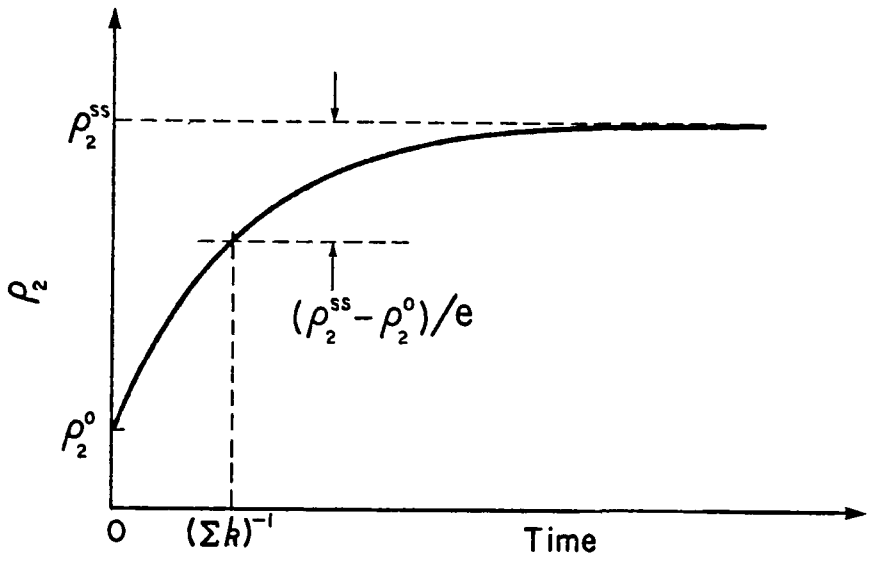

FIGURE 34: Schematic time dependence of the dislocation density at constant stress.

In general the stress is a function of time, and ρ_2^{ss} is a quasi-steady state value that is time dependent through its stress dependence. The quasi-steady state approximation is valid only if the rate of dislocation density change can follow the stress rate. If the stress rate is "too large", the system is in non-steady state, and its response is described by Eqs. (3.13) and (3.14). Steady state analysis is also a good approximation for studies of type (2') and (3') transitions that are associated with small dislocation redistribution.

3.2.2 YIELD POINT BEHAVIOR (118)

Yield drops are observed when specimens are tested in a hard machine at constant crosshead velocity. At the beginning of the test, that is for small strain, the relation between plastic strain rate and stress rate is given by Eq. (1.9). Neglecting the work hardening, this relation is written as

$$\dot{\sigma} = E' (S - \dot{\varepsilon}_p).$$

Equations (3.13) and (3.14), that describe the behavior of a system of two consecutive energy barriers, become

$$\dot{y} = {}_1k^1 + {}^2k_1 - y \Sigma k \tag{3.17}$$

$$\dot{\sigma} = E' \{S-\delta\rho_t [\eta (1-y) {}_1k^1 + (1-\eta)y {}_2k^2 - \eta y {}^1k_2 - (1-\eta)(1-y) {}^2k_1]\} \tag{3.18}$$

where the following notations were used:

$$y = \rho_2/\rho_t \quad , \quad \delta = \delta_1 + \delta_2 \quad , \quad \eta = \delta_1/\delta.$$

For illustration purposes the numerical solutions shown in Figs. 35 to 38 have been obtained for a system of symmetrical energy barriers associated with Ge. The activation parameters were found to be (73)
${}_1(\Delta G^{\ddagger})^1 = {}^2(\Delta G^{\ddagger})_1 = 3.6\ 10^{-19}$ J, ${}_2(\Delta G^{\ddagger})^2 = {}^1(\Delta G^{\ddagger})_2 = 2.9\ 10^{-19}$ J,
${}_1W^1 = {}^2W_1 = V_1\ \tau$, ${}_2W^2 = {}^1W_2 = V_2\ \tau$, $V_1 = 6500$ Å^3, $V_2 = 393$ Å^3.
To represent the condition that most of the contribution to the strain is produced after activation over the second energy barrier, the parameter η was chosen to be equal to 0.01. The initial values were:

$$\sigma\ (t = 0) = 0$$

$$y\ (t = 0) = \rho_2^{ss}\ (\sigma = 0)/\rho_t.$$

The calculations were stopped when the plastic strain rate was close to the crosshead velocity and, simultaneously, the stress close to its corresponding steady state value. The results are shown for a wide range of values for each parameter. Figure 35 shows that at low crosshead velocity, the steady state stress is small and no yield drop occurs. As the crosshead velocity increases, the steady state stress increases and the yield drop becomes more pronounced with oscillations around the steady state value. At high crosshead velocity, however, when the steady state stress is large, the yield drop disappears. As expected, the effect of decreasing temperature (Fig. 36) is identical to the effect of increasing crosshead velocity. Figure 37 shows that a soft machine, that is, the effect of small combined elastic modulus also causes the yield drop to disappear. As shown in Fig. 38, the effect of decreasing the product $\delta\rho_t$ is identical to increasing the crosshead velocity.

Non-steady state behavior is controlled by two factors: the amount of dislocation redistribution associated with a given stress change and the relaxation time $(\Sigma k)^{-1}$ that controls the rate of redistribution. Figure 39 shows that the extent of redistribution is small at low stress level, increases very rapidly as the stress increases, and levels off at high stress level. Figure 40 shows that the relaxation time is almost constant until the transition stress is reached, then decreases very rapidly as the stress increases. Non-steady state effects are important when the amount of dislocation redistribution is large or when the relaxation time is long. Because these two factors change in opposite directions when the steady state stress level increases, the amplitude of the yield drop goes through a maximum, at about the transition stress.

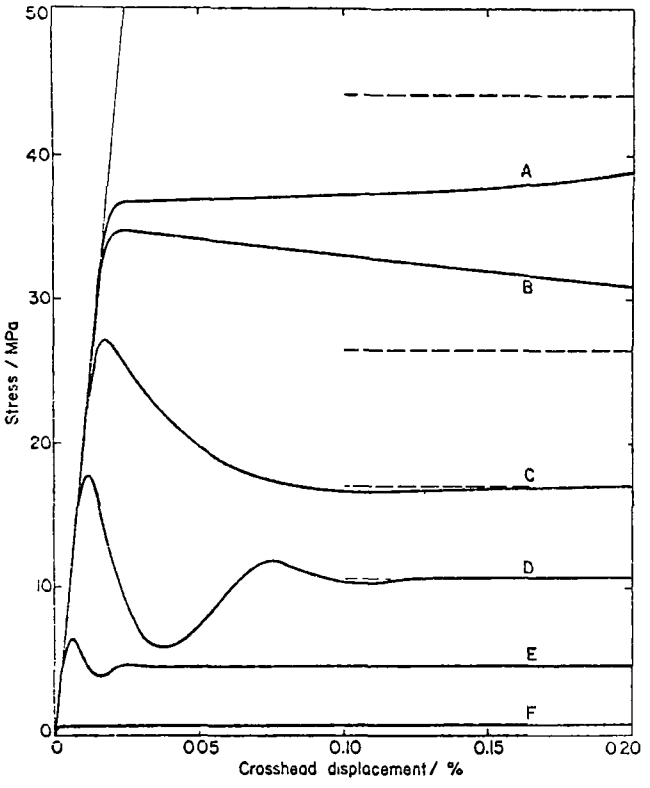

FIGURE 35

Calculated yield behavior as a function of strain rate. The activation parameters are those of Ge. $E' = 200$ GPa; $T = 650$ K; $\delta\rho_t = 0.1$; S (from A to F) = 2, 1, 10^{-1}, 10^{-2}, 10^{-4} min^{-1}.

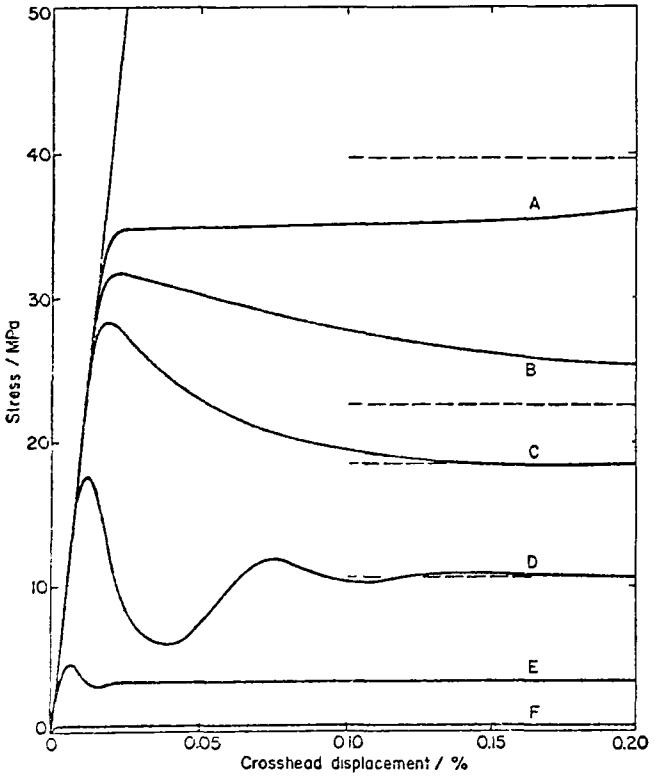

FIGURE 36

Calculated yield behavior as a function of temperature. Parameters as in Fig. 35; $S = 10^{-2}$ min^{-1}; T (from A to F) = 560, 580, 600, 650, 700, 750 K.

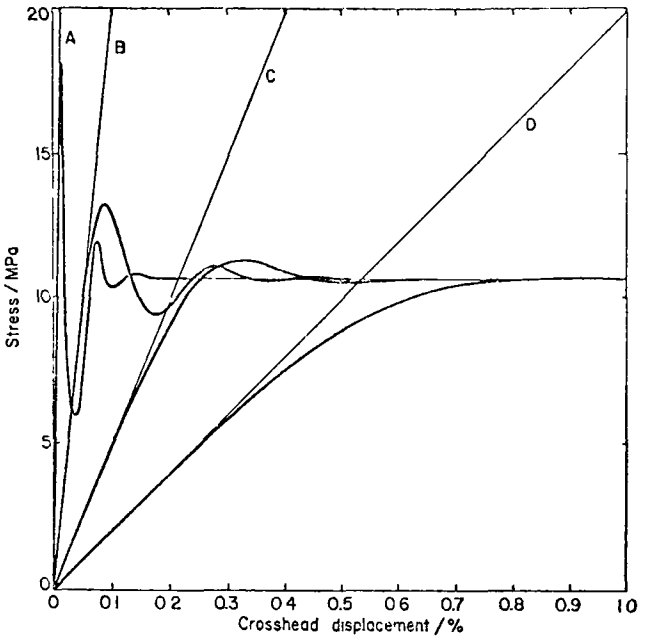

FIGURE 37: Calculated yield behavior as a function of machine stiffness. Parameters as in Fig. 35; $S = 10^{-2}$ min^{-1}; E' (from A to D) = 200, 20, 5, 2 GPa.

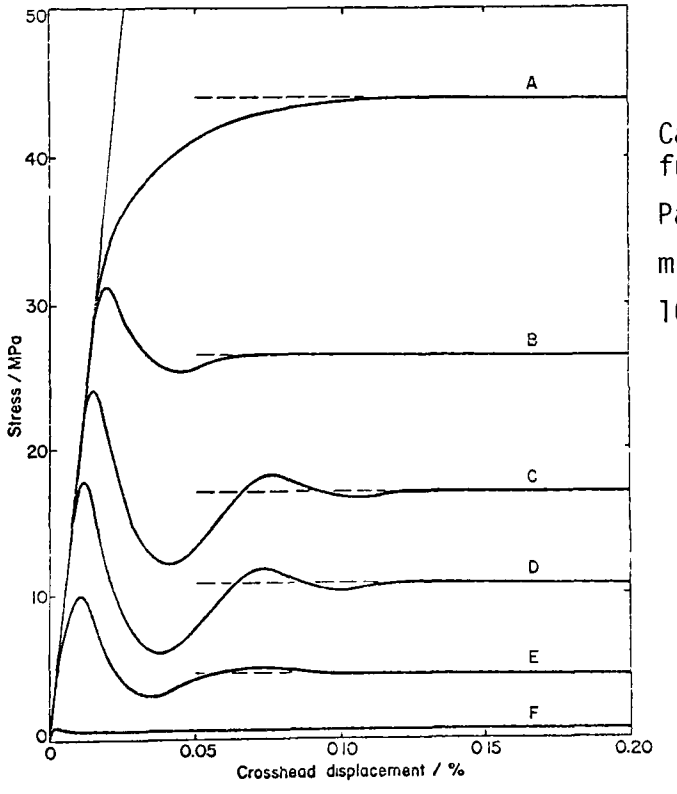

FIGURE 38

Calculated yield behavior as a function of the product $\delta\rho_t$. Parameters as in Fig. 35; $S = 10^{-2}$ min^{-1}; $\delta\rho_t$ (from A to F) = 5×10^{-4}, 10^{-3}, 10^{-2}, 10^{-1}, 1, 10.

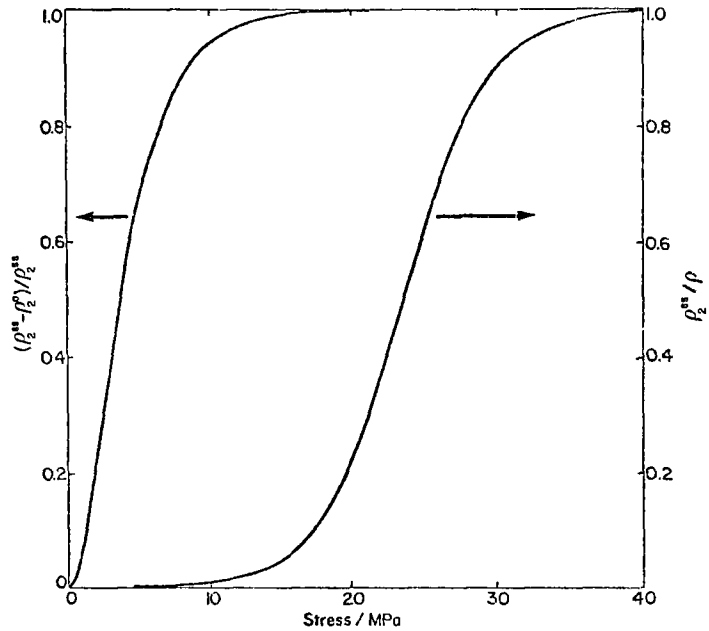

FIGURE 39: Stress dependence of the steady state dislocation density at 650 K.

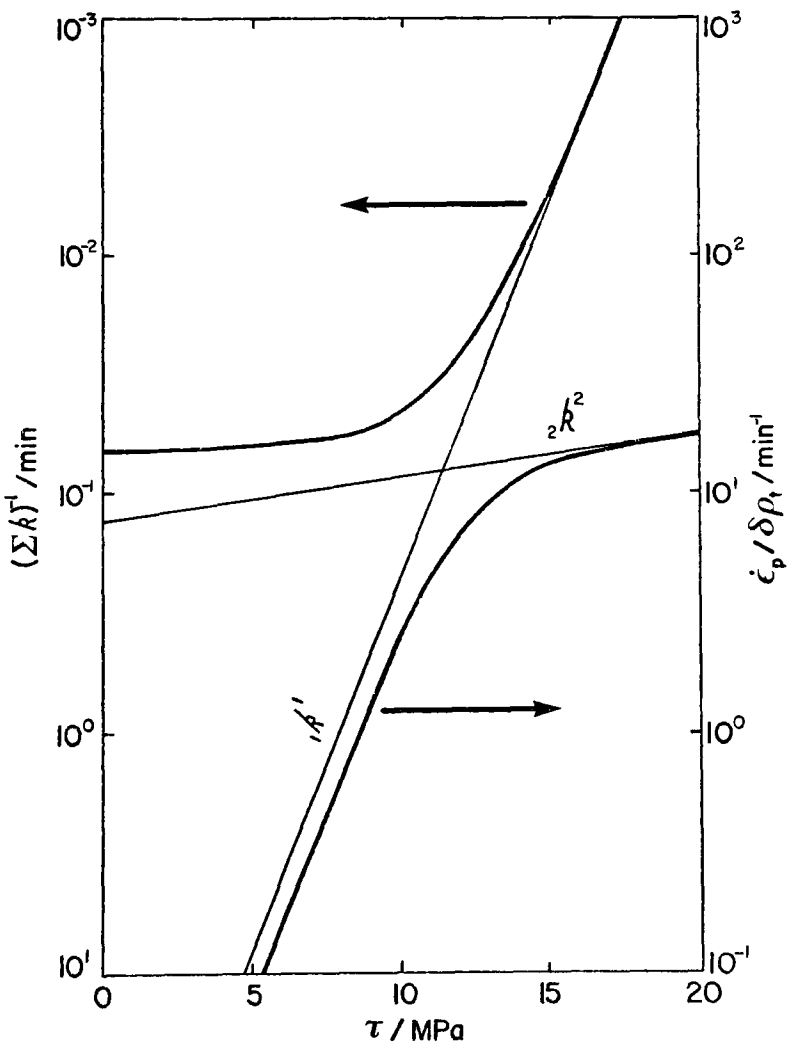

FIGURE 40: Shear stress dependence of the steady state strain rate and of the relaxation time at 650 K. The shear stress τ has been considered to be equal to one half of the normal stress.

3.2.3 REPEATED RELAXATION (119)

In a stress relaxation experiment, the stress is decreasing continuously, and consequently, in consecutive systems of energy barriers, dislocation redistribution occurs that may lead to non-steady state effects. These effects can be analyzed with Eqs. (3.17) and (3.18) that were used to determine yield drop effects. In stress relaxation, the pulling rate is zero. Using a Schmid factor of 1/2 to relate the shear stress to the normal stress, the behavior of the consecutive system is described as

$$\dot{y} = {}_1k^1 + {}^2k_1 - y\,\Sigma k \tag{3.19a}$$

$$\dot{\tau} = -\,1/2\,E'\,\delta\rho_t\left[\eta(1-y)\,{}_1k^1 + (1-\eta)y\,{}_2k^2 - \eta y\,{}^1k_2 - (1-\eta)(1-y)\,{}^2k_1\right] \tag{3.19b}$$

The numerical solutions of Eqs. 3.19a and b have been obtained for a system of two consecutive energy barriers associated with the first group of crystals. When the stress is expressed in MPa and the temperature in K, the activation parameters are:

$${}_1(\Delta G)^1/kT = (13383 - 1747x\tau)/T,\ {}_2(\Delta G)^2/kT = (17940 - 4026x\tau)/T,$$

$${}^1(\Delta G)_2/kT = (9600 + 436\ x\ \tau)/T,\ {}^2(\Delta G)_1/kT = (21723 + 4026x\tau)/T.$$

The temperature was 302 K, the combined elastic modulus E' was equal to 5000 MPa, and the product $\delta\rho_t$ equal to 0.0029. To represent the condition that most of the contribution to the strain is produced after activation over the second energy barrier, the parameter η was chosen to be 0.01. The initial values y_o and τ_o were equal to the steady-state values which would give a plastic strain rate of 0.002/min. For repeated relaxations, the initial density y_o was equal to its value at the end of the preceding test.

Figure 41 shows the effect of the initial dislocation density, y_o, on the stress dependence of the strain rate in the log $\dot{\varepsilon}_p$-vs-τ coordinate system. When y_o is equal to its steady state value, the non-steady state analysis gives almost the same result (curve A) as the steady state. The slope of the curve is proportional to the experimental activation volume and increases, characteristically, as the stress decreases. Because the dislocation density is a function of the stress, the initial value y_o in repeated relaxation depends on the duration of the preceding test. For the system considered, when the preceding test is long y_o is small, and the strain rate goes through a maximum in repeated relaxation (curves E and F). After sufficiently long time, however, the behavior becomes identical to the steady state prediction, independently of the preceding test.

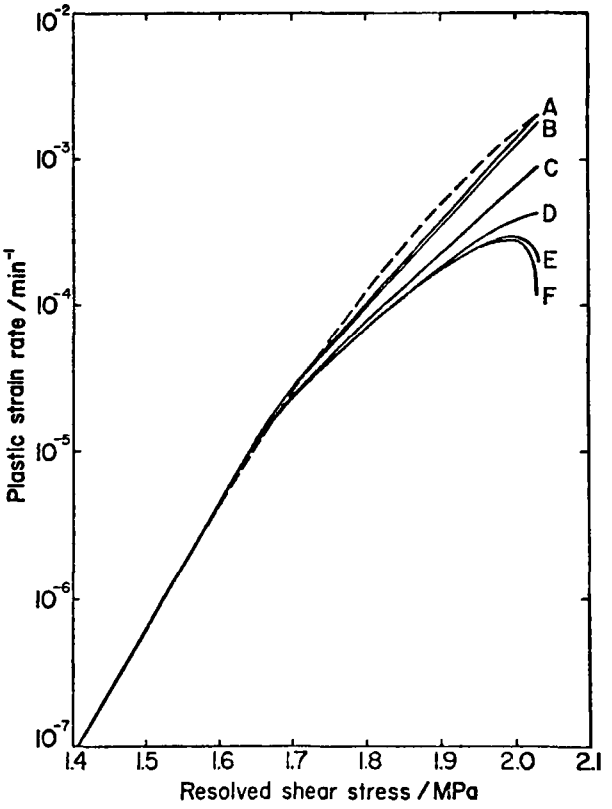

FIGURE 41: Effect of previous test duration on repeated stress relaxation. Curve A has been obtained from the steady-state initial conditions. From B to F the curves have been obtained after a preceding test of respectively 2 min, 12 min, 2 hours, 1 day, 1 week. Steady-state analysis gives always the same result (dashed curve).

This non-steady state behavior results, as in the case of yield-drop study, from the dislocation redistribution that should occur according to the relative heights of the consecutive energy barriers. The dislocation distribution lags behind its limiting value, the steady state value. This is illustrated for the system studied in Fig. 42, where the stress dependence of the dislocations ratio is represented for steady-state analysis and for stress relaxations corresponding to curves A, C, and E of Fig. 41. At the beginning of the repeated relaxation, the number of dislocations in front of the second energy barrier, ρ_2, is less than the steady-state concentration because it was

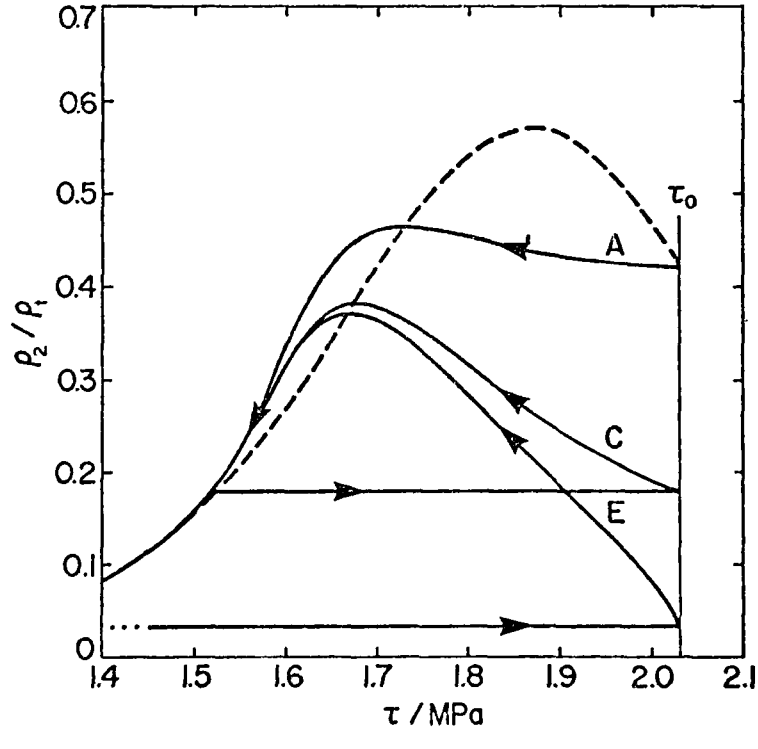

FIGURE 42: Stress dependence of dislocation distribution as obtained in stress relaxation. The dashed curve shows the steady state value. The curves correspond to curves A, C, E of Fig. 41.

taken equal to its value at the end of the previous relaxation. Because the strain is produced mainly after activation over the second energy barrier, the strain rate is low. However, at the high initial stress, the rate of activation over the first barrier is large and ρ_2 increases rapidly, producing the increasing plastic strain rate.

Figure 43 shows that the shape of the curve in the log $\dot{\varepsilon}$-vs-τ coordinate system does not depend on the initial stress, τ_0. Because of work-hardening, the same applied stress in repeated relaxation corresponds to a smaller effective stress. With the same initial dislocation density, the strain rate becomes smaller. When the strain

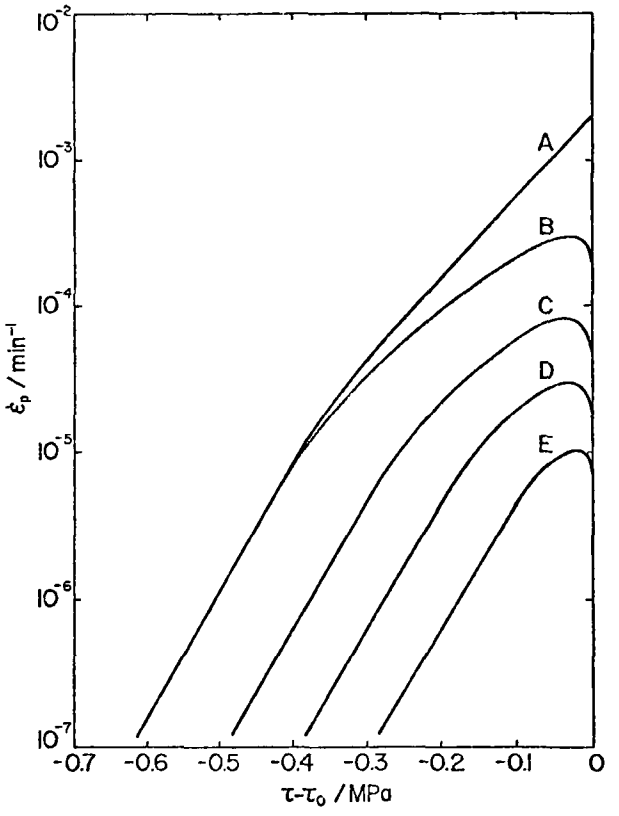

FIGURE 43: Effect of reloading stress on relaxation behavior. The curves have been plotted as a function of the relaxed stress. Curve A is the same as in Fig. 41 and its initial stress of 2.03 MPa corresponds to a steady-state strain rate of 2×10^{-3} min^{-1}; from B to E the initial stress, τ_0, is respectively 2.03, 1.9, 1.8, 1.7 MPa.

rate is plotted as a function of the stress change $(\tau-\tau_0)$ and not as a function of the effective stress, after appropriately long time, the curves become parallel rather than identical.

3.2.4 EXPERIMENTAL RESULTS

In Fig. 44 typical experimental results are compared to the calculated curves. Curve A of Fig. 43 has been fitted to the results of test 4.07 - a conventional relaxation. The curve has been shifted to the left by 0.05 MPa. An equivalent decrease of the load occurs in less than one second at the beginning of a conventional relaxation. The observed difference may thus result from transition effects in the equipment just after stopping the crosshead. A curve similar to curve C of Fig. 43 but starting at an initial stress of 1.93 MPa has been fitted, with a shift of 0.015 MPa, to the results of test 4.08 - a repeated relaxation. The good agreement between calculated curves and experimental results confirms the conclusion that the plastic flow in LiF is controlled by a system of two consecutive energy barriers.

It must be noticed that there is a difference of 0.1 MPa between the initial stresses of the calculated curves corresponding to the conventional and repeated relaxations, although the initial stresses of both tests were identical. This difference between measured and calculated results could be explained by a change of internal stress during the relaxation tests. This explanation, however, would not account for the identity of two consecutive repeated tests (tests 4.03-4.04 and 4.08-4.09 in Fig. 21 p. 45). The elucidation of this problem could lead to a better understanding of the deformation process in LiF, but is outside of the scope of this thesis.

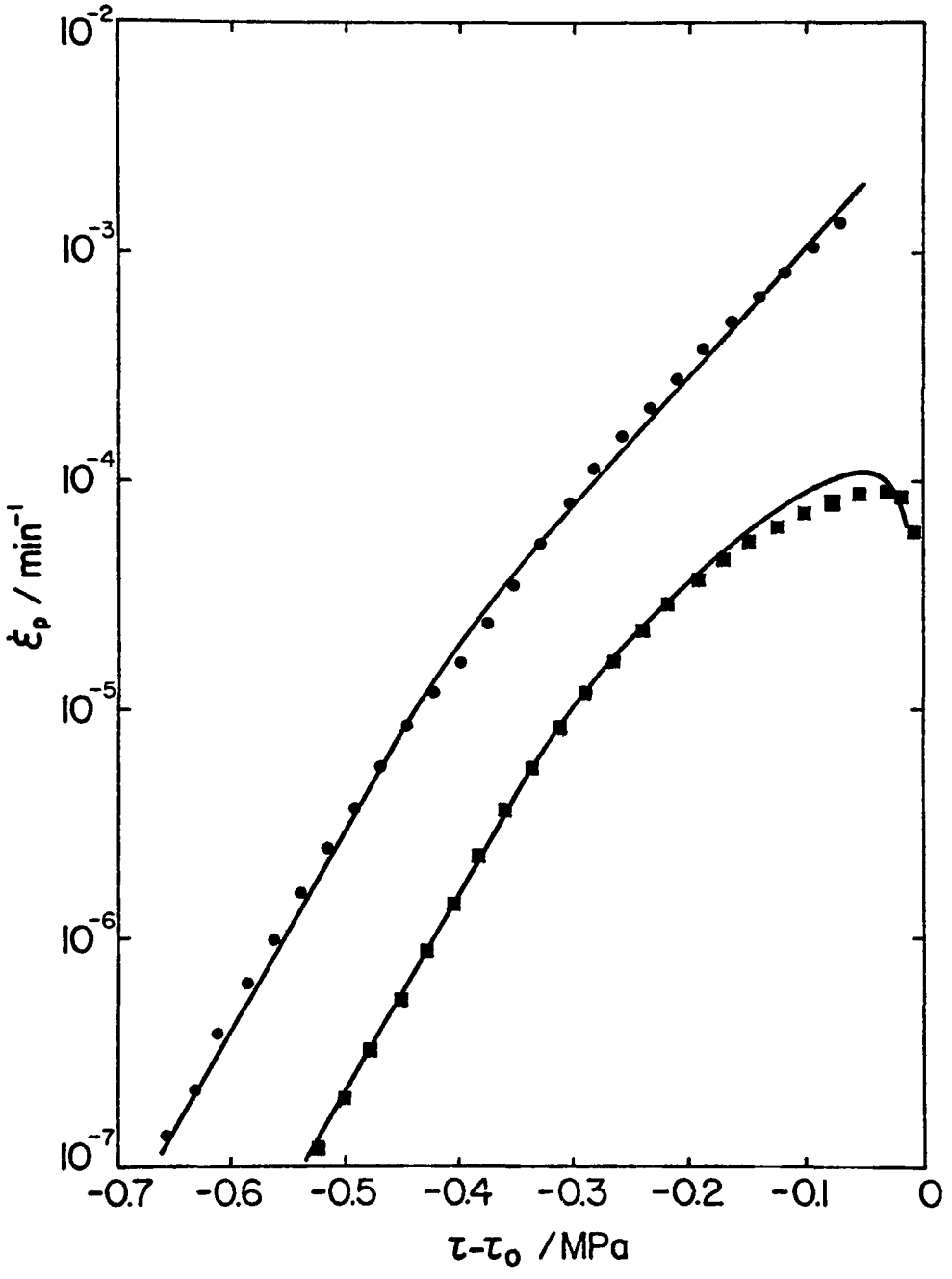

FIGURE 44: Calculated (curves) and experimental (points) rate diagrams during conventional (●) and repeated (■) stress relaxation.

It is interesting to compare the results obtained with crystals of two different batches. The activation volumes, 1300 and 2600 b^3, determined from the steady state analysis of the experimental results of specimen 26 are close to those obtained with specimens of the first batch ($_1V^1 = 1050\ b^3$ and $_2V^2 = 2400\ b^3$). The large experimental value, 3700 b^3, observed at low stress level with specimens of the first batch is a composite activation volume, $_1V^2 = {}_1V^1 + {}^1V_2 + {}_2V^2$. The product $\delta\rho_t$ of the second batch was 2×10^{-4}, that is one order of magnitude lower than that of the first group, 3×10^{-3}. To attain a specific strain rate, a low $\delta\rho_t$ must be compensated by a high rate of activation, that is a high effective stress. The high rate of activation could be responsible for the weak non-steady effects observed in specimen of groups II and III: at high stress level, the relaxation time is small and thus the dislocation redistribution is almost instantaneous. Furthermore, it is possible that the large activation volume (3700 b^3) was not observed in these groups because the stress was too large.

Only a few investigators have reported increasing strain rates at the beginning of stress relaxation experiments. This was noticed during relaxation of hair in low concentration of sodium sulfide. The proposed explanation involved a system of consecutive energy barriers: the sodium sulfide must diffuse into the hair before the reaction that leads to stress relaxation can take place. A well pronounced maximum has been reported recently (121) during pre-yield relaxation of pure iron. Formerly, delay time (122) had been observed in the same conditions. It is not fortuitous that in previous studies (123) it was concluded that the plastic deformation in iron is controlled by a consecutive energy barrier system.

CHAPTER 4

SUMMARY AND CONCLUSIONS

A functional relationship between parameters that control plastic flow is useful for engineering purposes. When plastic deformation results from thermally activated motion of dislocations, the plastic strain rate is usually expressed as

$$\dot{\varepsilon}_p = \dot{\varepsilon}_o \exp\left[-\left(\Delta G_{exp}/kT\right)\right] .$$

The analysis of the stress and temperature dependence of the two experimental terms, $\dot{\varepsilon}_o$ and ΔG_{exp}, must be based on deformation kinetics. This approach was utilized to study the behavior of LiF in stress relaxation experiments. The analysis has led to a comprehensive investigation of the properties of systems of two consecutive energy barriers.

It has been found that

1. In steady state flow there are two or three separate stress ranges where the rate of deformation is described by only one of the four ${}_ik^i$, ${}_ik^j$ rate constants.
2. No more than one of the two composite ${}_ik^j$ rate constants has an independent effect on the plastic strain rate. The four rate constants are effective only at low stress level when the plastic strain rate becomes very small.
3. Between two independent stress ranges there is a transition region where the strain rate is controlled by two rate constants. The

transition stress is temperature independent, and well defined by the properties of the system.

4. A methodology based on the transition stress can be utilized to determine the activation parameters. It has been applied to the analysis of the stress relaxation data of lithium fluoride.
5. The number of dislocations waiting in front of each energy barrier is stress dependent. Stress changes in a transition region may produce large redistributions of the dislocations. The redistribution occurs by non-steady state flow.
6. The non-steady state kinetics is described by a system of two differential equations. Non-steady state behavior is time dependent, and also depends on the testing condition: accordingly, the behavior of materials in which plastic flow is controlled by a consecutive energy barrier system can not be described by an "equation of state".
7. Non-steady state effects are well pronounced when the amount of dislocation redistribution is large, and when the relaxation time that controls the rate of redistribution is large.
8. In constant rate tests, the dislocation redistribution can produce yield drop effects. This is a new explanation of this phenomenon.
9. Dislocation redistribution can cause the strain rate to increase at the beginning of repeated stress relaxation experiments.
10. The behavior of LiF in stress relaxation is controlled by a system of two consecutive energy barriers. The properties of this system would explain both the stress and temperature dependence of the experimental activation volume, as well as the behavior in repeated relaxation. The calculated activation volumes and energies are in

agreement with the published values.

The theoretical and experimental parts of this study may be extended:

The application of the non-steady state kinetics to other testing conditions, for example creep and strain rate change tests, may elucidate behaviors that are now insufficiently understood.

The behavior of systems of two consecutive energy barriers remains to be investigated at low stress level.

The properties of systems of more than two consecutive energy barriers are to be determined, utilizing either the discrete approach (66) or a continuous method (124). This should be done for steady state and non-steady state conditions.

More experiments should be carried out on lithium fluoride. It would be interesting to compare the actual results with those of tests in compression. The effect of annealing and various doses of irradiation on the kinetics could be explored. The absence of difference between the first and second repeated relaxations remains to be elucidated.

Finally, this kinetics analysis could be utilized to analyze all published results that present a character associated with consecutive energy barriers.

REFERENCES

1. A. S. Krausz, Appl. Sc. Res. 26, 86 (1972).

2. A. Nadai, "Theory of Flow and Fracture of Solids", Vol. II, McGraw-Hill, New York, 1963.

3. J. A. Ewing, J. C. W. Humfrey, Phil. Trans. Roy. Soc. A200, 241 (1903).

4. E. R. Parker, "Brittle Behavior of Engineering Fracture", J. Wiley & Sons, New York, 1957.

5. P. Ludwig, "Elemente der Technologishen Mechanik", Verlag Julius Springer, Berlin, 1909.

6. R. Becker, Physik. Zeitschr. 26, 919 (1925).

7. J. H. Hollomon, C. Zener, J. Appl. Phys. 17, 69 (1946).

8. E. W. Hart, Acta Met. 18, 599 (1970).

9. "Constitutive Equations in Plasticity", Ed. Ali S. Argon, M.I.T. Press, Cambridge, 1975.

10. J. Eng. Mater. Techn. 98 (1976).

11. F. A. McClintock, A. S. Argon, "Mechanical Behavior of Materials", p. 190, Addison-Wesley, Reading, 1966.

12. E. Orowan, Z. Phys. 89, 605, 614, 634 (1934).

13. M. Polanyi, Z. Phys. 89, 660 (1934).

14. G. J. Taylor, Proc. Roy. Soc, A145, 362 (1934).

15. J. Frenkel, Z. Phys. 37, 572 (1926).

16. A. H. Cottrell, "Dislocations and Plastic Flow in Crystals", Oxford University Press, 1953.

17. J. Friedel, "Les Dislocations", Gauthiers-Villars, Paris, 1956.

18. H. G. van Bueren, "Imperfections in Crystals", Interscience, New York, 1960.

19. J. Weertman, J. R. Weertman, "Elementary Dislocation Theory", Macmillan, New York, 1964.

20. F. R. N. Nabarro, "Theory of Crystal Dislocations", Oxford Clarendon Press, 1967.

21. J. P. Hirth, J. Lothe, "Theory of Dislocations", McGraw-Hill, New York, 1968.

22. S. Amelinckx, in "Advances in Materials Research in the Nato Nations", Ed. H. Brooks, N. H. Mason, N. E. Promisel, G. H. Cooper, Pergammon Press, Oxford, 1963.

23. E. Orowan, Proc. Phys. Soc. 52, 8 (1940).

24. A. Seeger, Z. Naturforsch. 9a, 758, 819, 856 (1954).

25. Z. S. Basinski, Philos. Mag. 4, 393 (1959).

26. H. Conrad, H. Wiedersich, Acta Met. 8, 128 (1960).

27. H. Conrad, J. Metals, 16, 582 (1964).

28. J. P. Hirth, W. D. Nix, Phys. Stat. Sol. 35, 177 (1969).

29. H. Conrad, Mater. Sci. Eng. 6, 265 (1970).

30. S. Arrhenius, Z. Phys. Chem. 4, 226 (1889).

31. A. Marcellin, Ann Phys. 3, 158 (1915).

32. W. H. Rodebush, J. Am. Chem. Soc. 45, 606 (1923).

33. W. H. Rodebush, J. Chem. Phys. 1, 440 (1933).

34. W. H. Rodebush, J. Chem. Phys. 3, 242 (1935).

35. W. H. Rodebush, J. Chem. Phys. 4, 744 (1936).

36. O. K. Rice, H. Gershinowitz, J. Chem. Phys. 2, 853 (1934).

37. O. K. Rice, H. Gershinowitz, J. Chem. Phys. 3, 479 (1935).

38. H. Eyring, J. Chem. Phys. 3, 107 (1935).

39. W. F. K. Wynne-Jones, H. Eyring, J. Chem. Phys. 3, 492 (1935).

40. M. G. Evans, M. Polanyi, Trans. Far. Soc. 31, 875 (1935).

41. M. G. Evans, M. Polanyi, Trans. Far. Soc. 33, 448 (1937).

42. M. Polanyi, J. Chem. Soc. 629 (1937).

43. H. Eyring, J. Chem. Phys. 4, 283 (1936).

44. S. Glasstone, K. J. Laidler, H. Eyring, "The Theory of Rate Processes", McGraw-Hill, New York, 1941.

45. A. S. Krausz, H. Eyring, "Deformation Kinetics", Wiley-Interscience, New York, 1975.

46. K. J. Laidler, "Theories of Chemical Reaction Rates", McGraw-Hill, New York, 1969.

47. R. C. Gifkins, J. Mater. Sci. 5, 156 (1970).

48. J. C. M. Li in "Rate Processes in Plastic Deformation of Materials", edited by J. C. M. Li and A. K. Mukherjee, ASM, 1975.

49. A. S. Krausz, H. Eyring, J. Appl. Phys. 42, 2382 (1971).

50. T. O'D. Hanley, A. S. Krausz, J. Appl. Phys. 45, 2013 (1974).

51. E. Orowan, Z. Phys. 98, 382 (1935).

52. W. Kauzmann, Transact. Inst. Min. Metall. Eng. 143, 57 (1941).

53. G. Schoeck, Phys. Stat. Sol. 8, 499 (1965).

54. G. Alefeld, Z. Naturforsch. 17a, 899 (1962).

55. A. S. Krausz, Acta Met. 16, 897 (1968).

56. A. S. Krausz, Mater. Sci. Eng. 6, 260 (1970).

57. A. S. Krausz, Z. Naturforsch. 31a, 728 (1976).

58. A. S. Krausz, Mater. Sci. Eng. 26, 65 (1976).

59. A. G. Evans, R. D. Rawlings, Phys. Stat. Sol. 34, 9 (1969).

60. J. P. Hirth in "Inelastic Behavior of Solids", ed. M. F. Kanninen et al., McGraw-Hill, New York, 1970.

61. B. Chalmers, Proc. Roy. Soc. 156A, 427 (1936).

62. H. C. Heard, J. Geol. 71, 162 (1963).

63. S. J. Hahn, T. Ree, H. Eyring, Geol. Soc. Amer. Bull. 78, 773 (1967).

64. P. Guyot, J. E. Dorn, Can. J. Phys. 45, 983 (1867).

65. V. Celli, M. Kabler, T. Ninomiya, R. Thomson, Phys. Rev. 131, 58 (1963).

66. T. O'D. Hanley, A. S. Krausz, N. Krishna, J. Appl. Phys. 45, 2016 (1974).

67. D. N. Seidman, R. W. Balluffi in "Interactions Between Lattice Defects", ed. R. R. Hasiguti, Gordon and Breach Inc., New York, 1966.

68. J. Washburn in "Rate Processes in Plastic Deformation of Materials", ed. J. C. M. Li and A. K. Mukherjee, ASM, 1975.

69. N. F. Mott, Proc. Phys. Soc. B64, 729 (1951).

70. J. P. Hirth, J. Lothe, Can. J. Phys. 45, 809 (1967).

71. J. Diehl, G. P. Seidel, L. Niemann, Phys. Stat. Sol. 12, 405 (1965).

72. H. Conrad, Mater. Sci. Eng. 6, 265 (1970).

73. B. Faucher, A. S. Krausz, J. Appl. Phys. 49, 3946 (1978).

74. A. Nadai, "Theory of Flow and Fracture of Solids", Vol. 1, 2nd edition, McGraw-Hill, New York, 1950.

75. W. G. Johnston, J. Appl. Phys. 33, 2716 (1962).

76. P. Phillips, Phil. Mag. 9, 513 (1905).

77. E. N. da C. Andrade, Proc. Roy. Soc. A84, 1 (1910).

78. O. H. Wyatt, Proc. Phys. Soc. B66, 459 (1953).

79. A. S. Krausz, B. G. Craig, Acta Met. 14, 1807 (1966).

80. A. H. Cottrell, V. Aytekin, J. Inst. Met. 77, 389 (1950).

81. T. A. Trozera, J. Mote, J. E. Dorn, Trans. Amer. Soc. Met. 186, 1 (1960).

82. H. Conrad, L. Hays, G. Schoeck, H. Wiedersich, Acta Met. 9, 367 (1961).

83. P. Trouton, A. O. Rankine, Phil. Mag. 8, 538 (1904).

84. P. Feltham, Phil. Mag. 6, 259, 847 (1961); 8, 989 (1963).

85. P. Feltham, Phys. Stat. Sol. 3, 1340 (1963).

86. F. Guiu, P. L. Pratt, Phys. Stat. Sol. 6, 111 (1964).

87. G. B. Gibbs, Phil. Mag. 13, 317 (1966).

88. G. Sargent, H. Conrad, Scripta Met. 3, 43 (1969).

89. S. R. MacEwen, O. A. Kupcis, B. Ramaswami, Scripta Met. 3, 441, (1969).

90. C. N. Ahlquist, W. D. Nix, Scripta Met. 3, 679 (1969).

91. R. E. Reed-Hill, J. R. Donoso, Scripta Met. 9, 1305 (1975).

92. F. Guiu, Scripta Met. 3, 753 (1969).

93. K. Okazaki, Y. Aono, T. Kaneyuki, H. Conrad, Mater. Sci. Eng. 33, 253 (1978).

94. N. Krishna, M.Sc. Thesis, University of Ottawa, 1971.

95. C. H. Laforce, M.Sc. Thesis, University of Ottawa, 1977.

96. C. V. Briscoe, C. F. Squire, Phys. Rev. 106, 1175 (1957).

97. M. G. Akben, M.Sc. Thesis, University of Ottawa, 1977.

98. G. Baur, P. Lehr, Mem. Sci. Rev. Metall. 72. 551 (1975).

99. G. A. Sargent, Acta Met. 13, 663 (1965).

100. R. W. Rhode, T. V. Nordstrom, Scripta Met. 7, 317 (1973).

101. J. J. Gilman, W. G. Johnston, Sol. State Phys. 13, 147 (1962).

102. M. T. Sprackling, "The Plastic Deformation of Simple Ionic Crystals", Academic Press, London, 1976.

103. H. L. Fotedar, M. Srinivasan, D. A. Wilson, T. G. Stoebe, Mater. Sci. Eng. 7, 272 (1971).

104. H. L. Fotedar, T. G. Stoebe, Phys. Stat. Sol. A31, 399 (1975).

105. V. F. Gaiduchenya, A. A. Blistanov, M. P. Shaskol'skaya, Sov. Phys. Solid State 12, 27 (1970).

106. H. L. Fotedar, T. G. Stoebe, J. Physique 34, C9-367 (1973).

107. F. Guiu, T. G. Langdon, Phil. Mag. 30, 145 (1974).

108. B. Reppich, Acta Met. 20, 557 (1972); Scripta Met. 6, 1 (1972).

109. M. Cagnon, J. Physique 34, C9-217 (1973).

110. J. S. Nadeau, W. G. Johnston, J. Appl. Phys. 32, 2563 (1961).

111. R. L. Fleischer, Acta Met. 10, 835 (1962); J. Appl. Phys. 33, 3504 (1962).

112. G. B. Gibbs, Phil. Mag. 20, 611 (1969).

113. D. M. Barnett, W. D. Nix, Acta Met. 21, 1157 (1973).

114. B. J. Smirnov, B. A. Efimov, Phys. Stat. Sol. 16, 191 (1966).

115. J. J. Gilman, J. Appl. Phys. 33, 2703 (1962).

116. A. H. Cottrell, "Dislocations and Plastic Flow in Crystals", O.U.P. (1953).

117. W. G. Johnston, J. Appl. Phys. 33, 2716 (1962).

118. B. Faucher, A. S. Krausz, Scripta Met. 12, 175 (1978).

119. B. Faucher, A. S. Krausz, Scripta Met. 12, 913 (1978).

120. C. E. Reese. H. Eyring, Text. Res. J. 20, 743 (1950).

121. A. W. Sleeswyk, W. S. T. Maathius, 4th Int. Conf. on the Strength of Metals and Alloys, Nancy, France, Proceedings 1, 356 (1977).

122. K. Thomas, Nature 213, 172 (1967); 216, 149 (1967).

123. T. O'D. Hanley, A. S. Krausz, D. Maheshwari, Mater. Sci. Eng. 16, 155 (1974).

124. A. S. Krausz, B. Faucher, Scripta Met. (in press).

APPENDICES

APPENDIX A

NUMERICAL DIFFERENTIATION OF EXPERIMENTAL DATA

The smoothing of experimental data by spline functions developed by Reinsch[1] has been applied to the determination of stress and strain rates from experimental recordings.

Considering n experimental points (x_i, y_i), $i = 1, \ldots, n$ the smoothing function f(x) shall minimize

$$\int_{x_1}^{x_n} \left[\frac{d^2 g(x)}{dx^2}\right]^2 dx \tag{A.1}$$

among all functions g(x) such that

$$\sum_{i=1}^{n} \left[\frac{g(x_i) - y_i}{\delta y_i}\right]^2 \leq S, \quad g \in C^2 [x_1, x_n] \tag{A.2}$$

where δy_i are the estimated errors or standard deviations, S is a redundant smoothing index that may be used to control the extent of smoothing. Utilizing the methods of the calculus of variation, it is found that the function f(x) that satisfies Eqs. (A.1) and (A.2) is composed of cubic parabolas:

$$f(x) = a_i + b_i (x-x_i) + c_i (x-x_i)^2 + d_i (x-x_i)^3 \quad x_i \leq x \leq x_{i+1} \tag{A.3}$$

which join at their common end points such that f(x), $\frac{d f(x)}{dx}$, $\frac{d^2 f(x)}{dx^2}$ are continuous and

$$\lim_{h\to 0} \frac{d^3 f(x_i - h)}{dx^3} - \lim_{h\to 0} \frac{d^3 f(x_i + h)}{dx^3} = 2p \frac{f(x_i) - y_i}{\delta y_i^2} \tag{A.4}$$

where p is a Lagrangian parameter. The spline coefficients in Eq. (A.3) are determined from Eq. (A.4) and the continuity conditions. The

---

1. C. H. Reinsch, Num. Mathem. 10, (1967), D. G. Berghaus, J. P. Cannon, Exp. Mech. 13, 38 (1973).

Lagrangian parameter is then determined by iteration from the relation

$$\sum_{i=1}^{n} \left(\frac{f(x_i) - y_i}{\delta y_i}\right)^2 = S. \qquad (A.5)$$

In application to stress relaxation data, the function f is the stress or the corresponding value of the strain. Because the curvature of the smoothed-spline function is minimized, and because the stress and the strain are exponentially decreasing functions of the time, the variable x has been chosen equal to the logarithm of the time. The rates corresponding to the n data points are

$$\left(\frac{dy}{dt}\right)_i = b_i \cdot \frac{1}{t_i} = b_i \cdot e^{-x_i} \qquad (A.6)$$

Reinsch set the second and third derivative at the first and last data points equal to zero. It was found more satisfactory to measure the first derivative at the first point and to use this value in the calculation of the spline coefficients. The continuity conditions and Eq. (A.4) yield the relation

$$\Delta^2 y = A \cdot c$$

where $c = (c_0, c_1, \ldots, c_{n+1})^T$

$$\Delta^2 y = (\Delta^2_{y_0}, \Delta^2_{y_i}, \ldots \Delta^2_{y_{n+1}})^T$$

with $$\Delta^2_{y_i} = \frac{y_{i+1} - y_i}{x_{i+1} - x_i} - \frac{y_i - y_{i-1}}{x_i - x_{i-1}}$$

and A is a (n+2) x (n+2) band form matrix with five non-zero diagonals. The spline coefficients c_i obtained from $c = A^{-1} \Delta^2 y$, are functions of the Lagrangian parameter p. The derivatives b_i are calculated when Eq. (A.5) is satisfied.

In the following APL program, $\underline{A}$ is the matrix A, $\underline{C}$ is the vector c and $\underline{B}$ the derivatives calculated according to Eq. (A.6). The determination of the Lagrangian parameter is started with $L = \frac{1}{p} = 0$ and stopped when Eq. (A.5), which has been rewritten as $F(L) = L$, is satisfied within .01%. The calculated rates were always within the uncertainty of the measured derivatives. The program gives smooth curves as illustrated in the rate diagrams and it has been widely used (95, 97).

```
∇ RATE
 [1] 'ENTER STRESS'
 [2] SIG←⍞
 [3] 'ENTER LN TIME'
 [4] T←⍞
 [5] 'ENTER STRAIN( 0 IF NOT USED)'
 [6] EL←⍞
 [7] 'ENTER ERROR ON STRESS'
 [8] EC←⍞
 [9] 'ENTER ERROR ON STRAIN'
 [10] EEL←⍞
 [11] 'INITIAL STRESS RATE'
 [12] SIG0←⍞
 [13] 'INITIAL STRAIN RATE'
 [14] EL0←⍞
 [15] N←⍴T
 [16] Y←SIG←0×X←T←0×EY←N⍴ES
 [17] H←(1↓Y)-¯1↓X
 [18] A←((N+2),(N+2))⍴0
 [19] A[1;1]←A[N+1;N+1]←A⌈N+2;N+2]←1
 [20] DY←0 0,((((2↓Y)÷1↓H)+(¯2↓Y)÷¯1↓T)-(1↓¯1↓Y)×(÷(1↓H))+÷(¯1↓H)),0 0
 [21] DY[2]←(SIG0×÷X[1])-(Y[2]-Y[1])÷H[1]
 [22] L←L1←N÷+/EY*2+0×K←0
 [23] L←((L1>L),L1≤L)/(L1+(L1-L)÷2),L1
 [23.5] K←K+1
 [24] A←((L×EY[1]*2)÷H[1]*2),((L×(1↓¯1↓EY)*2)÷(1↓H)×¯1↓H),(L×FY[N]*2)÷H[(N-1)]*2
 [25] BE←A[1],((1↓¯1↓A)×(¯1↓H)÷1↓H)
 [26] GA←BE×((1↓EY)÷¯1↓EY)*2
 [27] B←(¯1↓A)+(1↓A)+BE+GA-H÷3
 [28] C←(2×1↓¯1↓A)+(¯1↓GA)+(1↓GA)+(¯1↓BE)+(1↓BE)+(2×(1↓H)+¯1↓H)÷3
 [29] A[2;2 3 4]←(-GA[1]+2×A[1]+H[1]÷3),(A[1]+A[2]+GA[1]-H[1]÷3),(-A[2])
 [30] I←2
 [31] I←I+1
 [32] A[I;]←((I-3)⍴0),A[I-2],(-B[I-2]),C[I-2],(-B[I-1]),A[I],(N-I)⍴0
 [33] →(I<N)/31
 [34] C←(⌹A)+.×DY
 [35] DN1←(((C[1]+C[3]-2×C[2])×EY[1]÷H[1])*2),(((C[N]+C[(N+2)]-2×C[(N+1)])×FY[N]÷H[(N-1)])*2)
 [36] DN←DN1,(((1↓¯1↓EY)×((1↓¯3↓C)÷¯1↓H)+((3↓¯1↓C)÷1↓H)-(2↓¯2↓C)×(÷1↓H)+÷¯1↓H)*2)
 [37] L1←(N*.5)÷(+/DN)*.5
 [38] →(((|L1-L)÷L1)>.0001)/23
 [39] 'L=  ';L1;'  (';K;')'
 [40] H1←H[1],H,H[(N-1)]
 [41] B1←(((¯3↓C)-1↓¯2↓C)×(¯1↓EY*2)÷¯2↓H1)+((2↓¯1↓C)-3↓C)×(1↓EY*2)÷2↓H1
 [42] B2←((2↓¯1↓C)-1↓¯2↓C)×((¯1↓EY*2)+1↓EY*2)÷H
 [43] B←((((L1×B1+B2)+(1↓Y)-¯1↓Y)÷H)-(H×(2×1↓¯2↓C)+2↓¯1↓C)÷3)÷¯1↓×T
 [44] →(EL=0)/63
 [45] →(Y=EL)/51
 [46] DSIG←B
 [47] Y←EL
 [48] SIG0←EL0
 [49] EY←N⍴EEL
 [50] →29
 [51] ELA←1E4
 [52] ''
 [53] DEP←B-DSIG÷ELA
 [54] X←⍉(6,(N-1))⍴(¯1↓SIG),(¯1↓EL),(¯1↓×T),DSIG,B,DEP
 [55] '       STRESS          STRAIN          TIME       STRESS RATE    STRAIN RATE     CORRECTED'
 [56] 14 4 EFT X[(⍳⌊(N-1)÷2);]
 [57] 14 4 EFT X[((⌊(N-1)÷2)+⍳⌈(N-1)÷2);]
 [60] 'COMB. ELAST. MOD. =  ';÷(÷ELA)-(X[N-1;2]-X[1;2])÷X[N-1;1]-X[1;1]
 [61] '-SIG/ε     ';'9999.' $ Z  ,(+/Z)÷⍴Z←-X[;4]÷X[;6]
 [62] →67
 [63] X←⍉(3,(N-1))⍴(¯1↓SIG),(¯1↓×T),B
 [64] '       STRESS          TIME       STRESS RATE'
 [65] 14 4 EFT X[(⍳⌊(N-1)÷2);]
 [66] 14 4 EFT X[((⌊(N-1)÷2)+⍳⌈(N-1)÷2);]
∇
```

APPENDIX B
THE EXPERIMENTAL RESULTS

TEST LIF: 2.01

TEMPERATURE = 302 (K)
INITIAL STRAIN = 0.20 (PCT)
TOTAL STRAIN = 0.20 (PCT)
INITIAL SHEAR STRESS = 8.360 (MPA)

SHEAR STRESS (MPA)	STRAIN RATE (/MIN)
8.314 *	1.70E-03
8.291	1.18E-03
8.268	8.00E-04
8.245	6.00E-04
8.222	4.50E-04
8.199	3.30E-04
8.176	2.25E-04
8.153	1.46E-04
8.130	9.80E-05
8.107	6.40E-05
8.084	4.60E-05
8.061	2.97E-05
8.038	1.98E-05
8.015	1.29E-05
7.992	8.80E-06
7.969	5.50E-06
7.946	3.32E-06
7.923	2.23E-06
7.900	1.51E-06
7.877	1.01E-06
7.855	6.40E-07
7.832	4.00E-07
7.809	2.60E-07
7.786	1.90E-07
7.763	1.30E-07

TEST LIF: 2.02

TEMPERATURE = 302 (K)
INITIAL STRAIN = 0.23 (PCT)
TOTAL STRAIN = 0.47 (PCT)
INITIAL SHEAR STRESS = 8.290 (MPA)

SHEAR STRESS (MPA)	STRAIN RATE (/MIN)
8.244	1.85E-03
8.221	1.23E-03
8.198	8.20E-04
8.175	5.40E-04
8.152	4.00E-04
8.129	2.86E-04
8.106	2.14E-04
8.083	1.43E-04
8.060	9.50E-05
8.037	6.50E-05
8 014	4.30E-05
7.991	2.83E-05
7.968	1.82E-05
7.945	1 18E-05
7.922	8.00E-06
7.899	5.20E-06
7.876	3.10E-06
7.853	1.90E-06
7 830	1.21E-06
7.807	7.30E-07
7.784	4.00E-07
7.761	2.30E-07
7.738	1.30E-07

TEST LIF: 2.03

TEMPERATURE = 302 (K)
INITIAL STRAIN = 0.20 (PCT)
TOTAL STRAIN = 0.70 (PCT)
INITIAL SHEAR STRESS = 8.272 (MPA)

SHEAR STRESS (MPA)	STRAIN RATE (/MIN)
8.240	1.58E-03
8.217	1.27E-03
8.194	9.90E-04
8.171	7.40E-04
8.148	5.30E-04
8.125	3.80E-04
8.101	2.72E-04
8.078	1.89E-04
8.055	1.30E-04
8.032	8.90E-05
8.009	6.10E-05
7.986	4.20E-05
7.963	2.79E-05
7.940	1.86E-05
7.917	1.18E-05
7.894	7.40E-06
7.871	5.20E-06
7.848	3.32E-06
7.824	2.13E-06
7.801	1.35E-06
7.778	8.40E-07
7.755	5.00E-07
7.732	3.00E-07
7.709	1.90E-07
7.686	1.30E-07

TEST LIF: 2.04

TEMPERATURE = 302 (K)
INITIAL STRAIN = 0.00 (PCT)
TOTAL STRAIN = 0.74 (PCT)
INITIAL SHEAR STRESS = 8.197 (MPA)

SHEAR STRESS (MPA)	STRAIN RATE (/MIN)
8.174	5.90E-04
8.151	4.60E-04
8.128	2.94E-04
8.105	1.82E-04
8.082	1.11E-04
8.058	7.00E-05
8.035	4.40E-05
8.012	2.85E-05
7.989	1.87E-05
7.966	1.18E-05
7.943	7.30E-06
7.920	4.70E-06
7.897	3.12E-06
7.874	2.06E-06
7.851	1.35E-06
7.828	8.80E-07
7.804	5.90E-07
7.781	4.10E-07
7.758	2.90E-07
7.735	1.90E-07
7.712	1.20E-07

* The accuracy of the stress values is of the order of 1%.

TEST LIF: 2.05

TEMPERATURE = 302 (K)
INITIAL STRAIN - 0.00 (PCT)
TOTAL STRAIN = 0.76 (PCT)
INITIAL SHEAR STRESS - 8.199 (MPA)

SHEAR STRESS (MPA)	STRAIN RATE (/MIN)
8.176	3.31E-05
8.152	3.53E-05
8.129	3.22E-05
8.106	2.82E-05
8.083	2.38E-05
8.060	1.92E-05
8.037	1.42E-05
8.014	1.06E-05
7.991	7.10E-06
7.968	4.81E-06
7.945	3.12E-06
7.922	1.95E-06
7.898	1.24E-06
7.875	7.60E-07
7.852	4.90E-07
7.829	3.00E-07
7.806	1.90E-07
7.783	1.20E-07

TEST LIF: 2.06

TEMPERATURE = 302 (K)
INITIAL STRAIN 0.21 (PCT)
TOTAL STRAIN = 1.00 (PCT)
INITIAL SHEAR STRESS 8.232 (MPA)

SHEAR STRESS (MPA)	STRAIN RATE (/MIN)
8.172	1.34E-03
8.149	9.20E-04
8.126	6.60E-04
8.102	5.20E-04
8.079	3.11E-04
8.056	2.19E-04
8.033	1.54E-04
8.010	1.04E-04
7.987	7.00E-05
7.964	4.80E-05
7.940	3.22E-05
7.917	2.17E-05
7.894	1.38E-05
7.871	8.70E-06
7.848	5.50E-06
7.825	3.52E-06
7.801	2.31E-06
7.778	1.52E-06
7.755	9.80E-07
7.732	5.70E-07
7.709	2.70E-07
7.686	1.40E-07

TEST LIF: 4.01

TEMPERATURE = 302 (K)
INITIAL STRAIN 0.20 (PCT)
TOTAL STRAIN - 0.20 (PCT)
INITIAL SHEAR STRESS 9.432 (MPA)

SHEAR STRESS (MPA)	STRAIN RATE (/MIN)
9.385	1.50E-03
9.362	1.26E-03
9.338	9.70E-04
9.315	7.40E-04
9.291	5.80E-04
9.268	4.40E-04
9.245	3.31E-04
9.221	2.51E-04
9.198	1.83E-04
9.174	1.34E-04
9.151	9.50E-05
9.128	6.70E-05
9.104	4.54E-05
9.081	3.04E-05
9.057	2.01E-05
9.034	1.30E-05
9.010	8.20E-06
8.987	5.20E-06
8.964	3.60E-06
8.940	2.22E-06
8.917	1.47E-06
8.893	1.00E-06
8.870	6.90E-07
8.847	4.80E-07
8.823	3.50E-07
8.800	2.40E-07
8.776	1.70E-07

TEST LIF: 4.02

TEMPERATURE = 302 (K)
INITIAL STRAIN 0.00 (PCT)
TOTAL STRAIN = 0.23 (PCT)
INITIAL SHEAR STRESS 9.369 (MPA)

SHEAR STRESS (MPA)	STRAIN RATE (/MIN)
9.341	3.35E-04
9.318	2.98E-04
9.294	2.50E-04
9.271	2.13E-04
9.247	1.79E-04
9.224	1.50E-04
9.200	1.24E-04
9.177	1.01E-04
9.154	8.20E-05
9.130	6.20E-05
9.107	4.70E-05
9.083	3.36E-05
9.060	2.34E-05
9.037	1.60E-05
9.013	1.06E-05
8.990	6.60E-06
8.966	3.90E-06
8.943	2.33E-06
8.920	1.28E-06
8.896	7.30E-07
8.873	4.00E-07
8.849	2.20E-07

TEST LIF: 4.03

TEMPERATURE =	302 (K)
INITIAL STRAIN	0.00 (PCT)
TOTAL STRAIN =	0.26 (PCT)
INITIAL SHEAR STRESS	9.379 (MPA)

SHEAR STRESS (MPA)	STRAIN RATE (/MIN)
9.344	5.90E-05
9.320	7.50E-05
9.297	7.50E-05
9.273	7.10E-05
9.250	6.40E-05
9.227	6.00E-05
9.203	5.35E-05
9.180	4.60E-05
9.156	3.85E-05
9.133	3.05E-05
9.110	2.25E-05
9.086	1.56E-05
9.063	1.02E-05
9.039	6.50E-06
9.016	4.30E-06
8.992	2.61E-06
8.969	1.56E-06
8.946	9.80E-07
8.922	5.80E-07
8.899	3.40E-07
8.875	2.20E-07
8.852	1.70E-07

TEST LIF: 4.04

TEMPERATURE =	302 (K)
INITIAL STRAIN	0.00 (PCT)
TOTAL STRAIN =	0.29 (PCT)
INITIAL SHEAR STRESS	9.379 (MPA)

SHEAR STRESS (MPA)	STRAIN RATE (/MIN)
9.347	5.50E-05
9.323	7.70E-05
9.300	7.70E-05
9.276	8.30E-05
9.253	7.30E-05
9.229	6.30E-05
9.206	5.60E-05
9.183	4.50E-05
9.159	3.50E-05
9.136	2.74E-05
9.112	2.06E-05
9.089	1.49E-05
9.065	1.02E-05
9.042	7.00E-06
9.019	4.70E-06
8.995	3.10E-06
8.972	1.92E-06
8.948	1.20E-06
8.925	7.10E-07
8.901	4.20E-07
8.878	2.40E-07

TEST LIF: 4.05

TEMPERATURE =	302 (K)
INITIAL STRAIN	0.20 (PCT)
TOTAL STRAIN =	0.51 (PCT)
INITIAL SHEAR STRESS	9.297 (MPA)

SHEAR STRESS (MPA)	STRAIN RATE (/MIN)
9.297	2.00E-03
9.273	1.80E-03
9.250	1.59E-03
9.226	1.23E-03
9.203	9.40E-04
9.179	7.30E-04
9.156	5.70E-04
9.132	4.33E-04
9.109	3.23E-04
9.085	2.41E-04
9.062	1.80E-04
9.038	1.31E-04
9.015	9.30E-05
8.991	6.50E-05
8.968	4.55E-05
8.944	3.01E-05
8.921	2.03E-05
8.898	1.32E-05
8.874	8.60E-06
8.851	5.30E-06
8.827	3.30E-06
8.804	1.98E-06
8.780	1.16E-06
8.757	6.60E-07
8.733	3.70E-07
8.710	2.10E-07

TEST LIF: 4.06

TEMPERATURE =	302 (K)
INITIAL STRAIN	0.10 (PCT)
TOTAL STRAIN =	0.64 (PCT)
INITIAL SHEAR STRESS	9.262 (MPA)

SHEAR STRESS (MPA)	STRAIN RATE (/MIN)
9.262	2.00E-03
9.238	1.75E-03
9.215	1.51E-03
9.191	1.17E-03
9.168	9.10E-04
9.144	7.10E-04
9.121	5.50E-04
9.097	4.23E-04
9.074	3.23E-04
9.050	2.39E-04
9.027	1.73E-04
9.003	1.22E-04
8.980	9.00E-05
8.956	6.30E-05
8.933	4.35E-05
8.909	2.98E-05
8.886	2.00E-05
8.862	1.30E-05
8.838	7.90E-06
8.815	5.00E-06
8.791	3.05E-06
8.768	1.86E-06
8.744	1.09E-06
8.721	7.00E-07
8.697	4.80E-07
8.674	3.30E-07
8.650	2.10E-07

TEST LIF: 4.07

TEMPERATURE = 302 (K)
INITIAL STRAIN 0.20 (PCT)
TOTAL STRAIN = 0.88 (PCT)
INITIAL SHEAR STRESS 9.213 (MPA)

SHEAR STRESS (MPA)	STRAIN RATE (/MIN)
9.213	2.00E-03
9.189	1.80E-03
9.166	1.62E-03
9.142	1.34E-03
9.119	1.06E-03
9.095	8.20E-04
9.072	6.40E-04
9.048	4.90E-04
9.025	3.76E-04
9.001	2.82E-04
8.977	2.10E-04
8.954	1.58E-04
8.930	1.14E-04
8.907	8.00E-05
8.883	5.30E-05
8.860	3.50E-05
8.836	2.40E-05
8.812	1.60E-05
8.789	1.20E-05
8.765	8.50E-06
8.742	5.70E-06
8.718	3.70E-06
8.695	2.48E-06
8.671	1.60E-06
8.648	1.00E-06
8.624	6.50E-07
8.600	3.90E-07
8.577	2.20E-07
8.553	1.40E-07

TEST LIF: 4.08

TEMPERATURE = 302 (K)
INITIAL STRAIN 0.00 (PCT)
TOTAL STRAIN = 0.92 (PCT)
INITIAL SHEAR STRESS 9.201 (MPA)

SHEAR STRESS (MPA)	STRAIN RATE (/MIN)
9.193	6.00E-05
9.170	9.90E-05
9.146	9.00E-05
9.122	8.00E-05
9.099	7.10E-05
9.075	6.20E-05
9.052	5.30E-05
9.028	4.40E-05
9.005	3.63E-05
8.981	2.88E-05
8.957	2.23E-05
8.934	1.67E-05
8.910	1.20E-05
8.887	8.40E-06
8.863	5.60E-06
8.840	3.60E-06
8.816	2.30E-06
8.792	1.44E-06
8.769	8.90E-07
8.745	5.40E-07
8.722	3.20E-07
8.698	2.00E-07
8.675	1.20E-07

TEST LIF: 4.09

TEMPERATURE = 302 (K)
INITIAL STRAIN 0.00 (PCT)
TOTAL STRAIN = 0.95 (PCT)
INITIAL SHEAR STRESS 9.215 (MPA)

SHEAR STRESS (MPA)	STRAIN RATE (/MIN)
9.196	6.40E-05
9.172	5.50E-05
9.149	4.50E-05
9.125	7.20E-05
9.102	7.60E-05
9.078	6.80E-05
9.054	5.70E-05
9.031	5.20E-05
9.007	3.90E-05
8.984	3.02E-05
8.960	2.24E-05
8.936	1.64E-05
8.913	1.16E-05
8.889	8.20E-06
8.866	5.60E-06
8.842	3.83E-06
8.819	2.63E-06
8.795	1.67E-06
8.771	1.15E-06
8.748	7.30E-07
8.724	4.30E-07
8.701	2.80E-07
8.677	1.80E-07

TEST LIF: 4.10

TEMPERATURE = 302 (K)
INITIAL STRAIN 0.20 (PCT)
TOTAL STRAIN = 1.19 (PCT)
INITIAL SHEAR STRESS = 9.170 (MPA)

SHEAR STRESS (MPA)	STRAIN RATE (/MIN)
9.123	1.40E-03
9.100	9.40E-04
9.076	7.80E-04
9.052	6.40E-04
9.029	5.20E-04
9.005	4.00E-04
8.981	3.11E-04
8.958	2.34E-04
8.934	1.75E-04
8.910	1.30E-04
8.887	9.40E-05
8.863	6.60E-05
8.840	4.75E-05
8.816	3.40E-05
8.792	2.40E-05
8.769	1.68E-05
8.745	1.16E-05
8.721	8.00E-06
8.698	5.40E-06
8.674	3.60E-06
8.650	2.38E-06
8.627	1.51E-06
8.603	9.30E-07
8.580	5.50E-07
8.556	3.20E-07
8.532	1.80E-07

TEST LIF: 6.01

TEMPERATURE = 302 (K)
INITIAL STRAIN - 0.12 (PCT)
TOTAL STRAIN = 0.12 (PCT)
INITIAL SHEAR STRESS 8.735 (MPA)

SHEAR STRESS (MPA)	STRAIN RATE (/MIN)
8.701	1.88E-03
8.677	1.68E-03
8.654	1.30E-03
8.630	1.02E-03
8.606	8.10E-04
8.582	6.20E-04
8.558	4.80E-04
8.534	3.55E-04
8.511	2.73E-04
8.487	2.02E-04
8.463	1.50E-04
8.439	1.10E-04
8.415	7.70E-05
8.391	5.50E-05
8.368	3.80E-05
8.344	2.65E-05
8.320	1.82E-05
8.296	1.24E-05
8.272	8.30E-06
8.248	5.80E-06
8.225	3.93E-06
8.201	2.68E-06
8.177	1.77E-06
8.153	1.22E-06
8.129	8.00E-07
8.105	5.30E-07
8.082	3.60E-07
8.058	2.40E-07
8.034	1.70E-07
8.010	1.00E-07

TEST LIF: 6.03

TEMPERATURE = 302 (K)
INITIAL STRAIN 0.00 (PCT)
TOTAL STRAIN - 0.18 (PCT)
INITIAL SHEAR STRESS 8.718 (MPA)

SHEAR STRESS (MPA)	STRAIN RATE (/MIN)
8.683	9.70E-05
8.659	9.70E-05
8.635	9.70E-05
8.611	1.02E-04
8.587	1.02E-04
8.563	9.70E-05
8.540	8.90E-05
8.516	7.80E-05
8.492	6.50E-05
8.468	6.00E-05

TEST LIF: 6.02

TEMPERATURE = 302 (K)
INITIAL STRAIN 0.00 (PCT)
TOTAL STRAIN = 0.15 (PCT)
INITIAL SHEAR STRESS - 8.716 (MPA)

SHEAR STRESS (MPA)	STRAIN RATE (/MIN)
8.680	1.30E-04
8.656	1.40E-04
8.632	1.35E-04
8.609	1.23E-04
8.585	1.10E-04
8.561	9.60E-05
8.537	8.30E-05
8.513	7.20E-05
8.489	6.00E-05
8.465	5.00E-05
8.442	4.11E-05
8.418	3.27E-05
8.394	2.58E-05
8.370	1.97E-05
8.346	1.44E-05
8.322	1.05E-05
8.299	7.20E-06
8.275	4.90E-06
8.251	3.23E-06
8.227	2.14E-06
8.203	1.39E-06
8.179	8.70E-07
8.155	5.50E-07
8.132	3.40E-07
8.108	2.10E-07

TEST LIF: 6.04

TEMPERATURE = 302 (K)
INITIAL STRAIN 0.00 (PCT)
TOTAL STRAIN = 0.18 (PCT)
INITIAL SHEAR STRESS 8.716 (MPA)

SHEAR STRESS (MPA)	STRAIN RATE (/MIN)
8.683	9.80E-04
8.659	9.00E-04
8.635	8.00E-04
8.611	7.40E-04
8.587	6.40E-04
8.563	5.60E-04
8.540	4.90E-04
8.516	4.05E-04
8.492	3.41E-04
8.468	2.73E-04
8.444	2.19E-04
8.420	1.73E-04
8.396	1.31E-04
8.373	9.80E-05
8.349	7.10E-05
8.325	5.10E-05
8.301	3.58E-05
8.277	2.45E-05
8.253	1.66E-05
8.229	1.06E-05
8.206	6.80E-06
8.182	4.24E-06
8.158	2.72E-06
8.134	1.71E-06
8.110	1.06E-06
8.086	6.40E-07
8.062	3.70E-07
8.039	2.10E-07
8.015	1.10E-07

TEST LIF: 7.01

TEMPERATURE = 302 (K)
INITIAL STRAIN 0.08 (PCT)
TOTAL STRAIN - 0.08 (PCT)
INITIAL SHEAR STRESS 8.955 (MPA)

SHEAR STRESS (MPA)	STRAIN RATE (/MIN)
8.911	1.29E-03
8.889	1.20E-03
8.867	1.09E-03
8.845	9.40E-04
8.823	7.70E-04
8.801	6.40E-04
8.779	4.90E-04
8.756	3.78E-04
8.734	2.86E-04
8.712	2.12E-04
8.690	1.55E-04
8.668	1.11E-04
8.646	7.60E-05
8.624	5.20E-05
8.602	3.42E-05
8.580	2.20E-05
8.557	1.39E-05
8.535	9.10E-06
8.513	5.70E-06
8.491	3.47E-06
8.469	2.11E-06
8.447	1.27E-06
8.425	7.30E-07
8.403	4.10E-07
8.381	2.20E-07
8.358	1.20E-07

TEST LIF 7.02

TEMPERATURE = 302 (K)
INITIAL STRAIN 0.00 (PCT)
TOTAL STRAIN = 0.11 (PCT)
INITIAL SHEAR STRESS 8.958 (MPA)

SHEAR STRESS (MPA)	STRAIN RATE (/MIN)
8.936	8.00E-05
8.914	1.32E-04
8.892	1.66E-04
8.870	1.87E-04
8.848	1.96E-04
8.825	1.94E-04
8.803	1.86E-04
8.781	1.71E-04
8.759	1.53E-04
8.737	1.35E-04
8.715	1.20E-04

TEST LIF: 7.03

TEMPERATURE = 302 (K)
INITIAL STRAIN 0.00 (PCT)
TOTAL STRAIN = 0.11 (PCT)
INITIAL SHEAR STRESS 8.923 (MPA)

SHEAR STRESS (MPA)	STRAIN RATE (/MIN)
8.870	2.00E-03
8.848	1.80E-03
8.825	1.60E-03
8.803	1.30E-03
8.781	1.07E-03
8.759	8.90E-04
8.737	7.00E-04
8.715	5.70E-04
8.693	4.70E-04
8.671	3.55E-04
8.648	2.79E-04
8.626	2.14E-04
8.604	1.61E-04
8.582	1.15E-04
8.560	8.20E-05
8.538	5.60E-05
8.516	3.80E-05
8.494	2.45E-05
8.472	1.53E-05
8.449	9.30E-06
8.427	5.40E-06
8.405	3.10E-06
8.383	1.76E-06
8.361	9.40E-07
8.339	4.80E-07
8.317	2.30E-07
8.295	1.30E-07

TEST LIF:20.01

TEMPERATURE =	300 (K)
INITIAL STRAIN =	0.07 (PCT)
TOTAL STRAIN =	0.07 (PCT)
INITIAL SHEAR STRESS	8.729 (MPA)

SHEAR STRESS (MPA)	STRAIN RATE (/MIN)
8.670	1.26E-03
8.624	9.25E-04
8.578	6.80E-04
8.532	4.97E-04
8.486	3.66E-04
8.440	2.70E-04
8.394	1.95E-04
8.349	1.37E-04
8.303	9.40E-05
8.257	6.50E-05
8.211	4.54E-05
8.165	3.15E-05
8.119	2.08E-05
8.073	1.43E-05
8.027	9.70E-06
7.982	6.50E-06
7.936	4.40E-06
7.890	3.00E-06
7.844	2.00E-06
7.798	1.37E-06
7.752	9.60E-07
7.706	6.60E-07
7.661	4.50E-07
7.615	2.80E-07
7.569	1.80E-07
7.523	1.10E-07

TEST LIF:20.02

TEMPERATURE =	300 (K)
INITIAL STRAIN =	0.00 (PCT)
TOTAL STRAIN =	0.14 (PCT)
INITIAL SHEAR STRESS	8.474 (MPA)

SHEAR STRESS (MPA)	STRAIN RATE (/MIN)
8.401	4.40E-04
8.355	3.01E-04
8.309	2.20E-04
8.263	1.65E-04
8.217	1.21E-04
8.171	8.70E-05
8.125	6.30E-05
8.079	4.43E-05
8.033	3.01E-05
7.988	2.02E-05
7.942	1.35E-05
7.896	8.90E-06
7.850	6.00E-06
7.804	3.82E-06
7.758	2.47E-06
7.712	1.65E-06
7.666	1.10E-06
7.620	7.20E-07
7.574	4.50E-07
7.528	2.80E-07
7.483	1.80E-07
7.437	1.30E-07

TEST LIF:20.03

TEMPERATURE =	300 (K)
INITIAL STRAIN =	0.00 (PCT)
TOTAL STRAIN =	0.19 (PCT)
INITIAL SHEAR STRESS	8.488 (MPA)

SHEAR STRESS (MPA)	STRAIN RATE (/MIN)
8.405	6.40E-04
8.359	4.50E-04
8.313	3.42E-04
8.267	2.62E-04
8.221	2.02E-04
8.175	1.50E-04
8.129	1.12E-04
8.083	8.00E-05
8.037	5.70E-05
7.992	3.92E-05
7.946	2.68E-05
7.900	1.80E-05
7.854	1.20E-05
7.808	8.00E-06
7.762	5.40E-06
7.716	3.50E-06
7.670	2.31E-06
7.624	1.49E-06
7.578	1.01E-06
7.532	6.80E-07
7.486	4.50E-07
7.440	3.20E-07
7.394	2.20E-07
7.349	1.50E-07

TEST LIF:21.01

TEMPERATURE =	300 (K)
INITIAL STRAIN =	0.06 (PCT)
TOTAL STRAIN =	0.06 (PCT)
INITIAL SHEAR STRESS -	8.592 (MPA)

SHEAR STRESS (MPA)	STRAIN RATE (/MIN)
8.497	1.63E-03
8.444	1.06E-03
8.391	7.60E-04
8.338	5.50E-04
8.285	3.90E-04
8.233	2.70E-04
8.180	1.86E-04
8.127	1.27E-04
8.074	8.40E-05
8.022	5.40E-05
7.969	3.43E-05
7.916	2.12E-05
7.863	1.33E-05
7.810	7.90E-06
7.758	4.65E-06
7.705	2.69E-06
7.652	1.59E-06
7.599	9.30E-07
7.547	5.50E-07
7.494	3.50E-07
7.441	2.10E-07
7.388	1.30E-07

TEST LIF:21.02

TEMPERATURE = 300 (K)
INITIAL STRAIN 0.00 (PCT)
TOTAL STRAIN = 0.10 (PCT)
INITIAL SHEAR STRESS 7.646 (MPA)

SHEAR STRESS (MPA)	STRAIN RATE (/MIN)
7.629	2.60E-06
7.602	1.06E-06
7.576	6.40E-07
7.550	4.70E-07
7.523	3.70E-07
7.497	2.90E-07
7.470	2.20E-07
7.444	1.90E-07
7.418	1.60E-07
7.391	1.20E-07

TEST LIF:21.03

TEMPERATURE = 300 (K)
INITIAL STRAIN - 0.00 (PCT)
TOTAL STRAIN = 0.12 (PCT)
INITIAL SHEAR STRESS - 7.931 (MPA)

SHEAR STRESS (MPA)	STRAIN RATE (/MIN)
7.894	1.90E-05
7.868	1.50E-05
7.842	1.30E-05
7.815	1.09E-05
7.789	9.30E-06
7.762	8.20E-06
7.736	6.80E-06
7.710	5.60E-06
7.683	4.60E-06
7.657	3.73E-06
7.630	3.15E-06
7.604	2.53E-06
7.578	1.93E-06
7.551	1.52E-06
7.525	1.13E-06
7.498	9.20E-07
7.472	7.00E-07
7.446	5.40E-07
7.419	4.00E-07
7.393	3.10E-07
7.366	2.20E-07
7.340	1.70E-07
7.314	1.30E-07
7.287	1.00E-07

TEST LIF 21.04

TEMPERATURE = 300 (K)
INITIAL STRAIN - 0.00 (PCT)
TOTAL STRAIN = 0.14 (PCT)
INITIAL SHEAR STRESS 8.208 (MPA)

SHEAR STRESS (MPA)	STRAIN RATE (/MIN)
8.186	2.70E-04
8.134	2.41E-04
8.081	1.96E-04
8.028	1.55E-04
7.975	1.17E-04
7.922	8.60E-05
7.870	5.90E-05
7.817	3 85E-05
7.764	2.38E-05
7.711	1.40E-05
7.658	8.20E-06
7.605	6.50E-06
7.553	2.51E-06
7.500	1 45E-06
7.447	8.20E-07
7.394	4.70E-07
7.341	2.80E-07
7.289	1.70E-07

TEST LIF:21.05

TEMPERATURE = 300 (K)
INITIAL STRAIN = 0.00 (PCT)
TOTAL STRAIN = 0.20 (PCT)
INITIAL SHEAR STRESS = 8.329 (MPA)

SHEAR STRESS (MPA)	STRAIN RATE (/MIN)
8.297	1.45E-03
8.271	1.29E-03
8.244	1.14E-03
8.218	1.00E-03
8.191	9.00E-04
8.165	7.90E-04
8.139	6.90E-04
8.112	6.00E-04
8.086	5.15E-04
8.059	4.40E-04
8.033	3.72E-04
8.006	3.13E-04
7.980	2.60E-04
7.954	2.13E-04
7.927	1.76E-04
7.901	1.43E-04
7.874	1.15E-04
7.848	9.10E-05
7.821	7.10E-05
7.795	5.54E-05
7.769	4.10E-05
7.742	3.25E-05
7.716	2.50E-05
7.689	1.90E-05
7.663	1 46E-05
7.636	1.18E-05
7.610	8.90E-06
7.584	6.50E-06
7.557	4.90E-06
7.531	3.72E-06
7.504	2.75E-06
7.478	2.08E-06
7.451	1.53E-06
7.425	1.14E-06
7.399	8.40E-07
7.372	6 30E-07
7.346	4.70E-07
7.319	3.30E-07
7.293	2.40E-07
7.267	1.70E-07

TEST LIF:21.06

TEMPERATURE = 300 (K)
INITIAL STRAIN 0.18 (PCT)
TOTAL STRAIN = 0.43 (PCT)
INITIAL SHEAR STRESS = 8.237 (MPA)

SHEAR STRESS (MPA)	STRAIN RATE (/MIN)
8.184	1.75E-03
8.157	1.24E-03
8.131	9.50E-04
8.104	7.40E-04
8.078	5.90E-04
8.051	4.80E-04
8.025	3.93E-04
7.998	3.19E-04
7.972	2.56E-04
7.945	2.05E-04
7.919	1.65E-04
7.892	1.29E-04
7.866	1.03E-04
7.839	8.00E-05
7.813	6.30E-05
7.786	4.90E-05
7.760	3.83E-05
7.733	2.92E-05
7.707	2.22E-05
7.680	1.70E-05
7.654	1.29E-05
7.627	1.00E-05
7.601	7.80E-06
7.575	6.00E-06
7.548	4.50E-06
7.522	3.44E-06
7.495	2.63E-06
7.469	1.99E-06
7.442	1.49E-06
7.416	1.13E-06
7.389	8.50E-07
7.363	6.20E-07
7.336	4.70E-07
7.310	3.40E-07
7.283	2.60E-07
7.257	2.00E-07
7.230	1.40E-07

TEST LIF:21.07

TEMPERATURE = 300 (K)
INITIAL STRAIN = 0.00 (PCT)
TOTAL STRAIN = 0.48 (PCT)
INITIAL SHEAR STRESS = 8.225 (MPA)

SHEAR STRESS (MPA)	STRAIN RATE (/MIN)
8.188	9.00E-04
8.161	7.20E-04
8.135	6.00E-04
8.108	5.10E-04
8.082	4.36E-04
8.055	3.70E-04
8.029	3.13E-04
8.002	2.66E-04
7.976	2.21E-04
7.949	1.83E-04
7.923	1.52E-04
7.896	1.23E-04
7.870	1.00E-04
7.843	8.00E-05
7.817	6.40E-05
7.790	5.00E-05
7.764	3.96E-05
7.737	3.05E-05
7.711	2.36E-05
7.684	1.80E-05
7.658	1.44E-05
7.631	1.10E-05
7.605	8.00E-06
7.578	6.20E-06
7.552	4.66E-06
7.525	3.55E-06
7.499	2.70E-06
7.472	2.04E-06
7.446	1.56E-06
7.419	1.18E-06
7.393	8.80E-07
7.366	6.70E-07
7.340	5.00E-07
7.313	3.80E-07
7.287	2.80E-07
7.260	2.20E-07

TEST LIF:21.08

TEMPERATURE = 300 (K)
INITIAL STRAIN 0.00 (PCT)
TOTAL STRAIN = 0.54 (PCT)
INITIAL SHEAR STRESS 8.238 (MPA)

SHEAR STRESS (MPA)	STRAIN RATE (/MIN)
8.193	9.60E-04
8.166	7.80E-04
8.140	6.60E-04
8.113	5.70E-04
8.087	4.84E-04
8.060	4.14E-04
8.034	3.46E-04
8.007	2.93E-04
7.981	2.43E-04
7.954	2.00E-04
7.927	1.64E-04
7.901	1.32E-04
7.874	1.06E-04
7.848	8.40E-05
7.821	6.60E-05
7.795	5.21E-05
7.768	4.08E-05
7.742	3.12E-05
7.715	2.39E-05
7.689	1.80E-05
7.662	1.38E-05
7.636	1.06E-05
7.609	8.00E-06
7.583	6.10E-06
7.556	4.60E-06
7.530	3.52E-06
7.503	2.65E-06
7.477	2.04E-06
7.450	1.54E-06
7.424	1.18E-06
7.397	8.90E-07
7.371	6.90E-07
7.344	5.30E-07
7.318	4.10E-07
7.291	3.10E-07
[illegible]	2.40E-07
[illegible]	1.90E-07

TEST LIF:21.09

TEMPERATURE = 300 (K)
INITIAL STRAIN 0.20 (PCT)
TOTAL STRAIN = 0.78 (PCT)
INITIAL SHEAR STRESS 8.239 (MPA)

SHEAR STRESS (MPA)	STRAIN RATE (/MIN)
8.186	1.46E-03
8.159	1.07E-03
8.132	8.30E-04
8.106	6.50E-04
8.079	5.20E-04
8.053	4.19E-04
8.026	3.40E-04
8.000	2.74E-04
7.973	2.20E-04
7.946	1.77E-04
7.920	1.40E-04
7.893	1.12E-04
7.867	8.70E-05
7.840	6.90E-05
7.814	5.33E-05
7.787	4.16E-05
7.760	3.16E-05
7.734	2.46E-05
7.707	1.87E-05
7.681	1.42E-05
7.654	1.12E-05
7.628	8.20E-06
7.601	6.50E-06
7.574	4.77E-06
7.548	3.78E-06
7.521	2.93E-06
7.495	2.16E-06
7.468	1.69E-06
7.441	1.23E-06
7.415	9.50E-07
7.388	7.80E-07
7.362	5.20E-07
7.335	3.80E-07
7.309	3.10E-07
7.282	2.30E-07
7.255	1.70E-07
7.229	1.40E-07

TEST LIF:21.10

TEMPERATURE = 300 (K)
INITIAL STRAIN 0.21 (PCT)
TOTAL STRAIN 1.05 (PCT)
INITIAL SHEAR STRESS 8.327 (MPA)

SHEAR STRESS (MPA)	STRAIN RATE (/MIN)
8.261	1.38E-03
8.234	1.06E-03
8.208	8.40E-04
8.181	6.80E-04
8.154	5.40E-04
8.128	4.42E-04
8.101	3.51E-04
8.074	2.85E-04
8.048	2.30E-04
8.021	1.83E-04
7.994	1.44E-04
7.968	1.14E-04
7.941	8.90E-05
7.914	7.10E-05
7.888	5.36E-05
7.861	4.21E-05
7.834	3.26E-05
7.808	2.53E-05
7.781	1.97E-05
7.755	1.55E-05
7.728	1.13E-05
7.701	9.00E-06
7.675	7.10E-06
7.648	5.20E-06
7.621	4.14E-06
7.595	3.27E-06
7.568	2.61E-06
7.541	1.98E-06
7.515	1.34E-06
7.488	1.03E-06
7.461	8.10E-07
7.435	5.80E-07
7.408	4.40E-07
7.381	3.40E-07
7.355	2.80E-07
7.328	2.20E-07

TEST LIF:21.11

TEMPERATURE = 300 (K)
INITIAL STRAIN 0.18 (PCT)
TOTAL STRAIN = 1.28 (PCT)
INITIAL SHEAR STRESS - 8.322 (MPA)

SHEAR STRESS (MPA)	STRAIN RATE (/MIN)
8.280	1.86E-03
8.253	1.29E-03
8.226	9.60E-04
8.200	7.50E-04
8.173	6.00E-04
8.146	4.78E-04
8.119	3.84E-04
8.093	3.04E-04
8.066	2.44E-04
8.039	1.91E-04
8.013	1.52E-04
7.986	1.20E-04
7.959	9.30E-05
7.932	7.30E-05
7.906	5.60E-05
7.879	4.40E-05
7.852	3.37E-05
7.826	2.64E-05
7.799	2.01E-05
7.772	1.55E-05
7.745	1.19E-05
7.719	9.20E-06
7.692	7.10E-06
7.665	5.45E-06
7.639	4.26E-06
7.612	3.29E-06
7.585	2.53E-06
7.559	1.94E-06
7.532	1.50E-06
7.505	1.14E-06
7.478	8.60E-07
7.452	6.50E-07
7.425	4.90E-07
7.398	3.60E-07
7.372	2.60E-07
7.345	1.90E-07

TEST LIF:21.12

TEMPERATURE = 300 (K)
INITIAL STRAIN 0.21 (PCT)
TOTAL STRAIN = 1.53 (PCT)
INITIAL SHEAR STRESS 8.327 (MPA)

SHEAR STRESS (MPA)	STRAIN RATE (/MIN)
8.273	1.87E-03
8.247	1.19E-03
8.220	8.80E-04
8.193	6.80E-04
8.166	5.40E-04
8.139	4.27E-04
8.113	3.39E-04
8.086	2.74E-04
8.059	2.17E-04
8.032	1.72E-04
8.006	1.37E-04
7.979	1.07E-04
7.952	8.50E-05
7.925	6.60E-05
7.898	5.14E-05
7.872	4.00E-05
7.845	3.09E-05
7.818	2.35E-05
7.791	1.81E-05
7.765	1.39E-05
7.738	1.08E-05
7.711	8.20E-06
7.684	6.30E-06
7.657	4.83E-06
7.631	3.75E-06
7.604	2.81E-06
7.577	2.16E-06
7.550	1.66E-06
7.524	1.29E-06
7.497	1.00E-06
7.470	7.80E-07
7.443	5.90E-07
7.417	4.50E-07
7.390	3.40E-07
7.363	2.70E-07
7.335	2.30E-07

TEST LIF:22.01

TEMPERATURE = 281 (K)
INITIAL STRAIN 0.06 (PCT)
TOTAL STRAIN = 0.06 (PCT)
INITIAL SHEAR STRESS 8.564 (MPA)

SHEAR STRESS (MPA)	STRAIN RATE (/MIN)
8.513	1.41E-03
8.463	1.10E-03
8.413	8.70E-04
8.363	7.00E-04
8.313	5.40E-04
8.263	4.26E-04
8.213	3.32E-04
8.163	2.57E-04
8.113	1.99E-04
8.063	1.50E-04
8.013	1.14E-04
7.963	8.60E-05
7.912	6.50E-05
7.862	4.80E-05
7.812	3.49E-05
7.762	2.61E-05
7.712	1.90E-05
7.662	1.38E-05
7.612	9.70E-06
7.562	7.20E-06
7.512	5.50E-06
7.462	4.10E-06
7.412	2.90E-06
7.362	2.12E-06
7.312	1.57E-06
7.261	1.13E-06
7.211	8.30E-07
7.161	6.10E-07
7.111	4.50E-07
7.061	3.10E-07
7.011	2.20E-07
6.961	1.60E-07

TEST LIF:23.01

TEMPERATURE =	281 (K)
INITIAL STRAIN	0.08 (PCT)
TOTAL STRAIN	0.08 (PCT)
INITIAL SHEAR STRESS	8.450 (MPA)

SHEAR STRESS (MPA)	STRAIN RATE (/MIN)
8.408	1.10E-03
8.356	8.60E-04
8.303	6.70E-04
8.251	5.20E-04
8.199	4.13E-04
8.147	3.23E-04
8.095	2.54E-04
8.042	1.98E-04
7.990	1.53E-04
7.938	1.18E-04
7.886	9.00E-05
7.833	6.90E-05
7.781	5.20E-05
7.729	3.90E-05
7.677	2.95E-05
7.624	2.21E-05
7.572	1.66E-05
7.520	1.23E-05
7.468	8.90E-06
7.416	6.30E-06
7.363	4.47E-06
7.311	3.17E-06
7.259	2.31E-06
7.207	1.67E-06
7.154	1.23E-06
7.102	8.80E-07
7.050	6.40E-07
6.998	4.50E-07
6.946	3.00E-07
6.893	2.00E-07
6.841	1.30E-07

TEST LIF:23.02

TEMPERATURE =	281 (K)
INITIAL STRAIN	0.00 (PCT)
TOTAL STRAIN =	0.17 (PCT)
INITIAL SHEAR STRESS	8.389 (MPA)

SHEAR STRESS (MPA)	STRAIN RATE (/MIN)
8.363	7.90E-04
8.311	6.60E-04
8.259	5.30E-04
8.206	4.20E-04
8.154	3.36E-04
8.102	2.70E-04
8.050	2.14E-04
7.997	1.70E-04
7.945	1.34E-04
7.893	1.05E-04
7.840	8.10E-05
7.788	6.10E-05
7.736	4.57E-05
7.684	3.41E-05
7.631	2.46E-05
7.579	1.77E-05
7.527	1.26E-05
7.475	8.90E-06
7.422	6.40E-06
7.370	4.50E-06
7.318	3.20E-06
7.265	2.20E-06
7.213	1.50E-06
7.161	1.03E-06
7.109	7.00E-07
7.056	4.80E-07
7.004	3.30E-07
6.952	2.20E-07
6.900	1.60E-07
6.847	1.10E-07

TEST LIF:23.03

TEMPERATURE =	281 (K)
INITIAL STRAIN	0.10 (PCT)
TOTAL STRAIN =	0.34 (PCT)
INITIAL SHEAR STRESS	8.472 (MPA)

SHEAR STRESS (MPA)	STRAIN RATE (/MIN)
8.430	1.89E-03
8.377	1.47E-03
8.325	1.12E-03
8.273	8.90E-04
8.220	7.00E-04
8.168	5.60E-04
8.116	4.41E-04
8.063	3.44E-04
8.011	2.68E-04
7.958	2.05E-04
7.906	1.56E-04
7.854	1.12E-04
7.801	8.10E-05
7.749	5.80E-05
7.697	4.11E-05
7.644	2.92E-05
7.592	2.09E-05
7.540	1.48E-05
7.487	1.06E-05
7.435	7.60E-06
7.383	5.50E-06
7.330	3.86E-06
7.278	2.70E-06
7.225	1.88E-06
7.173	1.31E-06
7.121	9.40E-07
7.068	6.30E-07
7.016	4.20E-07
6.964	3.00E-07
6.911	2.10E-07
6.859	1.50E-07

TEST LIF:23.04

TEMPERATURE =	281 (K)
INITIAL STRAIN	0.20 (PCT)
TOTAL STRAIN =	0.63 (PCT)
INITIAL SHEAR STRESS	8.543 (MPA)

SHEAR STRESS (MPA)	STRAIN RATE (/MIN)
8.507	1.83E-03
8.454	1.38E-03
8.402	1.05E-03
8.349	8.00E-04
8.297	6.30E-04
8.244	4.94E-04
8.191	3.82E-04
8.139	2.96E-04
8.086	2.27E-04
8.034	1.73E-04
7.981	1.32E-04
7.929	1.00E-04
7.876	7.50E-05
7.824	5.60E-05
7.771	4.12E-05
7.719	3.05E-05
7.666	2.25E-05
7.614	1.65E-05
7.561	1.20E-05
7.509	9.70E-06
7.456	8.20E-06
7.404	4.74E-06
7.351	4.39E-06
7.299	3.71E-06
7.246	2.95E-06
7.194	1.63E-06
7.141	1.30E-06
7.089	8.50E-07
7.036	6.00E-07
6.984	4.10E-07
6.931	2.90E-07
6.879	2.10E-07
6.826	1.40E-07

TEST LIF:24.02

TEMPERATURE = 258 (K)
INITIAL STRAIN = 0.00 (PCT)
TOTAL STRAIN = 0.04 (PCT)
INITIAL SHEAR STRESS = 10.181 (MPA)

SHEAR STRESS (MPA)	STRAIN RATE (/MIN)
10.111	9.50E-04
10.062	1.00E-03
10.012	9.90E-04
9.963	9.60E-04
9.913	9.10E-04
9.863	8.60E-04
9.814	8.00E-04
9.764	7.40E-04
9.715	6.80E-04
9.665	6.10E-04
9.616	5.50E-04
9.566	5.00E-04
9.517	4.39E-04
9.467	3.89E-04
9.417	3.38E-04
9.368	2.92E-04
9.318	2.49E-04
9.269	2.12E-04
9.219	1.79E-04
9.170	1.51E-04
9.120	1.27E-04
9.070	1.06E-04
9.021	8.70E-05
8.971	7.00E-05
8.922	5.60E-05
8.872	4.40E-05
8.823	3.47E-05
8.773	2.72E-05
8.723	2.10E-05
8.674	1.63E-05
8.624	1.28E-05
8.575	1.00E-05
8.525	7.70E-06
8.476	5.80E-06
8.426	4.30E-06
8.377	3.17E-06
8.327	2.31E-06
8.277	1.69E-06
8.228	1.22E-06
8.178	8.70E-07
8.129	6.20E-07
8.079	4.50E-07
8.030	3.30E-07
7.980	2.40E-07

TEST LIF:24.03

TEMPERATURE = 258 (K)
INITIAL STRAIN = 0.00 (PCT)
TOTAL STRAIN = 0.45 (PCT)
INITIAL SHEAR STRESS 9.182 (MPA)

SHEAR STRESS (MPA)	STRAIN RATE (/MIN)
9.157	1.13E-03
9.108	1.03E-03
9.058	8.30E-04
9.008	6.80E-04
8.958	5.60E-04
8.909	4.57E-04
8.859	3.75E-04
8.809	3.05E-04
8.759	2.48E-04
8.709	1.98E-04
8.660	1.57E-04
8.610	1.23E-04
8.560	9.70E-05
8.510	7.50E-05
8.461	5.80E-05
8.411	4.44E-05
8.361	3.35E-05
8.311	2.53E-05
8.262	1.87E-05
8.212	1.39E-05
8.162	1.02E-05
8.112	7.50E-06
8.062	5.50E-06
8.013	4.05E-06
7.963	2.80E-06
7.913	2.06E-06
7.863	1.46E-06
7.814	1.04E-06
7.764	7.40E-07
7.714	5.20E-07
	E-07

TEST LIF:24.04

TEMPERATURE = 258 (K)
INITIAL STRAIN = 0.21 (PCT)
TOTAL STRAIN = 0.35 (PCT)
INITIAL SHEAR STRESS 9.347 (MPA)

SHEAR STRESS (MPA)	STRAIN RATE (/MIN)
9.297	1.68E-03
9.248	1.40E-03
9.198	1.15E-03
9.148	9.40E-04
9.099	7.70E-04
9.049	6.40E-04
8.999	5.20E-04
8.949	4.29E-04
8.900	3.56E-04
8.850	2.90E-04
8.800	2.34E-04
8.751	1.89E-04
8.701	1.51E-04
8.651	1.18E-04
8.601	9.20E-05
8.552	7.20E-05
8.502	5.60E-05
8.452	4.25E-05
8.402	3.25E-05
8.353	2.45E-05
8.303	1.87E-05
8.253	1.41E-05
8.204	1.07E-05
8.154	8.00E-06
8.104	6.00E-06
8.054	4.44E-06
8.005	3.20E-06
7.955	2.30E-06
7.905	1.60E-06
7.856	1.11E-06
7.806	7.70E-07
7.756	5.50E-07
7.706	3.80E-07
7.657	2.60E-07
7.607	1.80E-07
7.557	1.30E-07

TEST LIF:24.04

TEMPERATURE = 258 (K)
INITIAL STRAIN = 0.17 (PCT)
TOTAL STRAIN = 0.70 (PCT)
INITIAL SHEAR STRESS 9.045 (MPA)

SHEAR STRESS (MPA)	STRAIN RATE (/MIN)
9.031	1.60E-03
8.981	1.40E-03
8.931	1.10E-03
8.881	8.90E-04
8.831	7.20E-04
8.781	5.70E-04
8.731	4.54E-04
8.681	3.57E-04
8.631	2.79E-04
8.581	2.17E-04
8.532	1.69E-04
8.482	1.30E-04
8.432	1.00E-04
8.382	7.60E-05
8.332	5.80E-05
8.282	4.34E-05
8.232	3.23E-05
8.182	2.42E-05
8.132	1.78E-05
8.083	1.33E-05
8.033	9.70E-06
7.983	7.00E-06
7.933	5.00E-06
7.883	3.57E-06
7.833	2.53E-06
7.783	1.79E-06
7.733	1.27E-06
7.683	8.80E-07
7.634	6.10E-07
7.584	4.30E-07
7.534	3.10E-07

TEST LIF:24.05

TEMPERATURE = 258 (K)
INITIAL STRAIN 0.16 (PCT)
TOTAL STRAIN 0.92 (PCT)
INITIAL SHEAR STRESS = 9.025 (MPA)

SHEAR STRESS (MPA)	STRAIN RATE (/MIN)
9.000	1.62E-03
8.950	1.36E-03
8.900	1.10E-03
8.850	8.60E-04
8.800	6.90E-04
8.750	5.40E-04
8.700	4.30E-04
8.650	3.35E-04
8.600	2.60E-04
8.550	2.03E-04
8.500	1.56E-04
8.450	1.18E-04
8.400	8.90E-05
8.350	6.70E-05
8.300	5.10E-05
8.250	3.80E-05
8.200	2.84E-05
8.150	2.16E-05
8.100	1.60E-05
8.050	1.17E-05
8.000	8.50E-06
7.950	6.10E-06
7.900	4.43E-06
7.850	3.13E-06
7.800	2.21E-06
7.750	1.57E-06
7.700	1.08E-06
7.650	7.60E-07
7.600	5.20E-07
7.550	3.70E-07
7.500	2.60E-07
7.450	1.70E-07

TEST LIF:25.01

TEMPERATURE 258 (K)
INITIAL STRAIN 0.07 (PCT)
TOTAL STRAIN = 0.07 (PCT)
INITIAL SHEAR STRESS =11.133 (MPA)

SHEAR STRESS (MPA)	STRAIN RATE (/MIN)
11.101	9.80E-04
11.055	7.30E-04
11.010	5.90E-04
10.964	4.60E-04
10.918	3.71E-04
10.872	3.04E-04
10.826	2.60E-04
10.780	2.26E-04
10.734	2.01E-04
10.688	1.80E-04
10.643	1.61E-04
10.597	1.44E-04
10.551	1.28E-04
10.505	1.11E-04
10.459	9.50E-05
10.413	8.40E-05
10.367	7.10E-05
10.321	6.00E-05
10.276	5.10E-05
10.230	4.16E-05
10.184	3.39E-05
10.138	2.70E-05
10.092	2.15E-05
10.046	1.63E-05
10.000	1.26E-05
9.954	9.60E-06
9.909	7.30E-06
9.863	5.60E-06
9.817	4.16E-06
9.771	3.13E-06
9.725	2.34E-06
9.679	1.75E-06
9.633	1.30E-06
9.588	9.70E-07
9.542	7.20E-07
9.496	5.40E-07
9.450	3.90E-07
9.404	3.00E-07
9.358	2.30E-07
	0E-07

TEST LIF:24.06

TEMPERATURE 258 (K)
INITIAL STRAIN - 0.11 (PCT)
TOTAL STRAIN 1.12 (PCT)
INITIAL SHEAR STRESS 9.118 (MPA)

SHEAR STRESS (MPA)	STRAIN RATE (/MIN)
9.068	2.91E-03
9.018	2.41E-03
8.968	1.92E-03
8.918	1.50E-03
8.868	1.20E-03
8.818	9.40E-04
8.768	7.40E-04
8.717	5.80E-04
8.667	4.45E-04
8.617	3.42E-04
8.567	2.64E-04
8.517	2.01E-04
8.467	1.53E-04
8.417	1.14E-04
8.367	8.60E-05
8.317	6.40E-05
8.267	4.70E-05
8.216	3.48E-05
8.166	2.55E-05
8.116	1.87E-05
8.066	1.36E-05
8.016	9.80E-06
7.966	7.10E-06
7.916	5.10E-06
7.866	3.66E-06
7.816	2.56E-06
7.766	1.83E-06
7.715	1.28E-06
7.665	9.00E-07
7.615	6.30E-07
7.565	4.60E-07
7.515	3.20E-07
7.465	2.30E-07
7.415	1.60E-07

TEST LIF:25.02

TEMPERATURE 258 (K)
INITIAL STRAIN 0.20 (PCT)
TOTAL STRAIN 0.38 (PCT)
INITIAL SHEAR STRESS =10.137 (MPA)

SHEAR STRESS (MPA)	STRAIN RATE (/MIN)
10.123	1.79E-03
10.077	1.91E-03
10.031	1.52E-03
9.985	1.20E-03
9.939	9.50E-04
9.893	7.40E-04
9.847	5.90E-04
9.801	4.63E-04
9.755	3.60E-04
9.709	2.79E-04
9.663	2.12E-04
9.617	1.60E-04
9.571	1.19E-04
9.525	8.80E-05
9.479	6.40E-05
9.433	4.58E-05
9.387	3.30E-05
9.341	2.30E-05
9.295	1.59E-05
9.249	1.08E-05
9.203	7.30E-06
9.157	4.92E-06
9.111	3.29E-06
9.065	2.18E-06
9.019	1.43E-06
8.973	9.50E-07
8.927	6.10E-07
8.881	4.20E-07
8.835	2.80E-07
8.789	1.90E-07
8.743	1.30E-07

TEST LIF:25.03

TEMPERATURE = 258 (K)
INITIAL STRAIN 0.00 (PCT)
TOTAL STRAIN = 0.46 (PCT)
INITIAL SHEAR STRESS = 10.154 (MPA)

SHEAR STRESS (MPA)	STRAIN RATE (/MIN)
10.131	5.10E-04
10.108	7.10E-04
10.085	8.20E-04
10.062	8.70E-04
10.039	8.80E-04
10.016	8.80E-04
9.993	8.70E-04
9.970	8.50E-04
9.947	8.20E-04
9.924	7.90E-04
9.901	7.50E-04
9.878	7.10E-04
9.855	6.80E-04
9.809	6.00E-04
9.763	5.10E-04
9.717	4.41E-04
9.671	3.60E-04
9.625	3.01E-04
9.579	2.41E-04
9.533	1.92E-04
9.487	1.51E-04
9.441	1.15E-04
9.395	8.80E-05
9.348	6.30E-05
9.303	4.43E-05
9.256	3.07E-05
9.210	2.11E-05
9.164	1.44E-05
9.118	9.90E-06
9.072	6.60E-06
9.026	4.47E-06
8.980	2.92E-06
8.934	1.86E-06
8.888	1.23E-06
8.842	8.30E-07
8.796	5.60E-07
8.750	3.70E-07
8.704	2.40E-07
8.658	1.60E-07

TEST LIF:26.01

TEMPERATURE = 319 (K)
INITIAL STRAIN 0.14 (PCT)
TOTAL STRAIN = 0.14 (PCT)
INITIAL SHEAR STRESS 9.082 (MPA)

SHEAR STRESS (MPA)	STRAIN RATE (/MIN)
9.065	2.33E-03
9.020	2.14E-03
8.975	1.72E-03
8.931	1.41E-03
8.886	1.11E-03
8.841	8.90E-04
8.797	7.00E-04
8.752	5.50E-04
8.707	4.27E-04
8.663	3.24E-04
8.618	2.45E-04
8.573	1.83E-04
8.529	1.33E-04
8.484	9.30E-05
8.439	6.40E-05
8.395	4.27E-05
8.350	2.81E-05
8.306	1.81E-05
8.261	1.14E-05
8.216	7.70E-06
8.172	4.67E-06
8.127	2.80E-06
8.082	1.64E-06
8.038	9.50E-07
7.993	5.60E-07
7.948	3.60E-07
7.904	2.40E-07
7.859	1.60E-07
7.814	1.10E-07

TEST LIF:26.02

TEMPERATURE = 319 (K)
INITIAL STRAIN 0.00 (PCT)
TOTAL STRAIN = 0.22 (PCT)
INITIAL SHEAR STRESS 9.161 (MPA)

SHEAR STRESS (MPA)	STRAIN RATE (/MIN)
9.117	1.83E-03
9.072	2.12E-03
9.027	2.21E-03
8.982	2.18E-03
8.938	2.09E-03
8.893	1.96E-03
8.848	1.80E-03
8.804	1.62E-03
8.759	1.43E-03
8.714	1.25E-03
8.670	1.06E-03
8.625	8.90E-04
8.580	7.20E-04
8.536	5.70E-04
8.491	4.38E-04
8.446	3.30E-04
8.402	2.41E-04
8.357	1.73E-04
8.312	1.23E-04
8.267	8.50E-05
8.223	5.70E-05
8.178	3.75E-05
8.133	2.50E-05
8.089	1.54E-05
8.044	9.30E-06
7.999	5.40E-06
7.955	3.05E-06
7.910	1.73E-06
7.865	9.70E-07
[illegible]	5.50E-07

TEST LIF:26.03

TEMPERATURE = 319 (K)
INITIAL STRAIN 0.19 (PCT)
TOTAL STRAIN = 0.50 (PCT)
INITIAL SHEAR STRESS 8.524 (MPA)

SHEAR STRESS (MPA)	STRAIN RATE (/MIN)
8.515	2.06E-03
8.470	1.93E-03
8.425	1.36E-03
8.380	1.03E-03
8.335	7.90E-04
8.291	5.90E-04
8.246	4.47E-04
8.201	3.33E-04
8.156	2.40E-04
8.111	1.74E-04
8.066	1.23E-04
8.022	8.50E-05
7.977	5.50E-05
7.932	3.57E-05
7.887	2.30E-05
7.842	1.45E-05
7.798	8.70E-06
7.753	5.10E-06
7.708	2.90E-06
7.663	1.66E-06
7.618	9.30E-07
7.574	5.40E-07
7.529	3.10E-07
7.484	1.80E-07
7.439	1.10E-07

TEST LIF:26.04

TEMPERATURE =	319 (K)
INITIAL STRAIN	0.00 (PCT)
TOTAL STRAIN =	0.56 (PCT)
INITIAL SHEAR STRESS	8.529 (MPA)

SHEAR STRESS (MPA)	STRAIN RATE (/MIN)
8.520	2.85E-04
8.475	2.86E-04
8.430	2.89E-04
8.385	2.74E-04
8.340	2.51E-04
8.296	2.25E-04
8.251	1.97E-04
8.206	1.65E-04
8.161	1.37E-04
8.116	1.12E-04
8.071	9.10E-05
8.026	6.70E-05
7.982	4.90E-05
7.937	3.55E-05
7.892	2.48E-05
7.847	1.68E-05
7.802	1.06E-05
7.757	6.80E-06
7.713	4.04E-06
7.668	2.42E-06
7.623	1.39E-06
7.578	7.90E-07
7.533	4.60E-07
7.488	2.80E-07
7.444	1.70E-07

TEST LIF:26.05

TEMPERATURE =	319 (K)
INITIAL STRAIN	0.19 (PCT)
TOTAL STRAIN =	0.82 (PCT)
INITIAL SHEAR STRESS	8.353 (MPA)

SHEAR STRESS (MPA)	STRAIN RATE (/MIN)
8.317	2.05E-03
8.272	1.52E-03
8.227	1.17E-03
8.182	8.90E-04
8.137	6.70E-04
8.092	5.00E-04
8.047	3.85E-04
8.002	2.79E-04
7.957	1.99E-04
7.912	1.41E-04
7.867	1.00E-04
7.822	6.60E-05
7.777	4.38E-05
7.733	2.89E-05
7.688	1.91E-05
7.643	1.19E-05
7.598	7.20E-06
7.553	4.20E-06
7.508	2.30E-06
7.463	1.30E-06
7.418	7.20E-07
7.373	4.30E-07
7.328	2.50E-07
7.283	1.50E-07

TEST LIF:26.06

TEMPERATURE =	305 (K)
INITIAL STRAIN	0.12 (PCT)
TOTAL STRAIN =	1.00 (PCT)
INITIAL SHEAR STRESS	7.600 (MPA)

SHEAR STRESS (MPA)	STRAIN RATE (/MIN)
7.559	1.68E-03
7.514	1.24E-03
7.469	9.10E-04
7.424	6.60E-04
7.379	4.85E-04
7.334	3.68E-04
7.289	2.67E-04
7.244	1.96E-04
7.199	1.44E-04
7.154	1.03E-04
7.109	7.30E-05
7.064	5.10E-05
7.019	3.52E-05
6.974	2.41E-05
6.928	1.67E-05
6.883	1.15E-05
6.838	8.00E-06
6.793	5.40E-06
6.748	3.70E-06
6.703	2.45E-06
6.658	1.58E-06
6.613	1.03E-06
6.568	6.40E-07
6.523	4.00E-07
6.478	2.50E-07
6.433	1.50E-07

TEST LIF:26.07

TEMPERATURE =	294 (K)
INITIAL STRAIN	0.17 (PCT)
TOTAL STRAIN =	1.23 (PCT)
INITIAL SHEAR STRESS	7.913 (MPA)

SHEAR STRESS (MPA)	STRAIN RATE (/MIN)
7.877	1.56E-03
7.832	1.15E-03
7.787	8.60E-04
7.741	6.30E-04
7.696	4.65E-04
7.651	3.40E-04
7.606	2.49E-04
7.561	1.80E-04
7.516	1.30E-04
7.471	9.20E-05
7.425	6.60E-05
7.380	4.60E-05
7.335	3.33E-05
7.290	2.33E-05
7.245	1.62E-05
7.200	1.13E-05
7.155	7.90E-06
7.109	5.40E-06
7.064	3.76E-06
7.019	2.56E-06
6.974	1.75E-06
6.929	1.18E-06
6.884	8.00E-07
6.839	5.30E-07
6.793	3.50E-07
6.748	2.10E-07
6.703	1.40E-07

TEST LIF:26.08

TEMPERATURE = 282 (K)
INITIAL STRAIN 0.20 (PCT)
TOTAL STRAIN = 1.49 (PCT)
INITIAL SHEAR STRESS = 8.141 (MPA)

SHEAR STRESS (MPA)	STRAIN RATE (/MIN)
8.110	1.81E-03
8.064	1.23E-03
8.019	9.00E-04
7.974	6.60E-04
7.929	4.93E-04
7.883	3.59E-04
7.838	2.66E-04
7.793	1.92E-04
7.748	1.38E-04
7.702	9.80E-05
7.657	6.90E-05
7.612	4.90E-05
7.567	3.35E-05
7.521	2.32E-05
7.476	1.62E-05
7.431	1.15E-05
7.386	8.10E-06
7.340	5.70E-06
7.295	3.85E-06
7.250	2.63E-06
7.205	1.79E-06
7.159	1.21E-06
7.114	8.10E-07
7.069	5.30E-07
7.024	3.60E-07
6.979	2.30E-07
6.933	1.50E-07

TEST LIF:26.09

TEMPERATURE = 274 (K)
INITIAL STRAIN 0.20 (PCT)
TOTAL STRAIN = 1.75 (PCT)
INITIAL SHEAR STRESS 8.376 (MPA)

SHEAR STRESS (MPA)	STRAIN RATE (/MIN)
8.335	1.62E-03
8.289	1.20E-03
8.244	8.80E-04
8.199	6.40E-04
8.153	4.74E-04
8.108	3.48E-04
8.062	2.56E-04
8.017	1.83E-04
7.972	1.31E-04
7.926	9.40E-05
7.881	6.70E-05
7.836	4.70E-05
7.790	3.21E-05
7.745	2.21E-05
7.700	1.53E-05
7.654	1.05E-05
7.609	7.20E-06
7.563	5.20E-06
7.518	3.50E-06
7.473	2.40E-06
7.427	1.50E-06
7.382	9.80E-07
7.337	6.70E-07
7.291	4.40E-07
7.246	2.90E-07
7.200	2.20E-07
7.155	1.70E-07

TEST LIF:33.01

TEMPERATURE = 305 (K)
INITIAL STRAIN 0.13 (PCT)
TOTAL STRAIN 0.13 (PCT)
INITIAL SHEAR STRESS 7.897 (MPA)

SHEAR STRESS (MPA)	STRAIN RATE (/MIN)
7.799	2.24E-03
7.750	2.09E-03
7.701	1.73E-03
7.652	1.38E-03
7.603	1.04E-03
7.554	8.00E-04
7.505	5.70E-04
7.456	4.15E-04
7.407	2.98E-04
7.357	2.15E-04
7.308	1.52E-04
7.259	1.05E-04
7.210	7.30E-05
7.161	4.80E-05
7.112	3.08E-05
7.063	1.86E-05
7.014	1.08E-05
6.965	6.80E-06
6.916	4.07E-06
6.867	2.56E-06
6.818	1.51E-06
6.769	8.40E-07
6.720	4.60E-07
6.671	2.80E-07
6.622	1.85E-07

TEST LIF:33.02

TEMPERATURE = 305 (K)
INITIAL STRAIN 0.00 (PCT)
TOTAL STRAIN 0.24 (PCT)
INITIAL SHEAR STRESS 7.897 (MPA)

SHEAR STRESS (MPA)	STRAIN RATE (/MIN)
7.873	6.70E-04
7.848	4.50E-04
7.823	3.54E-04
7.799	2.81E-04
7.774	2.33E-04
7.750	1.89E-04
7.725	1.52E-04
7.701	1.25E-04
7.676	1.02E-04
7.652	8.30E-05
7.627	6.60E-05
7.603	5.20E-05
7.578	4.30E-05
7.554	3.36E-05
7.529	2.64E-05
7.505	2.10E-05
7.480	1.66E-05
7.456	1.29E-05
7.431	9.80E-06
7.407	7.70E-06
7.382	6.20E-06
7.357	4.70E-06
7.333	3.67E-06
7.308	2.83E-06
7.284	2.21E-06
7.259	1.60E-06
7.235	1.13E-06

TEST LIF:33.03

TEMPERATURE = 305 (K)
INITIAL STRAIN 0.14 (PCT)
TOTAL STRAIN = 0.46 (PCT)
INITIAL SHEAR STRESS 7.446 (MPA)

SHEAR STRESS (MPA)	STRAIN RATE (/MIN)
7.416	1.52E-03
7.366	1.02E-03
7.317	7.50E-04
7.267	5.50E-04
7.217	4.09E-04
7.167	2.99E-04
7.118	2.19E-04
7.068	1.59E-04
7.018	1.13E-04
6.968	8.20E-05
6.918	5.40E-05
6.869	3.78E-05
6.819	2.63E-05
6.769	1.76E-05
6.719	1.16E-05
6.670	7.50E-06
6.620	4.80E-06
6.570	3.04E-06
5.520	1.85E-06
6.471	1.21E-06
6.421	8.00E-07
6.371	5.60E-07
6.321	3.50E-07
6.271	2.10E-07

TEST LIF:33.05

TEMPERATURE = 305 (K)
INITIAL STRAIN 0.18 (PCT)
TOTAL STRAIN = 0.67 (PCT)
INITIAL SHEAR STRESS - 7.387 (MPA)

SHEAR STRESS (MPA)	STRAIN RATE (/MIN)
7.272	8.00E-04
7.232	6.20E-04
7.182	4.48E-04
7.132	3.37E-04
7.083	2.48E-04
7.033	1.78E-04
6.983	1.31E-04
6.933	9.00E-05
6.883	6.50E-05
6.833	4.60E-05
6.783	3.10E-05
6.733	2.12E-05
6.684	1.45E-05
6.634	9.80E-06
6.584	6.50E-06
6.534	4.29E-06
6.484	2.74E-06
6.434	1.80E-06
6.384	1.15E-06
6.334	7.10E-07
6.285	4.30E-07
6.235	2.67E-07
6.185	1.67E-07

TEST LIF:33.06

TEMPERATURE = 305 (K)
INITIAL STRAIN 0.00 (PCT)
TOTAL STRAIN = 0.70 (PCT)
INITIAL SHEAR STRESS - 7.409 (MPA)

SHEAR STRESS (MPA)	STRAIN RATE (/MIN)
7.334	4.35E-04
7.284	2.74E-04
7.234	1.89E-04
7.184	1.40E-04
7.135	1.03E-04
7.085	7.80E-05
7.035	5.70E-05
6.985	4.26E-05
6.935	3.14E-05
6.885	2.26E-05
6.835	1.63E-05
6.785	1.16E-05
6.735	8.10E-06
6.686	5.70E-06
6.636	3.80E-06
6.586	2.63E-06
6.536	1.77E-06
6.486	1.16E-06
6.436	7.80E-07
6.386	5.50E-07
6.336	3.80E-07

TEST LIF:33.07

TEMPERATURE 303 (K)
INITIAL STRAIN 0.17 (PCT)
TOTAL STRAIN = 0.90 (PCT)
INITIAL SHEAR STRESS 8.240 (MPA)

SHEAR STRESS (MPA)	STRAIN RATE (/MIN)
8.191	1.00E-03
8.142	7.90E-04
8.093	6.50E-04
8.044	4.90E-04
7.995	3.50E-04
7.946	2.27E-04
7.897	1.46E-04
7.848	9.10E-05
7.799	5.30E-05
7.750	3.40E-05
7.701	2.06E-05
7.652	1.23E-05
7.603	7.20E-06
7.554	4.04E-06
7.505	2.13E-06
7.456	1.16E-06
7.407	6.60E-07
7.357	4.80E-07
7.308	2.20E-07

TEST LIF:33.08

TEMPERATURE =	303 (K)
INITIAL STRAIN	0.00 (PCT)
TOTAL STRAIN =	1.00 (PCT)
INITIAL SHEAR STRESS	7.946 (MPA)

SHEAR STRESS (MPA)	STRAIN RATE (/MIN)
7.897	8.20E-05
7.873	7.70E-05
7.848	7.40E-05
7.823	7.00E-05
7.799	6.50E-05
7.774	6.00E-05
7.750	5.20E-05
7.725	4.60E-05
7.701	4.00E-05
7.676	3.31E-05
7.652	2.72E-05
7.627	2.21E-05
7.603	1.78E-05
7.578	1.46E-05
7.554	1.13E-05
7.529	9.00E-06
7.505	7.10E-06
7.480	5.70E-06
7.456	4.42E-06
7.431	3.47E-06
7.407	2.75E-06
7.382	2.14E-06
7.357	1.65E-06
7.333	1.27E-06
7.308	9.90E-07
7.284	7.70E-07
7.259	5.90E-07
7.235	4.60E-07
7.210	3.50E-07
7.186	2.75E-07
7.161	2.10E-07

TEST LIF:33.09

TEMPERATURE =	303 (K)
INITIAL STRAIN =	0.17 (PCT)
TOTAL STRAIN =	1.30 (PCT)
INITIAL SHEAR STRESS	8.314 (MPA)

SHEAR STRESS (MPA)	STRAIN RATE (/MIN)
8.289	8.90E-04
8.240	5.60E-04
8.191	3.71E-04
8.142	2.48E-04
8.093	1.65E-04
8.044	1.10E-04
7.995	7.10E-05
7.946	4.50E-05
7.897	2.86E-05
7.848	1.75E-05
7.799	1.07E-05
7.750	6.40E-06
7.701	3.81E-06
7.652	2.22E-06
7.603	1.26E-06
7.554	7.40E-07
7.505	4.30E-07
7.456	2.40E-07
7.407	1.40E-07

TEST LIF:33.10

TEMPERATURE =	306 (K)
INITIAL STRAIN	0.19 (PCT)
TOTAL STRAIN =	1.60 (PCT)
INITIAL SHEAR STRESS	7.933 (MPA)

SHEAR STRESS (MPA)	STRAIN RATE (/MIN)
7.903	1.59E-03
7.853	1.02E-03
7.802	7.30E-04
7.752	5.40E-04
7.702	4.03E-04
7.651	3.01E-04
7.601	2.22E-04
7.551	1.62E-04
7.500	1.18E-04
7.450	8.60E-05
7.400	6.10E-05
7.349	4.34E-05
7.299	3.09E-05
7.249	2.17E-05
7.198	1.53E-05
7.148	1.08E-05
7.098	7.40E-06
7.047	5.20E-06
6.997	3.48E-06
6.947	2.37E-06
6.896	1.57E-06
6.846	9.60E-07
6.796	6.60E-07
6.745	4.30E-07
6.695	2.80E-07
6.645	1.80E-07

TEST LIF:33.11

TEMPERATURE =	306 (K)
INITIAL STRAIN	0.17 (PCT)
TOTAL STRAIN =	1.80 (PCT)
INITIAL SHEAR STRESS	7.949 (MPA)

SHEAR STRESS (MPA)	STRAIN RATE (/MIN)
7.919	1.66E-03
7.868	1.11E-03
7.818	7.60E-04
7.767	5.60E-04
7.717	4.20E-04
7.666	3.06E-04
7.616	2.27E-04
7.566	1.66E-04
7.515	1.23E-04
7.465	8.80E-05
7.414	6.30E-05
7.364	4.50E-05
7.313	3.18E-05
7.263	2.26E-05
7.213	1.56E-05
7.162	1.09E-05
7.112	7.60E-06
7.061	5.10E-06
7.011	3.40E-06
6.960	2.25E-06
6.910	1.50E-06
6.859	9.30E-07
6.809	5.80E-07
6.759	3.40E-07
6.708	2.00E-07